Y3.At7:
36/9-4

POWER REACTOR TECHNOLOGY

A Quarterly Technical Progress Review

Prepared for DIVISION OF TECHNICAL INFORMATION, USAEC, by
ARGONNE NATIONAL LABORATORY

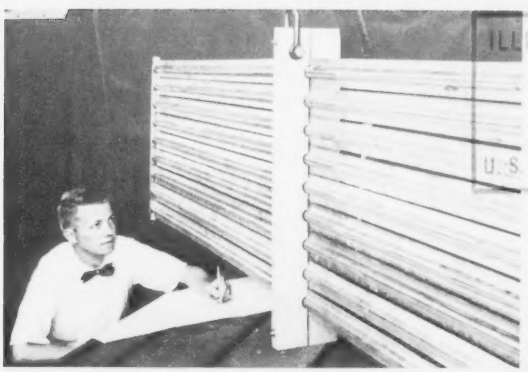

ILLINOIS STATE LIBRARY
JUL 17 1967
U.S. Supt. of Documents Deposit

Fall 1966

● VOLUME 9

● NUMBER 4

Rankine-cycle space power ... page 194

TECHNICAL PROGRESS REVIEWS

The United States Atomic Energy Commission publishes the Technical Progress Reviews to meet the needs of industry and government for concise summaries of current nuclear developments. Issued quarterly, each journal digests and evaluates the latest findings in a specific area of nuclear technology and science.

The journals are:

Isotopes and Radiation Technology
P. S. Baker, A. F. Rupp, and Associates
Oak Ridge National Laboratory

Nuclear Safety
Wm. B. Cottrell, W. H. Jordan, J. P. Blakely, and Associates
Nuclear Safety Information Center, Oak Ridge National Laboratory

Power Reactor Technology
Argonne National Laboratory

Reactor Materials
E. M. Simons and Associates
Battelle Memorial Institute

All are available from the U. S. Government Printing Office. See the back cover for ordering instructions.

The views expressed in this publication do not necessarily represent those of the United States Atomic Energy Commission, its divisions or offices, or of any Commission advisory committee or contractor.

Availability of Reports Cited in This Review

United States Atomic Energy Commission (USAEC) reports are available at USAEC depository libraries and are sold by the Clearinghouse for Federal Scientific and Technical Information (CFSTI), National Bureau of Standards, U. S. Department of Commerce, 5285 Port Royal Road, Springfield, Va. 22151. All reports sold by CFSTI are $3.00 for printed copy and $0.65 for microfiche. Each separately bound part of a report is priced as a separate report. Some reports may not be available because of their preliminary nature; however, the information contained in them will generally be found in later progress or topical reports on the subject.

Other U. S. Government agency reports identified in this journal generally are available from CFSTI.

Private-organization reports should be requested from the originator.

United Kingdom Atomic Energy Authority (UKAEA) and Atomic Energy of Canada Limited (AECL) reports are available at USAEC depository libraries. UKAEA reports are sold by Her Majesty's Stationery Office, London; AECL reports are sold by the Technical Information Officer, Atomic Energy of Canada Limited, Chalk River, Ontario, Canada. UKAEA and AECL reports issued after March 1, 1967, are sold by CFSTI to purchasers in the United States and its territories.

Contents

Power Reactor Technology

Vol. 9, No. 4

APPLICATIONS	New Departures in High-Flux Research Reactors *Bernard I. Spinrad*	153
PHYSICS	Zone-Loaded Critical Experiments for Fast Breeders *George J. Fischer, Armando Travelli, and Daniel A. Meneley*	162
CONTROL AND DYNAMICS	Let's Apply Optimal Control and Nonlinear Analysis *Ronald R. Mohler*	169
FLUID AND THERMAL TECHNOLOGY	Improved Design Predictions Through Liquid-Metal Heat-Transfer Research *Ralph P. Stein*	174
OPERATING EXPERIENCE	NPD Performance Indicates Merit of On-Power Refueling *Karl K. Brown*	180
ENERGY CONVERSION	Recent Developments in Liquid-Metal MHD Power Systems *Michael Petrick*	187
	Component Development—Key to Rankine-Cycle Space Applications *Edward J. Croke*	194
INDEX	Volume 9	215

LIMITED COVERAGE OF FUEL PROCESSING

The Technical Progress Review *Reactor Fuel Processing* was terminated with the Vol. 9, No. 4, issue. Limited coverage of fuel processing will begin in this journal with the Winter issue, Vol. 10, No. 1.

Issued quarterly by the U. S. Atomic Energy Commission. Use of funds for printing this publication approved by the Director of the Bureau of the Budget on July 8, 1966.

Power Reactor Technology

is a quarterly review of developments in reactor technology — including new concepts and applications as well as research results, analysis, and experience with existing or new components and systems. Prepared by Argonne National Laboratory at the request of the Division of Technical Information of the U. S. Atomic Energy Commission, *Power Reactor Technology* is intended for reactor designers and other technical specialists concerned with the interplay among reactor development, design, construction, operation, and economics. Thus this quarterly journal reports and interprets progress in the power-reactor field in terms of its significance to the reactor designer. Its scope includes research and development in the various technical specialties in the field as well as design and construction practices, reactor concepts, applications, economics, and operating experience.

Some articles summarize and critically evaluate reported developments; others review a topic broadly so that designers can interpret new developments, experience, and trends. All, however, call the reader's attention to reports and publications that merit study. Because any appraisal involves the reviewer's opinion of the significance of the work reported, readers are urged to consult the references for additional information and the judgments of the original authors. If a reader has information that causes his evaluation to reinforce, modify, or contradict the opinions of our reviewers, he is encouraged to write to the Editor.

For reasonably timely coverage, articles often must be based on fragmentary information. Thus, whenever appropriate, continuity will be maintained from one issue to another by use of subject headings that reflect parts of the following scope of the journal:

CONCEPTS and APPLICATIONS: Progress in evaluating the applicability and economics of various reactor types and systems (including unconventional approaches), as well as of fuel resources and cycles, for utility central-station generation of electricity, auxiliary power, process radiation and heat, desalting, and propulsion — and for terrestrial, undersea, aerospace, and other advanced uses.

ANALYSIS and EXPERIMENTATION: Advancements in the techniques of reactor physics, fluid and thermal technology, power conversion, fuel elements, materials, mechanics, control and dynamics, and reactor safety.

SYSTEMS and COMPONENTS: Experience as reflected in design and construction practice, components, systems technology, and operating performance of various specific types of reactors — including pressurized- and boiling-water reactors, molten-salt, organic-, gas-, and liquid-metal-cooled reactors, as well as generally applicable aspects of research and test reactors.

At Argonne National Laboratory, the Reactor Engineering Division (L. J. Koch, Director) has the principal responsibility for the preparation of *Power Reactor Technology*, with the regular assistance of the Reactor Physics Division (R. A. Avery, Director) and the occasional assistance of other Laboratory divisions (Metallurgy, Chemical Engineering, Chemistry, Reactor Operations, and Idaho). Thus, unless noted otherwise, the reviewers and authors of articles are Laboratory staff members. The editors will welcome interpretive review articles contributed by readers outside the Laboratory.

JAMES J. DUTTON, *Editor*
DAVID H. LENNOX, *Technical Editor;* KARL K. BROWN, *Managing Editor*
EDWARD J. CROKE and RAYMOND GOLD, *Associate Editors*
BARBARA A. SCHMEH, *Assistant Editor*

Argonne National Laboratory

Y3.At7:
36/9-4

ILLINOIS STATE LIBRARY
JUL 17 1967
U. S. Supt. of Documents Deposit

New Departures in High-Flux Research Reactors

By Bernard I. Spinrad

The present generation of high-flux research reactors—heterogeneous, water cooled and moderated (light and heavy), with projected beam and irradiation fluxes of 1 to 5×10^{15} thermal neutrons/(cm^2)(sec)—represents the penultimate in research-reactor performance, according to their designers. That is, although they may be improved by design refinements as we learn more about actual system performance with regard to hot-channel factors, coolant flow patterns, burnout safety margins, and so on, it is unlikely that this improvement could lead to more than a factor of ~3 in available flux. (If this were not the case, these improvements would be the subject of vigorous research and development and would be incorporated in the most recent proposals.)

To go further in obtaining greater neutron fluxes for experimental purposes, it is necessary to overcome the limitations of present reactor types and to find new reactor concepts that are more amenable to very-high-flux design. After discussing methods by which present limitations can be overcome by relatively moderate design changes, this article considers a number of specific new concepts. Even though several of the new approaches might be able to deliver ~10^{17} neutrons/(cm^2)(sec), they, too, have foreseeable limits. It is likely that a flux greater than 2×10^{17} will never be achieved in a steady-state research reactor. However, if it were possible to "hire" the Jackass Flats hydrogen pumping capability for an occasional—and, indeed, very expensive—hour, fluxes up to 5×10^{17} might be contemplated with reactor designs appropriate for 50 Mw/liter operation. A similar complex (Fig. 1) that uses stored helium to cool a reactor (Fig. 2) might be more attractive from the standpoint of operating cost. Helium would be safer to handle than hydrogen, and there would be a greater variety of reactor materials that can tolerate it.

Overcoming Limitations

The major factor that limits the advance of fluxes in present types of research reactors is the power density, which is restricted by conflicting requirements of heat transfer, heat transport, and core materials. Designs now have coolant flows of 6 to 15 m/sec, core pressure drops of 5 to 10 atm, and core power densities of 1 to 3 Mw/liter. Typical heat-transfer rates are ~200 watts/cm^2, and system pressures are tens of atmospheres to suppress boiling. The materials and heat-transfer technologies do not permit much increase in power density with present reactor concepts. But, for experiment irradiation purposes, we can (1) alter the fissile material to obtain greater neutron-production rates, (2) take greater advantage of geometry, and (3) use the core flux more effectively. These steps lead to consideration of flux traps, core life, criticality, and power shape and their influence on reactor design and operation.

ALTERING THE FISSILE MATERIAL

Per fission yielding ν neutrons, the critical reactor core absorbs ν/k_∞ neutrons, where k_∞ is the infinite multiplication factor of the core. Therefore the excess neutrons produced per fission are $\nu(k_\infty - 1)/k_\infty$. Without parasitic absorption, the maximum value k_∞ can assume is η. Table 1 lists values of $\nu(\eta - 1)/\eta$, which represents the maximum number of neutrons that can be made available per fission, for three fissile isotopes. It is apparent that ^{239}Pu is a very superior fuel in the fast-energy range. Uranium-233 is the best fuel in the intermediate-energy range, and ^{239}Pu and ^{233}U are about equally good in thermal reactors.

Unfortunately, ^{235}U is the most available fuel and is used preferably. Its use in an intermediate-reactor core results in only half as many neutrons being

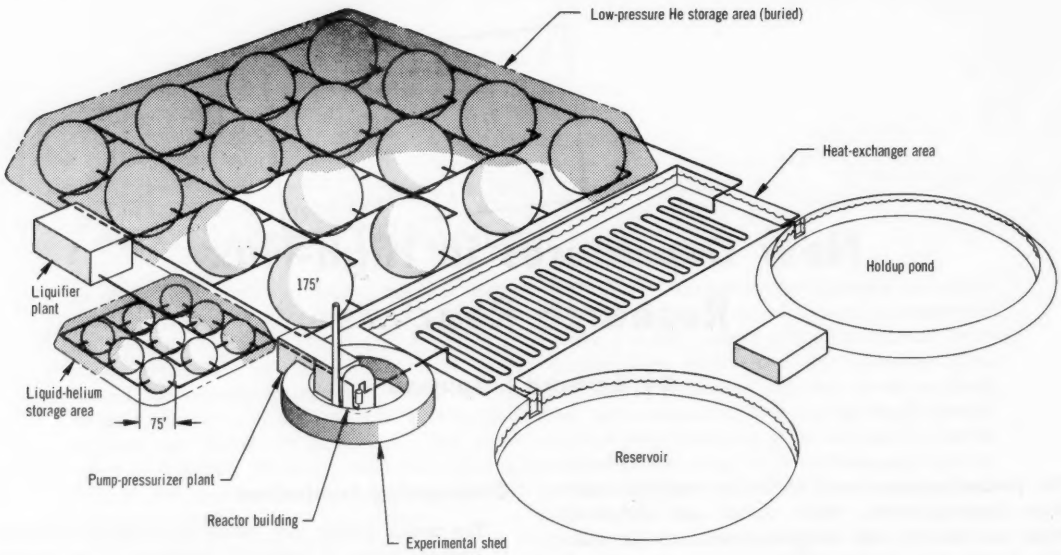

Fig. 1 Helium system for cooling reactor (Fig. 2) that might produce 5×10^{17} neutrons/(cm²)(sec). Coolant storage complex might be dubbed "Helium Hill."

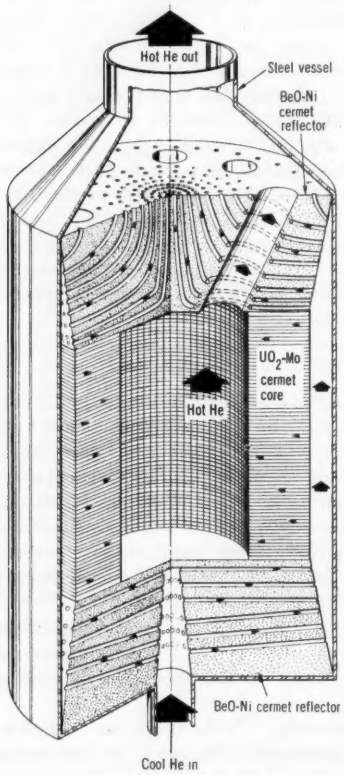

Fig. 2 Research-reactor concept capable of 50 Mw/liter operation to produce 5×10^{17} neutrons/(cm²)(sec).

available as in a plutonium-fueled fast core, and two-thirds as many as in a ^{233}U- or ^{239}Pu-fueled thermal reactor. Uranium-233 is the least available fuel. It would appear worthwhile, therefore, to explore the possibility of using ^{239}Pu, which is plentiful, to fuel research reactors. The desirability of ^{239}Pu is enhanced by its high neutron-absorption cross section at all energies, which makes it rather easy for the infinite multiplication factor to approach η.

Table 1 AVAILABLE NEUTRONS PER FISSION $[\nu(\eta-1)/\eta]$

Energy range	^{233}U	^{235}U	^{239}Pu
Thermal	1.41	1.26	1.43
Intermediate	1.39	0.96	1.28
Fast	1.50	1.41	1.90

TAKING ADVANTAGE OF GEOMETRY

Experiments are generally located in the reflector of the reactor system. To examine the geometrical factors, let us take the reactor as a sphere emitting Q neutrons, and let τ be the reflector age, a the core radius, L the reflector diffusion length, and D the diffusion coefficient for thermal neutrons. To enhance the ratio of thermal neutrons to high-energy neutrons, the experiment is usually located in the reflector at a distance of about $\sqrt{\tau}$ from the core edge. The unperturbed thermal flux is usually within a factor of 2 of $QL/(a + \sqrt{\tau})(a + L + \sqrt{\tau})D$.

The properties of moderators are such that the maximum flux is obtained in light water when $a \leq 15$

cm, in beryllium or BeO when 15 cm $\leq a \leq$ 30 cm, and in D_2O when $a \geq 30$ cm. More importantly, the flux increases for each moderator as a decreases—i.e., the diffusion processes merely serve to smear out the basic $1/r^2$ law. With moderator optimization taken into account, the unperturbed neutron flux follows a $1/r$ law up to about 1 m, whereas current (more appropriate for large beam setups) follows a $1/r^2$ law.

Thus it is obvious that the more the source can be compressed the more flux we will have—so the incentive is for high power density.

To some extent this argument may be slightly softened by the use of "external flux traps" or a "neutron hohlraum." External flux trapping, a means of leading more than the geometrical share of neutrons to an experiment, is usually done by putting some hydrogenous moderator around the experiment (when the reflecting material is beryllium or D_2O). In a neutron hohlraum the core and a small quantity of reflector are placed in a large cavity in a block of dense moderator. Even in these cases the advantages of high-power-density cores persist.

USING THE CORE FLUX

Under circumstances where the backgrounds can be made acceptable, it is desirable to get close to the source to obtain high flux for an experiment. In fact, in principle, it is possible to extract neutrons directly from the core. In this circumstance the previous arguments are not valid. Instead, one must examine core criticality and power density more closely.

If the core power density is PD (in megawatts per liter) and the macroscopic fission cross section is Σ_f, then the flux is

$$\phi = \frac{PD}{\Sigma_f} \times 3.25 \times 10^{13} \qquad (1)$$

The macroscopic fission cross section is related to the critical mass and volume by

$$\Sigma_f = \left(\frac{N_0 \sigma_f}{A}\right)\left(\frac{M}{V}\right) \qquad (2)$$

where N_0 = Avogadro's number
σ_f = the microscopic fission cross section
A = the molar mass
M = the critical mass
V = the core volume

Then

$$\phi = \frac{(3.25 \times 10^{13})\,A}{N_0 \sigma_f} PD \left(\frac{V}{M}\right)$$

$$= \frac{(3.25 \times 10^{13})\,A}{N_0 \sigma_f} \left(\frac{P}{M}\right) \qquad (3)$$

where P is total power.

Thus, to get high core flux, we attempt to attain a highly dilute core (small M/V) or a small critical mass, depending on whether power density or power is limiting. Additionally, we may get high epithermal fluxes by making the core undermoderated, and thereby achieving small values of σ_f. However, this factor is counterbalanced by the fact that critical masses of intermediate reactors tend to be large.

FLUX TRAPS

The ultimate in penetrating the core is to use the flux at its center. This poses no problem for lightly loaded reactors. However, heavily loaded small reactors immersed in a moderator have peak core flux at the outer edge and peak thermal flux in the moderating reflector at ~1 root age from the core.

This effect also can be observed in the center of the core. Geometrically, if one takes a slab core and deforms it into a cylindrical or spherical annulus, the thermal-neutron-flux peaks on both sides persist—and one of these peaks now can be at the center of the annulus. This peak is known as a flux trap and has been well investigated.[1–3] The most definitive study is that of Ergen.[4,5] However, it is now well known that the performance of a flux trap depends strongly on core configuration.

The following heuristic points have emerged as a result of the many investigations of moderator islands in research-reactor cores.[6]

- There is a limiting ratio of core-to-moderator blackness, below which no flux peak in a moderator island is possible. This does not mean that experimental fluxes in moderator islands embedded in cores of low absorption are necessarily low; such cores are characterized by already well-thermalized spectra. The flux trap in such cores has degenerated to a simple filter removing virgin-neutron background. Small quantities (dimensions small compared to thermal-neutron-diffusion length in the moderator) of materials such as D_2O or beryllium are optimal. In fact, maximum experimental flux per unit core power density can be obtained from such systems.
- The flux-trap principle peaks the thermal-neutron flux most dramatically when cores of high blackness to thermal neutrons are used, which means that, in the core, thermal-neutron flux is strongly depressed.

It follows from these two principles that the actual value of thermal-neutron flux in the center of a moderator island only mildly depends on core blackness and, in fact, is higher for cores of low blackness: the flux produced by thermalization of fast neutrons in the island is essentially additive to core flux.

The preceding argument assumes that "other things are equal." In practice, other things are not equal. For example, two idealizations of the moderator island assume that (1) the total source strength is constant (i.e., fast-neutron current at the edge of the island = $Q/4\pi a^2$, where Q is the available neutrons) and (2) fast current is constant at the edge. It turns out that geometrical factors prohibit flux peaking in

the former case, which is appropriate to large power-limited cores. Per unit source the maximum flux is attained with a vanishing island. However, the source entering a small island is more nearly described by a constant entering current from a power-density-limited reactor (Case 2). Nevertheless, this current may be made somewhat larger by maximizing the inward leakage to the flux trap relative to outward leakage. To do this:

- The core should be as thin as possible.
- The core should be externally reflected by a good fast-neutron reflector, particularly one with a high scattering cross section for epithermal neutrons. Beryllium and nickel are recommended.

These two arguments can also be arrived at by simply examining the contribution to fast-neutron current entering the island from fission sources originating at various points in the core. The contribution is greatest for sources close to the island and can be somewhat enhanced by a good external reflector. The two points of view are therefore functionally related.

So far, we have not commented on steps to maximize flux within the island. The following points should be considered:

- The "fast" neutrons leaking in should actually be as soft as possible.
- The neutron-absorption cross section of the flux-trap medium should be low, and the diffusion coefficient for thermal neutrons in it should also be low, to permit high flux buildup and to inhibit thermal-neutron migration from trap to core.

All these criteria are difficult to satisfy at once. For example, H_2O, D_2O, and beryllium can all function as flux-trap media of approximately equal efficiency, but the dimensions of the optimum trap vary greatly and the optima emphasize different properties of the media (the low age and thermal-neutron-diffusion coefficient of water, the low absorption by D_2O, and the intermediate properties of beryllium).

Although, ideally, the flux trap is completely surrounded by core, in practice not too much harm is done by penetrating the core with a beam tube. As with irradiation experiments, not too many neutrons must be extracted by means of a beam or the flux will be depressed. About half the neutrons in the trap may be used.

CORE LIFE AND REFUELING

Very-high-flux research reactors will operate at quite high power—100 to 1000 Mw, and maybe even more. At these powers, fissile fuel is destroyed quite rapidly. At 100 Mw, about 1 kg is destroyed in 10 days, and at 1000 Mw, in 1 day.

For fluid-fuel reactors the problems of burnup are solvable by straightforward engineering.

For fixed-fuel reactors the rapid attrition of the fuel profoundly affects reactor design, both (1) because it is desirable to have operating time long compared to refueling time and (2) because of the changes in core characteristics due to having a time variation in fuel and poison concentrations. Conventional techniques [as used at the Materials Testing Reactor (MTR), the Engineering Test Reactor (ETR), and CP-5, for example] embody a refueling operation, performed after the reactor has been shut down and permitted to cool off, in which the fuel elements are replaced gradually and one at a time. The reloading shutdown takes 2 days to a week, depending on the cooling time adopted, the mechanisms available, and safety restrictions adopted. Thus cycle times of 20 to 70 days are necessary to achieve 90% operating time.

Even with a short time—20 days—and a 100-Mw power, 2 kg of fuel is burned. Because thermal reactors are characterized by critical masses of 1 to 5 kg, this means that something of the order of an extra critical mass must be provided initially. (Actually, it is desirable economically to provide initially two or three extra critical masses so that core fabrication can be amortized over a longer period.)

Control System. The large overload of fuel requires that there be an elaborate control system. The fresh core must be held down, either by burnable or movable poison or by controlling leakage. Since leakage neutrons are what the experimenter wants, the latter method should be preferred, especially since core poisons additionally restrict neutron availability per unit power. Unfortunately, reactor designers have so far chosen the "conventional" approach of control rods rather than the "unconventional" one of reflector motion—to the experimenter's disadvantage.

To fulfill the requirements of core life, several expedients are, fortunately, available. In addition to the use of fluid fuel, which has several obvious advantages for the long run, two points may be capitalized:

1. Intermediate- and, particularly, fast-reactor cores show relatively less reactivity swing over a large fractional core burnup. This not only makes control generally easier but also makes it more feasible to adopt leakage control. Moreover, such reactors do not show large xenon-buildup effects when shut down briefly.
2. There is no physical reason for not having brief shutdowns for partial refueling, or, in the limit, designing for on-line refueling. The required engineering development to permit this, and to satisfy appropriate safety requirements, must ultimately be done.

CRITICALITY AND POWER SHAPE

Up to this point we have assumed that the high-flux reactor core can be made critical with an assumed volume, reflector material, configuration, and low parasitic core absorption. But this is not always the

case. Nearly all reactor types of potential utility can be made critical in volumes of 100 liters or more. However, attempts to capitalize on geometric factors by going to smaller cores require a progressive restriction of reactor type, and the smallest cores must be either proton-moderated or fast—a fact well illustrated in the choice of concepts for development as space nuclear power reactors.

Small cores pose another problem. They tend to be relatively black to low-energy neutrons. Therefore, when immersed in a pure moderator, they see a large reentrant low-energy flux, which creates a power spike at the interface. Although this is desirable experimentally—it produces neutrons close to the experiment—it is undesirable from the viewpoint of the core designer on three counts: (1) the power spike is a region of unusually high burnup and thus is not constant over life, (2) it limits total system power because the maximum power density is at the spike, and (3) the spike is likely to consist largely of epithermal fissions, the energy range least productive of experimental neutrons.

Consider New Concepts

The most compact reactor systems that can be made critical are the proton-moderated thermal reactors and fast reactors. In view of our familiarity through experience with them, water-moderated and -cooled reactors should be considered first.

SMALL-CORE H_2O REACTORS

There exists a body of information on the critical properties of these systems with H_2O reflectors (p. 182 ff in Ref. 7). As practical solutions, with fission products, ^{236}U, etc., water-reflected reactors can be made to go critical in a variety of sizes. Cores from 20 to 100 liters in volume all would require < 3 kg of ^{235}U and would be quite thermal in their power spectra. A small core might have a 20-liter volume, a k_∞ of 1.68, and a ^{235}U concentration of 100 g/liter; a middle-sized one would have $V = 50$ liters, $k_\infty = 1.40$, and $c = 36$ g/liter; a large one, $V = 100$ liters, $k_\infty = 1.25$, and $c = 25$ g/liter.

These cores would all be power-density limited. The "figure of merit," power times availability factor times geometry factor, could be approximated by $[\text{volume}/(r+6)^2]\,[(k_\infty - 1)/k_\infty]$. The results for the three sizes are almost identical.

Beryllium Reflector. The substitution of beryllium for H_2O as reflector would reduce critical-core radii by 6 to 7 cm. The result would be to permit a critical volume of ~20 liters at a k_∞ of ~1.39 and a volume of ~7 liters at k_∞ of ~1.7.

The smaller beryllium-reflected system may be profitably examined. For one thing, high power densities are more readily attained in small sizes than in large ones. Moreover, more concentrated systems can tolerate structural neutron poisons more readily than can dilute ones.

Although I have computed 7 liters as critical volume, reduced water density at power makes 10 liters a safer volume for a reactor of $k_\infty = 1.7$ and $c = 100$ g/liter. At 10 Mw/liter and a flow area of 50 cm^2 in the outlet pipe, this would have, as a homogeneous reactor with allowed temperature rise of 200°C, a coolant flow velocity of ~25 m/sec in the piping. The realization of such a reactor would probably be as an aqueous slurry.

Fluxes at beam locations would be several times 10^{15}. The major problems would be slurry circulation, radiolysis, and radiation damage to the container. It is probable that these could only be solved by using disposable (or, at least, dismountable) quick-connect primary components.

HEAVY-WATER REACTORS

A crucial difficulty with light-water reactors is that, unless they are quite small, the critical mass of fuel must compete with a significant quantity of water absorber for neutrons. Systems of more relaxed size—100 liters or more—have a low k_∞ and thus a small availability of excess neutrons per unit power. If one wants to keep the bulk of the fissions in the thermal range and yet have a large-volume core, the obvious step is to replace light water by very weakly absorbing heavy water.

A practical heavy-water core, with some fission products and xenon, could go critical at a 100-liter volume with a k_∞ of 1.88 and a ^{235}U concentration of about 6 g/liter. This is as estimated for a D_2O reflector, which is a convenient experimental medium. If, in some way, 1000 Mw could be extracted, the mean thermal flux would be greater than 4×10^{16}, and the peak would approach 10^{17}.

The core would, as a sphere, have a radius of slightly under 30 cm. At an experimental point 40 cm from the core center, the current would be about 1.8×10^{15} neutrons/(cm^2)(sec), and the small-beam flux would be close to 6×10^{16}.

The great improvement over the light-water system comes from several factors: (1) the artificial one of this article—had I chosen 200 Mw at 10 Mw/liter or 100 Mw at 5 Mw/liter, 20 liters would be the optimum-size core (although D_2O systems can be made critical at this size, their concentration approaches that of H_2O systems), (2) the higher k_∞ of D_2O cores makes them more productive of experimental neutrons for a given power, and (3) the higher flux/current ratio of D_2O reflectors, which again becomes apparent only in large sizes.

In summary to this point: D_2O systems with core sizes up to 100 liters have intrinsic neutronic advantages over H_2O reactors. If 10 Mw/liter core power can be attained, D_2O reactors are very attractive.

The low critical concentration—cited as 6 g/liter—makes it feasible to reconsider solution cores for this concept.

Central Zone. The very high core fluxes also make it attractive to consider locating experiments in an unfueled central zone. The peak core thermal flux for a constant-power reactor occurs with the core of minimum critical mass. According to my estimate this would occur with a core of ~120 liters—only slightly larger than the one just postulated—at which size the critical concentration would be 5 g/liter. A 10^{17} flux would be attainable in a central D_2O tube in such a reactor. (Not yet a flux trap; in D_2O it takes a very "gray" annular core and a large gap to develop maximum flux.)

The flux in a homogeneous reactor can of course be improved further by on-site fuel processing to remove fission products, with a consequent decrease in critical mass; this can be done for this reactor. There is only one other engineering problem that was not mentioned in the discussion of high power density from homogeneous reactors—the problem that all structural parts, including core pot and entrance pipes, must be very weak neutron absorbers. Otherwise, the virtues of the low absorption in D_2O would be seriously compromised. Materials such as beryllium, BeO, carbon, and magnesium, with zirconium as a possible cladding material, must be used.

As a possible alleviation of the high pipe flow rates, an "octopus" or "dodecapus," as sketched in Fig. 3, might be used. Such a reactor would have neutron production to some extent in the arms; and I can think of no easy way to figure out its real critical properties.

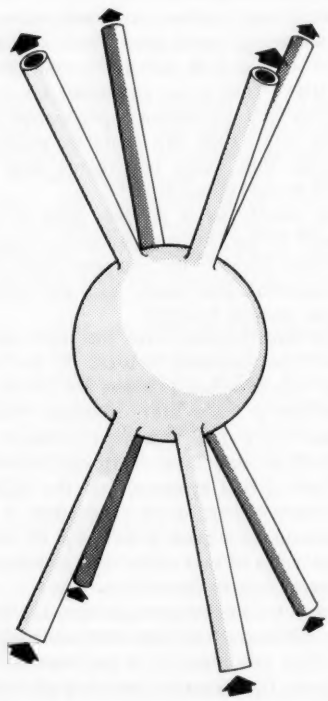

Fig. 3 Octopus-style homogeneous reactor would distribute out-of-core flow over four loops.

SMALL FAST REACTORS

Concentrated fast reactors are the smallest that can be made. For example, the critical mass of a ^{235}U sphere in a tub of H_2O is only about 23 kg (p. 582 of Ref. 7), corresponding to a core volume of 1.225 liters and a core radius of 6.64 cm. In D_2O the critical radius is ~5.6 cm. Even a bare sphere (such as Godiva) has a radius of only 8.4 cm. Plutonium spheres are even smaller; a high-density plutonium sphere in a thick beryllium reflector has a critical radius of < 3.2 cm.

These systems thus approach the "point source," and so the possibility of capitalizing on geometry must again be examined.

Selecting a point at radius 15 cm in a beryllium reflector as our experimental location, and assuming that a plutonium source has $\nu = 2.9$ and $k_\infty = 2$ (to account for the rather large fraction of epithermal fission), we have a net neutron availability of 4.7×10^{16} neutrons/Mw, a neutron current of 1.66×10^{13}/Mw at the experiment, and a thermal-neutron flux of almost 3×10^{14}/Mw.

A conservative example of the virtue of this system is illustrated below. It is conservative because performance could be markedly improved through use of plutonium and incorporation of very primitive internal cooling.

Let us consider a concentrated uranium sphere immersed in a 5-cm-thick sphere of H_2O. The critical radius would be under 7 cm, and the total assembly radius[7] would be 12 cm. The thermal conductivity of uranium is good enough that this assembly could operate at 8 kw for a uranium temperature rise of 200°C. At this power, given $k_\infty = 2.2$, the beam current from the water surface would be 1.9×10^{11} neutrons/(cm^2)(sec). In a graphite hohlraum this current may be somewhat intensified. This beam current is about what one would get from a 10^{12} flux research reactor—admittedly, not a high-flux system, but extremely good performance when compared with a 100-kw swimming pool! When such a reactor is opened for cooling, it can still be quite small. We consider now the next largest size, that of the Experimental Breeder Reactor I (EBR-I)[8] and Clementine.[9]

The EBR-I, as an example, has a core of a little over 6 liters, corresponding to a sphere of ~11-cm radius. With a most conservative cooling system, it produced 1 Mw of power. Its k_∞ was about 2.1.

Sodium Coolant. We now know how to achieve power densities of 1 Mw/liter in large sodium-cooled fast reactors, and so it would be straightforward engineering to do the same for a 6-liter fast reactor. The use of beryllium instead of uranium for the blanket would markedly increase reactivity, making it pos-

sible to use smaller rods and more sodium in the core. So a power density higher than 1 Mw/liter can be predicted for this type of system. Sodium coolant flow of 15 m/sec seems possible, and, at 30% core porosity and 10-cm core radius, this would amount to a mass flow rate of 115 kg/sec. Because heat capacity is ~1.25 joules/(g)(°C), a temperature rise of 400°C would permit a power of 57.5 Mw, or almost 10 Mw/liter.

Short Core-Residence Time. The key to this high power density is the small core size, which permits the coolant to have a very short core-residence time. Of course, all the numbers cited are advances over current practice (EBR-II, for example, has a core 2.5 times as long, sodium velocity $\frac{1}{2}$ as great, and temperature rise $\frac{1}{3}$ to $\frac{1}{4}$ as much, in achieving somewhat less than 1 Mw/liter). Nevertheless, the sodium route is one of the more straightforward ways of achieving high power density.

At 60 Mw in a 10-liter ^{235}U-fueled core with a beryllium reflector, we might achieve $k_\infty = 2.1$. With an experimental position at 24 cm, the experimental current would be 3.4×10^{14}, and the small-beam flux, around 7×10^{15}.

Hydrogen Coolant. A somewhat larger core could undoubtedly be built of refractory materials. We have investigated tungsten–UO_2 cermet fast-reactor systems for nuclear-rocket application. At about 50 liters and up, it becomes possible to extract 1000 Mw from them when the coolant is hydrogen, which can achieve high flow rates in small passages without unusual pressure drop and has a very high heat capacity per unit weight. The refractory core permits the heat source to sustain a high driving temperature difference for heat transfer to the bulk coolant.

Such a system — 1000 Mw, 20-cm radius, $k_\infty \sim 1.8$ — would yield the impressive flux of $\sim 1.6 \times 10^{17}$. Unfortunately, it is probably too costly to supply many cores of this type, and the cost of using hydrogen as a coolant is also extreme — as is likewise the hazard. Nevertheless, it indicates that technology in itself does not limit power density.

CAVITY AND THIN-SHELL REACTORS

It has been often observed, in this article and elsewhere, that a major limit to power density in heterogeneous reactors is a relatively long coolant-flow path through the core. Pressure drop increases with length, and temperature rise is constrained to some maximum. It is for these reasons that smaller cores may have higher power densities.

It is clear that shorter coolant path lengths can be achieved with radial coolant flow. For a more-or-less compact core, only a factor of 2 reduction in flow length is possible, and this is hardly worth the design difficulty. However, there are core types for which the fuel configuration can be a thin annular section. For such cores, quite short flow paths can be realized by radial flow.

The most intriguing of these systems are the D_2O flux-trap cores and their close relatives, D_2O cavity reactors. Several reactor systems of this general sort were investigated some years ago.[10] The basic observation is that, in a large body of moderator (D_2O being the best example), a spherical shell of fuel just thick enough to be black to thermal neutrons will be critical.[4,5] If the shell is made larger, its blackness can be reduced to some limiting value, which is that required for criticality in a thin slab. Moreover, if the interior of the shell is evacuated, only a slight increase in blackness keeps the system critical; and, if the contents of the shell are dispersed uniformly within the sphere (the cavity reactor), again only a little more fuel is required.

Cavity Reactor. The cavity reactor is often conceived in terms of a fissioning gas with temperatures approaching those of plasmas. It is a possible core for plasma-reactor schemes, such as those of Refs. 11 to 13. The cavity reactor may also be fueled with a suspension of fissioning "dust"; as such, it is effectively a gas-phase homogeneous reactor of potential quite similar to that of the large homogeneous heavy-water solution. Problems of corrosion and plateout are replaced by problems of erosion and adhesion.

Thin-Shell Reactor. The existence of thin-shell critical assemblies presents a more novel reactor concept. Figure 4 illustrates a possible configura-

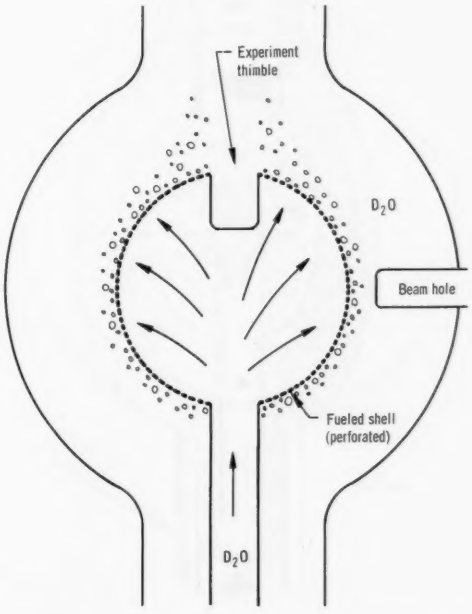

Fig. 4 Colander type D_2O thin-shell reactor.

tion: The core is a thin shell of a strong fueled material—such as a stainless-steel–urania cermet. This shell is perforated with a very large number of small holes, possibly drilled or punched at the time of fabrication, and probably clad by a chemical or electrochemical technique. The shell has at least one reentrant thimble for high-flux irradiations and a stem for coolant entry. Coolant is pumped in, forced through the holes of the colander, and dumped into the main moderator vessel.

Although the inlet pipe must contain the high flows characteristic of homogeneous reactors and the shell must support significant pressure, the high-temperature outlets of the homogeneous reactor have disappeared, and pressure drops do not approach those of parallel-flow heterogeneous systems. The D_2O may be permitted to evaporate and superheat in passing—it will recondense in the outer tank. (Not shown is the main cooling system, which withdraws warm moderator from the tank and returns part of the cold moderator by downward circulation around the outside of the shell.)

For those who are concerned with the strength of such a colander, an alternate scheme has been proposed.[14] The reactor shell is now solid (Fig. 5). The coolant is dispersed by flow through a nozzle head and impinges on the inner surface of the shell. The velocity of the coolant jets is high enough so that they can cut through the steam which comes off that surface, impinge on it, and be evaporated. The outer surface of the shell would be vapor bound in stable film boiling but not at a high enough temperature to burn out.

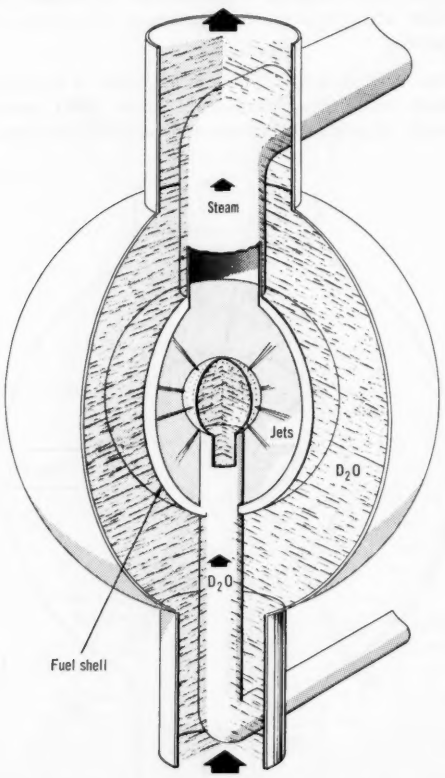

Fig. 5 Sprinkler type D_2O thin-shell reactor.

Finally, the scheme may be reduced to more conventional terms by reverting to parallel flow in small tubes of some appreciable length. Such a reactor looks like the colander of Fig. 4, with the thin shell replaced by a tubular fueled structure of 2 to 10 cm thickness (and flow length).[15]

The thin shell may also be used in reactors of more normal flow design. D_2O flux traps may be simulated by heterogeneous designs consisting of individual fuel elements spaced around a cylindrical annulus or a pseudospherical "basket." The large radius of optimal D_2O flux traps permits, in fact, enough space for a pressure-tube reactor design, which might make on-line reloading more feasible.

Another version of a thin-shell reactor is one computed by Ergen.[4,5] It seems possible to build a beryllium-moderated version in which the shell contains circulating molten salt. The excellent characteristics of molten salts as possible homogeneous reactor fuels (high permissible temperature rise and high gravimetric heat capacity) make a 100-Mw power for such a system credible. Ergen's calculation predicts a 7×10^{15} central-island flux for this case.

This article is based on a paper presented at the Symposium on Intense Neutron Sources,[16] Santa Fe, N. Mex., Sept. 19–23, 1966.

References

1. J. W. Webster, A Critical Assembly Having Maximum Sensitivity, USAEC Report IDO-16248, Phillips Petroleum Co., Aug. 31, 1953.
2. M. Osredkar and R. Stephenson, A Low Power, High Thermal-Flux Experimental Nuclear Reactor, *J. Nucl. Energy*, 5: 210 (1957).
3. M. Osredkar and R. Stephenson, Thermal Flux in the Central Moderator Zone of Thermal and Fast Reactors, in *Proceedings of the Second United Nations International Conference on the Peaceful Uses of Atomic Energy, Geneva, 1958*, Vol. 10, p. 174, United Nations, New York, 1958.
4. W. K. Ergen, Homogeneous High-Flux Reactor, USAEC Report CF-58-3-68, Oak Ridge National Laboratory, Mar. 31, 1958.
5. W. K. Ergen, The Highest Thermal Neutron Fluxes Obtainable from Fission Reactors, in *Proceedings of the Second United Nations International Conference on the Peaceful Uses of Atomic Energy, Geneva, 1958*, Vol. 10, p. 182, United Nations, New York, 1958.
6. C. N. Kelber, B. I. Spinrad and L. J. Templin, Advanced High-Flux Research Technology, *Trans. Amer. Nucl. Soc.*, 5(2): 425 (1962).
7. Argonne National Laboratory, Reactor Physics Constants, USAEC Report ANL-5800 (2nd ed.), July 1963.
8. H. V. Lichtenberger et al., Operating Experience and Experimental Results Obtained from a NaK-Cooled

Fast Reactor, in *Proceedings of the International Conference on the Peaceful Uses of Atomic Energy, Geneva, 1955*, Vol. 3, p. 345, United Nations, New York, 1956.
9. E. T. Jurney et al., The Los Alamos Fast Plutonium Reactor, USAEC Report LA-1679, Los Alamos Scientific Laboratory, May 1954.
10. G. Safonov, Externally Moderated Reactors, Report R-316, The Rand Corp., July 1957.
11. J. L. Kerrebrock and R. V. Meghreblian, Vortex Containment for the Gaseous Fission Rocket, Report JPL-TR-34-205, Jet Propulsion Laboratory, September 1961.
12. D. F. Spencer, Thermal and Criticality Analysis of the Plasma Core Reactor, Report JPL-TR-32-189, Jet Propulsion Laboratory, January 1962.
13. H. Weinstein and R. G. Ragsdale, A Coaxial Flow Reactor — A Gaseous Nuclear-Reactor Concept, *Amer. Rocket Soc.*, Preprint 1518-60, December 1960.
14. D. H. Lennox, Argonne National Laboratory, personal communication, 1961.
15. J. T. Weills, Conceptual Study of a Spherical Geometry Reactor with a High Flux Central Region, *Trans. Amer. Nucl. Soc.*, 5(2): 437 (November 1962).
16. Proceedings of the Symposium on Intense Neutron Sources, Santa Fe, N. Mex., Sept. 19–23, 1966 (to be published by the European Nuclear Energy Agency).

Zone-Loaded Critical Experiments for Fast Breeders

By George J. Fischer, Armando Travelli, and Daniel A. Meneley

Physics uncertainties—among others—limit the technology of the large fast power breeder, a reactor that might be fueled with 2000 kg of plutonium in a 6000-liter core and be capable of 1000 Mw(e). Some of these uncertainties influence safety analyses. Others relate to the behavior of the nuclear fuel over the fuel cycle and influence calculations of such parameters as doubling time and reactivity swing over core lifetime. These uncertainties force appropriate conservative design decisions that tend to lower the economic potential of the fast breeder.

Experiments on zero-power critical assemblies can effectively test the degree of uncertainty of many important calculations. They can also provide useful basic data to help reduce the uncertainties. There are some difficulties involved in straightforward mockup experiments, however. These difficulties will be discussed here; it is largely because of them that zone-loaded experiments are important.

A cross section of the material arrangement of a typical zone-loaded critical experiment is shown in Fig. 1. It is a zero-power critical assembly[1] and contains only a small fraction of the full core of interest. This fraction of the full $^{239}Pu-^{238}U$ fueled large breeder core is mounted as a center zone inside a "driver" region that supplies the additional reactivity needed to achieve criticality. A "buffer" or "filter" zone may be used between these two regions to improve such characteristics as the neutron-energy spectrum near the edge of the center zone. The driver is fueled with ^{235}U, which is more readily available than plutonium.

This article presents the reasons why zone-loaded experiments are important and describes a number of physics questions that can be answered through these experiments. It also discusses the limitations of the zone-loaded method, the safety aspects of this type of critical loading, and the major needs for further development of the concept. An example is given of a critical test of the ability of the analyst to predict full-core reactor properties on the basis of analysis of a zone-loaded critical experiment.

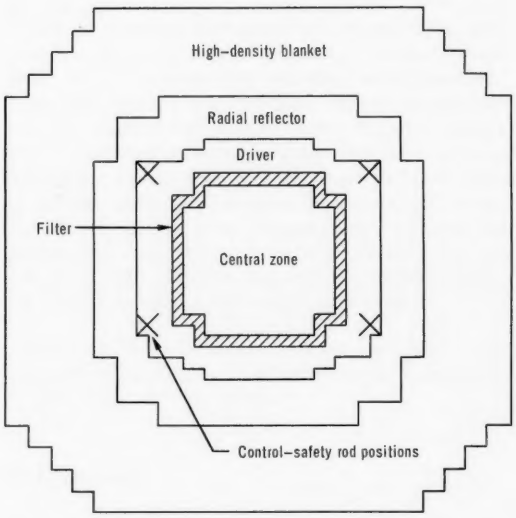

Fig. 1 Cross-section view of zone-loading assembly. Reactor materials are often loaded into matrix tubes of ~2- by 2-in. cross section, which gives the rectangular profile.[1]

Why Zone-Loaded Experiments?

Among the important advantages of zone-loaded experiments are:

- Smaller and presently available reactors such as ZPR-VI (Fig. 2) can be used effectively.
- Much smaller inventories of materials such as ^{239}Pu or ^{233}U fuels are needed in many cases.

- Cost of items directly related to reactor size is reduced.
- A program of survey type experiments on zone-loaded reactors could provide important basic data for a range of breeder-reactor compositions, possibly years sooner than these data might otherwise be obtained.
- There may be safety and health advantages to the use of zone-loaded mockups.

Difficulties involved in straightforward full-core mockups are numerous. The 6000-liter core, for example, would require a very large investment in fuel plates and other mockup materials — in amounts that usually are not obtainable at present. (Many nations will be forced into doing zone-loaded experiments because of limited availability of these materials.) Even when the materials are on hand, from 4 to 8 weeks would be needed just to assemble one full-core critical experiment. The radioactivity from ^{240}Pu, fission products, and possibly ^{233}U and its associated isotopes, all or some of which might need to be included, would be a hazard to operating personnel. Decay heat from these materials would induce reactor drift, which could limit the precision of reactivity measurements. Because of the high operating costs for facilities in which zero-power critical assemblies are built and because of the pressing need for experimental data, especially sodium-void and Doppler-effect measurements, it is essential that these facilities be employed with maximum effectiveness.

Physics Needs of the Fast Power-Breeder Reactor Program

Phenomena of particular concern in the difficult area of safety of the sodium-cooled large fast breeder — and comparatively difficult to calculate accurately — are the sodium-void effect and the Doppler effect. For some relatively simple and typical accident calculations that include both effects, sodium expulsion has been calculated to add reactivity at rates of 2 to 100 dollars per second. Addition of 1 dollar of reactivity to a reactor operating at a steady state (delayed critical) makes the reactor prompt critical — a dangerous condition in which the

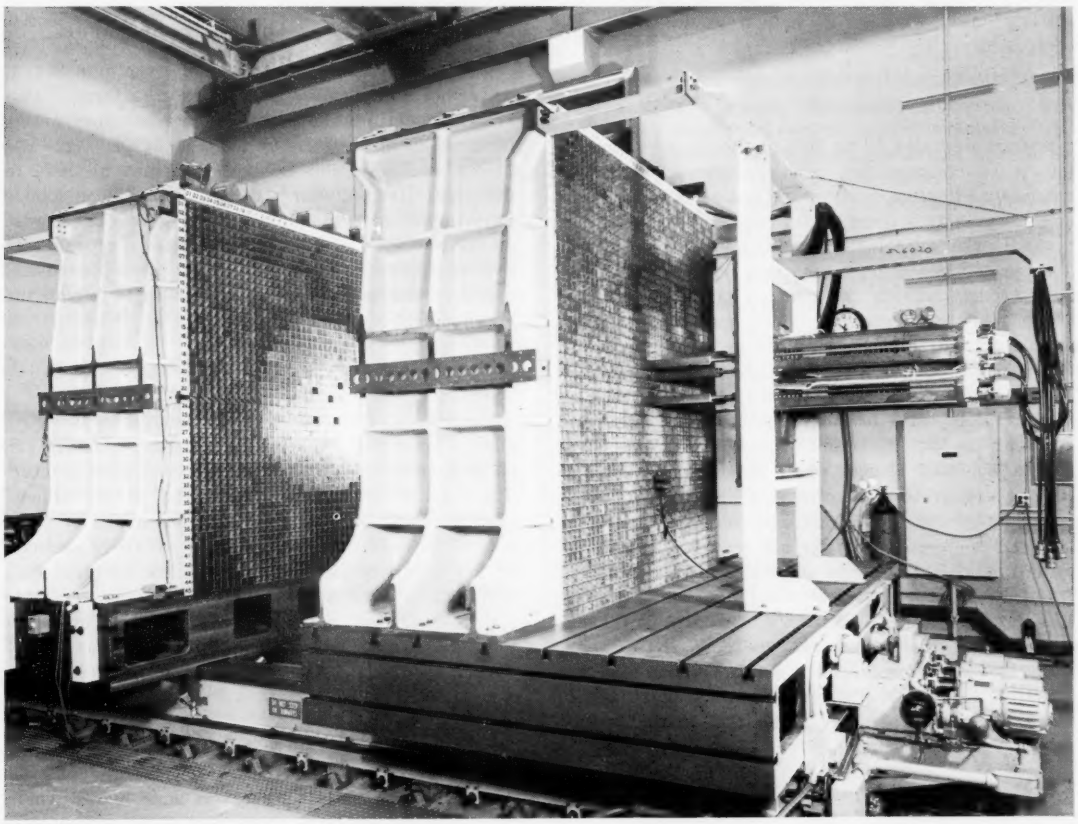

Fig. 2 Zero-power critical assembly ZPR-VI.

power doubles every few thousandths of a second. It is very important that careful experiments be performed to check the ability of the theoretician to calculate these two phenomena. In addition, since these effects have been calculated to be highly sensitive to the presence of higher plutonium isotopes, fission products, and the nature of the clad materials, the experiments must include these materials.

THE DOPPLER EFFECT

The Doppler effect is a prompt shutdown mechanism that operates primarily by absorbing neutrons in the energy range from about 1 to 15 kev, the low-energy tail of the neutron-energy spectrum of a fast reactor. This absorption takes place primarily in the fertile atoms, which exceed the fissile atoms by ratios of about 7:1 to 9:1, in the fissile isotopes, and, to a smaller extent, in structural materials. The effect occurs as a response to temperature changes, as in the heating of the fuel during a power surge. An objective of fast reactor designs is to achieve a Doppler-effect shutdown mechanism sufficiently strong that possible gains of positive reactivity upon voiding of sodium would be safely controlled.

THE SODIUM-VOID PROBLEM

Sodium occupies 50 to 70% of the core volume in the more common fast power-reactor designs. A relatively effective moderator because of its modest atomic weight, sodium shifts the neutron spectrum toward lower energies. In addition, sodium also has a large and broad resonance that peaks at 2.85 kev and strongly affects the neutron population in the 1- to 4-kev energy range, which contributes to the Doppler effect. Full or partial loss of sodium coolant, such as might follow pump failure or a transient, reverses these spectral effects. There is thus a spectral component of the reactivity change associated with the loss of sodium.

This spectral change which accompanies sodium voiding usually adds reactivity. Loss of sodium in a region about the reactor core center of some large fast power-breeder designs can increase reactivity by several dollars. On the other hand, loss of sodium from any reactor region in which there is a spatial flux gradient (as near the core boundary) increases the leakage of neutrons from the core and thereby tends to reduce the reactivity in competition with the spectral component. This reactivity change is the other component of the sodium-void effect and is called the leakage component.

OTHER NEEDS

In addition to the sodium-void and Doppler effects, there are many other uncertainties to be resolved. The theoretical physicist would like to check his cross-section choices for the materials in the reactor by means of material-worth measurements and of neutron-energy-spectrum measurements. He would like to check the reliability of some of his simplifying assumptions and procedures, such as the spatial dependence of his cross sections, heterogeneity corrections, choice of transport approximations, coupling between modules for a modular concept, and the change of this coupling with reactor operation. There are engineering problems that are sometimes difficult to calculate or important to verify. These include worths of partially inserted rods and effectiveness of shielding, for which additional approximations must be introduced and checked.

Plutonium became available for zero-power fast critical experimentation only a few years ago. Because physicists associated with the critical assemblies employing plutonium were required to devote a large part of the assembly availability time to mockup experiments, very little good basic experimental work on the reactor physics of plutonium–uranium fueled fast reactors exists.

Usefulness of Zone-Loaded Experiments

The central zone of the assembly[1] shown in Fig. 1, Assembly 45A of ZPR-III, mocked up a large ^{239}Pu–^{238}U monocarbide fast breeder reactor very satisfactorily with the use of only 51 kg of ^{239}Pu. The 21-cm radius of this central zone may be close to the lower limit of what is desirable on a zone-loaded experiment. A cylindrical geometry was used, with an axial core length of 91 cm chosen as a representative fast breeder core height. The zone-loaded assemblies discussed here will be assumed to have the arrangement of this assembly.

MEASURING NEUTRON-ENERGY SPECTRA

Many physics measurements related to the neutron-energy spectrum of large fast breeder reactors can be performed satisfactorily in a zone-loaded reactor. The most direct measurement is that of central neutron spectra. The experiments performed by Bennett, Gold, and Huber[2] provide an excellent example of the accuracy and resolution of the spectral data that can be obtained from a zone loading. Valuable energy-spectrum measurements in the direction of the axial blanket are equally possible in zone-loaded cores.

MEASURING SODIUM-VOID EFFECTS

Sodium-void measurements of several types can be performed satisfactorily on zone-loaded reactors.[1,3,4] The spectral component of the sodium-void effect is easily measured at the center of the zone loading, as are variations in the spectral effect due

to composition changes. Also straightforward are measurements of the important effects of channeled loss of sodium (related to the accidental voiding of a fuel subassembly). The leakage component of the sodium-void effect in the axial direction may also be measured. These experiments should be limited to one or more channels around the axis of the reactor. They frequently are sufficient to verify theoretical methods.

Care must be taken, of course, that the flux perturbations due to any measurement, especially if made at some radial distance away from the axis of the central zone, do not extend to a region where the neutron spectrum is affected by the buffer and driver zones. Although these effects might be compensated for to a considerable degree, it is always desirable to keep the measurement as free from uncertainties as possible.

As another precaution, the analyst must remain aware of the possibility that, in the approach of first-order perturbation theory, the denominator term

$$\oint \left\{ \left(\sum_j \phi_j^+ \chi_j \right) \times \left(\sum_k (\nu \Sigma_f)_k \phi_k \right) \right\} dVol$$

may change upon removal of sodium over a significant region of the central zone.

MEASURING THE DOPPLER EFFECT

Doppler-effect measurements have been made at or near the center of the zone loadings of the ZPR-III reactor on Assemblies 43, 43A (Ref. 5), 45, and 45A (Ref. 1) and in zone-loaded Assembly 4Z of ZPR-VI at Argonne.[6] Atomics International has performed Doppler-effect measurements in zone-loaded assemblies that employed thermal drivers.[7] All these measurements used small samples, which allowed much freedom in such matters as the nature of materials that surrounded the samples to be heated.

Experimental difficulties in Doppler-effect measurements made thus far in zone-loaded assemblies are only in small part different from the difficulties that would be found in equivalent measurements on nonzoned assemblies. Particular care must be taken, however, in attempting to measure the change in Doppler reactivity effects when sodium is removed from the environment surrounding the heated sample. It is very easy for the domain in which the sodium is removed to become sufficiently large that the Doppler element "sees" the presence of the buffer zone.

With moderate care, multiple-sample and "pot" type Doppler-effect measurements should be successful in zone-loaded assemblies.

KINETICS STUDIES

Rossi-alpha type kinetics measurements can be performed in zone loadings and apparently can be interpreted to predict the full-core kinetic characteristics with considerable confidence.[8] This property was demonstrated first in ZPR-III experiments on a coupled fast thermal-reactor concept,[9] a form of zone loading.

EQUIVALENCE TO MODULAR FAST BREEDER SYSTEMS

The physics of the modular concepts can be related clearly to the physics of the zone-loaded concepts. The radius of the central zone can be increased so that its reactivity grows, and the nature of the buffer zone can be changed to approximate the blanket region between modules. By letting the driver region, now with perhaps the same fuel as the central zone, represent a simplification of the modules external to the central module, we achieve a "zone-loading" representation of the modular concept which is particularly amenable to analysis. Much of the statics and dynamics of the physics of interaction of the modules could be checked by this type of experiment. For instance, the change of the coupling between the modules with coolant loss or fissile isotope buildup in the blanket could be measured readily.

EQUIVALENCE TO FUEL-IRRADIATION FACILITIES

Some proposed fast reactor fuel-irradiation facilities are, in a sense, zone-loaded reactors. They frequently employ a central region containing fuel elements whose irradiation characteristics are to be learned, a buffer region to shape power distribution or neutron-energy spectrum, and a driver fuel chosen largely for its power density, burnup, and fabrication characteristics. Thus techniques learned during zone-loaded critical-assembly design can be useful to designers of fuel-irradiation facilities.

Limitations of Zone-Loading Procedures

A not unimportant difficulty of the zone-loading procedure as compared to the single-zone procedure is that the physicist must be more careful about the design and interpretation of some experiments. For example, the removal of sodium from a large portion of the central zone is an experimental variation that must be attempted only with caution. For such an experiment the best choice of buffer-zone composition becomes a matter of concern. For certain regions, transport-theory calculations may predict spectrum distributions significantly different from those predicted by diffusion-theory calculations. Greater care must be taken in the procedure for collapsing multigroup cross sections from ultrafine data because the spectrum over some of the groups may change considerably within short distances. However, awareness of these difficulties should assure satisfactory interpretation of zone-loaded experiments.

ESTIMATING REACTIVITY CHANGES

Another difficulty arises in trying to predict from the result of a reactivity measurement in a zone-loaded reactor the result that the same measurement would have yielded if it had been made in the full reactor that the center zone of the zone-loaded reactor represents. A simple example of this difficulty is found when a reactivity measurement is to be made at the center of the zone loading and when a perfect match of real and adjoint neutron-energy spectra with the corresponding spectra in the single-zone reactor has been achieved over the region of the reactor affected by the perturbation. A satisfactory approximation to this condition is achieved relatively easily with careful design of the zone loading.

If this measurement were to be interpreted by means of first-order perturbation theory, the expression for the perturbation of k would be

$$\frac{\Delta k}{k} = \frac{\sum_{i,j} \int_{\text{reactor}} \phi_j^+ \Delta[\chi_j \nu_i \Sigma_{f_i}/k + \Sigma_{i\to j} - \Sigma_{t_i} \delta_{i,j}] \phi_i \, dVol}{\sum_{i,j} \int_{\text{reactor}} \phi_j^+ [\chi_j \nu_i \Sigma_{f_i}/k] \phi_i \, dVol} \quad (1)$$

where all terms have their usual definitions. Both integrals extend over the entire reactor, but, of course, the terms in the numerator are nonzero only over the regions in which the perturbation is made. With the assumption that the real and adjoint fluxes in the zone loading match those of the full core over the region of the perturbation, the only difficulty in relating worth measurements made at the center of the two cores lies in the calculation of the denominator terms for the two reactors. For the full core this calculation is relatively straightforward. For the zone loading, each of the zones adds several sources of uncertainty. The results of an investigation of some of the more difficult calculational aspects of this problem are given in the subsection entitled "A Test of the Zone-Loading Method."

ESTIMATING CRITICAL MASS

The critical mass of a large fast power breeder cannot be directly determined by a zone-loading experiment. However, this is not necessarily a severe limitation. Many large power breeders will employ several zones of different enrichments to provide power flattening. Small changes in the location of the interfaces between the zones will result in criticality of the actual reactor. Many important indirect questions (e.g., material worth and detailed neutron-energy spectra at the core center and near the axial blanket) used to check the ability to calculate critical mass can be answered very well by a zone loading. Again, recent cross-section measurements and refinements in multigroup cross-section preparation procedures have improved the ability to estimate critical mass. Whereas errors in predicting critical mass were 30 to 40% for difficult cases a year or two ago, errors larger than 10% may be expected to be relatively unusual in the near future. The problem of predicting the critical mass of a large reactor by zone-loading procedures has been treated with some success recently in France.[10]

Safety Aspects of Zone-Loaded Critical Experiments

It would be thoroughly misleading to pretend that the issue of safety of zone-loaded critical experiments, even relative to that of full-core loaded reactors, can be adequately treated in a few sentences. The statements made here are intended only to point out important aspects of a complex problem.

A full-core (nonzone loaded) loading on a zero-power critical reactor can require from several hundred to several thousand kilograms of highly toxic plutonium fuel. If, in spite of the very considerable precautions taken in the design and operation of these reactors, a severe accident were to occur (definitely a highly improbable event), the containment of the reactor might be ruptured and very dangerous materials dispersed for several miles downwind. For this reason, operators of fast reactor critical experiments give much attention to safety.

An obvious aspect of the relative safety of the two types of experiments is that the zone-loaded reactor would contain 50 to 200 kg of ^{239}Pu in the central zone, approximately one-tenth as much as the full-core reactor mockup. The driver region of the zone-loaded core usually would be fueled with 200 to 300 kg of the far less toxic ^{235}U.

SHUTDOWN MECHANISMS

An important prompt shutdown mechanism of the critical assembly comes from the Doppler effect. This is achieved if the fertile ^{238}U is mixed with the ^{239}Pu in a ratio of about 3 : 1 when the fuel plates or rods are fabricated and if the assembly is composed of such other materials that the real and adjoint neutron-energy spectrum in the kiloelectron-volt region is sufficiently large. This second requirement may not be satisfied. It is especially difficult to provide an adequately soft spectrum in the driver region of a zone-loaded assembly. Furthermore, the driver fuel of older reactors may consist of ^{235}U separated from the ^{238}U. Under these conditions the ^{235}U will undergo many more fissions than the ^{238}U and therefore will heat more rapidly during an incident. Any Doppler effect in a driver of this type might add to the reactivity rather than subtract from it because of the generally positive nature of the ^{235}U Doppler effect.

Separated driver fuel, however, has better reactivity-loss characteristics through expansion on heating than does mixed driver fuel.

A Test of the Zone-Loading Method

How well can reactor analysts use data from a zone-loaded reactor experiment to predict the results for the same measurements in the full nonzoned core? We were recently given the opportunity, and challenge, to make such an analytical study and prediction. Although the success of the analytical prediction made for our test experiment does not assure the credibility of all analyses of zone-loading experiments, the study demonstrates that successful predictions of the properties of large fast breeder reactors can be based on zone-loaded experiments.

We were asked to analyze zone-loaded Assembly 4Z (in ZPR-VI) and to predict the results of the more crucial subsequent experiments on Assembly 5, a single-zone 2600-liter core of the same composition as the zone-loaded core. The assignment was resolved into several parts. One study was that of the deviation from the "correct" answer which results from the simplifying assumptions an analyst frequently makes in the course of his work. Examples of these approximations are the use of diffusion theory vs. transport theory and the use of one-dimensional calculations vs. the much more costly multidimensional calculations. A second study concentrated on the difficulties of evaluating the denominator terms of Eq. 1. Because of the nature of the construction of Assembly 4Z, it was evident that the accuracy of any prediction of Doppler, sodium-void, or other worth measurement would be sensitive to how well this term was calculated. The third objective was to predict the critical mass of Assembly 5. Much of the detail and physics of these studies has been published.[13] Only a summary of the results is given here.

A number of interesting results were obtained from the first study. It was shown that transport theory predicted very different behavior of the neutron flux, in certain energy intervals, near the edge of the central zone and through the filter and driver regions. The ^{238}U fission activity was significantly different, so that, if Assembly 4Z had been a fuel-irradiation facility, diffusion theory would have rather poorly predicted the power density due to ^{238}U fission. Other results showed cancellations of detail effects in Assembly 4Z, in some cases, which would help generate false confidence in the predictions of simpler methods.

In the important area of predicting analytically the worths of measurements of reactivity made at the center of the full core from those at the center of the zoned Assembly 4Z, it was predicted that the ratio of these worth measurements would be a constant and that the value of this constant would be 1.003. (Heterogeneity effects in the driver were not accounted for in the prediction because of the complexity of the geometry used.)

It was also predicted that the critical mass of the core of Assembly 5 would be 1664 kg of ^{235}U, with an uncertainty of ±150 kg mainly due to uncertainties in the cross sections used in the calculations.

These predictions were tested when Assembly 5 was built. It was found that the weighted average of the ratios of the reactivity worths of a large number of materials measured in the two assemblies was 1.003 ± 0.002, against the predicted value of 1.003. This agreement must be considered partly fortuitous. The experimental critical mass, corrected for edge effects, was close to 1580 kg of ^{235}U, 84 kg less than predicted but well within the estimated uncertainty of the calculation.

VIOLENT DISASSEMBLY

The most improbable but also the most severe accidents are those for which all other accident-termination mechanisms have failed and the accident is shut down by violent disassembly. The acceleration of material is caused by gradients in the hydraulic pressure generated by heating of reactor material, especially the fuel, which may melt or vaporize. The local pressure in a region is usually proportional to the power density there.

If a nonzoned large reactor is mocked up on the facility at the time of the accident, it may be the type that employs several regional fuel enrichments to obtain a flattened (economically desirable) power distribution. The flattened power distribution, however, leads to very small pressure gradients in a severe accident. Thus disassembly and shutdown of nuclear multiplication processes would be achieved only after large amounts of nuclear energy had been released.

A safety aspect of common zone-loading designs of the form represented by Fig. 1 is that they frequently are constructed, for practical reasons, with power densities in the driver zones which are from 1.5 to 3 times larger than those of the central zone. Thus, during a severe nuclear incident, very large pressures would occur, most probably, in the driver zone well before they would occur at other locations. Also, there usually is a large gradient in power density across the driver in the direction away from the reactor center, a very desirable safety characteristic. We have studied the neutronic and hydrodynamic behavior of several zone-loaded fast reactor experiments for severe accident conditions. The accident code Ax-1 (Ref. 11) and a more recent ANL code, PREAX,[12] able to handle meltdown histories as well as severe accidents were used. The calculations show that initial high pressures in the driver region begin to drive the inner boundary of the driver toward the center of the core (a reactivity-adding mechanism) and at the same time to drive most of the remainder of the driver outward (a reactivity-losing mechanism). A very short interval of time over which the reactor gains a very small amount of reactivity was seen, followed by a relatively rapid shutdown.

Because of the high power density of the driver, disassembly pressures in the driver region began early in the history of severe accidents calculated for zone-loaded reactors. Since small displacements of the driver produced rapid reactivity loss, nuclear-

energy release for accidents in zone-loaded reactors tended to be smaller than for comparable accidents in critical assemblies mounted with the equivalent full-core loadings.

Broad generalizations of this type, of course, must not be used to conclude that all zone-loaded experiments are inherently safe. This problem deserves much more careful attention than it has received.

Improvements Needed

Limited inventories of nuclear materials, especially isotopes of plutonium, make zone-loaded experiments the only available experimental means for many laboratories to study large fast power-breeder reactors. For others, the technique is an exceptionally useful research procedure. For these reasons, it is important to continue to extend the understanding and capabilities of the procedure.

Some rather basic practical questions have not yet been adequately resolved. An example is the question of what minimal amount of plutonium fuel, containing a varied enrichment of higher isotopes, should be purchased to study satisfactorily the physics of large power breeders having this fuel composition.

BETTER CROSS SECTIONS

Particularly needed for successful analysis of zone-loaded assemblies is an analytical tool which would produce spatially dependent multigroup cross sections from ultrafine cross sections and which would take into account the flux-perturbing presence of materials in adjacent regions. One such procedure is being developed by D. Meneghetti, A. Rago, and K. Phillips at Argonne.

HETEROGENEITY CORRECTIONS

The coarse plate structures used as mockup materials on zero-power critical experiments approximate only roughly the structures of power reactors, and they create a problem that has been recognized for some years. A satisfactory correction is especially needed for zone-loaded cores because driver regions are relatively thin and because they often include materials highly transparent to neutrons.

EXTENSIONS AND TESTS

There is a serious need to examine ways in which the zone-loading technique might be extended for even greater usefulness. There is also a need to identify clearly those cases in which zone-loading methods could lead to misinterpreted results. Finally, there is a need to specify a set of experiments that would most clearly test analytical procedures.

Further development of the zone-loaded reactor concept as an experimental research tool is important to fast breeder-reactor development and is also an intriguingly complex problem for the analyst.

References

1. G. J. Fischer et al., Doppler Effect Measurements in Plutonium-Fueled Fast Power Breeder Spectra, *Nucl. Sci. Eng.*, 25: 37-46 (1966).
2. E. F. Bennett, R. Gold, and R. J. Huber, Spectrum Measurements in a Large Plutonium-Fueled Fast Reactor, in Proceedings of the International Conference on Fast Critical Experiments and Their Analysis, October 10–13, 1966, USAEC Report ANL-7320, Argonne National Laboratory (to be published).
3. J. Gasidlo and P. Amundson, Reactor Development Program Progress Report, January 1965, USAEC Report ANL-7003, Argonne National Laboratory, Feb. 18, 1965.
4. R. A. Karam et al., Measured Physics Parameters in a Zoned Fast Uranium Carbide Core, Assembly 4Z, USAEC Report ANL-7281, Argonne National Laboratory, January 1967.
5. G. J. Fischer et al., Doppler Coefficient Measurements for U-238 in Fast Reactor Spectra, *Nucl. Sci. Eng.*, 18: 290 (1964).
6. C. E. Till, R. A. Lewis, and R. N. Hwang, Recent Doppler Effect Measurements in ZPR-6 and -9 and Comparisons with Theory, in Proceedings of the International Conference on Fast Critical Experiments and Their Analysis, October 10–13, 1966, USAEC Report ANL-7320, Argonne National Laboratory (to be published).
7. S. G. Carpenter et al., Dependence of the Doppler Coefficient of Reactivity for Heavy Elements on Chemical Form, Surface-to-Mass Ratio and Neutron Spectrum, in Proceedings of the International Conference on Fast Critical Experiments and Their Analysis, October 10–13, 1966, USAEC Report ANL-7320, Argonne National Laboratory (to be published).
8. G. S. Brunson et al., A Survey of Prompt Neutron Lifetimes in Fast Critical Systems, USAEC Report ANL-6681, Argonne National Laboratory, August 1963.
9. R. Avery et al., Coupled Fast-Thermal Critical Experiment, in *Proceedings of the Second United Nations International Conference on the Peaceful Uses of Atomic Energy, Geneva, 1958*, Vol. 12, p. 151, United Nations, New York, 1958.
10. F. Storrer and J. M. Chaumont, The Application of Space-Energy Synthesis to the Interpretation of Fast Multizone Critical Experiments, in Proceedings of the International Conference on Fast Critical Experiments and Their Analysis, October 10–13, 1966, USAEC Report ANL-7320, Argonne National Laboratory (to be published).
11. D. Okrent et al., Ax-1, A Computing Program for Coupled Neutronics–Hydrodynamics Calculations on the IBM-704, USAEC Report ANL-5977, Argonne National Laboratory, May 1959.
12. G. J. Fischer, D. A. Meneley, and L. Volodka, Argonne National Laboratory, personal communication, May 1966.
13. G. J. Fischer and A. Travelli, Zone Loading Studies, in Proceedings of the International Conference on Fast Critical Experiments and Their Analysis, October 10–13, 1966, USAEC Report ANL-7320, Argonne National Laboratory (to be published).

Let's Apply Optimal Control Theory and Nonlinear Analysis

By Ronald R. Mohler, University of New Mexico

Reactor-control problems traditionally have been solved—or at least satisfied—by trial-and-error techniques with digital- and analog-computer simulations based on classical linear-systems theory. With the aid of recently developed ["modern"] systems theory, i.e., optimal control and nonlinear stability analysis, we may achieve more precise solutions and gain the dual benefits of increased safety and economy.

Rather than the theoretical details of optimal control and nonlinear analysis, this article deals with results and their implications, constructively criticizes certain areas, and indicates some of the pitfalls into which researchers have stumbled.

Some of the easier reactor-control problems are discussed. You are most fortunate, though, if your reactor fits such cases. Tough practical problems unfortunately are the ones confronting reactor engineers. With the computations as involved as they are, it is no wonder the simplest possible problems are solved first. If the work is to be applied in everyday practice, however, systems people must dirty their sometimes sterile computations with practicality. Also, more cooperation is needed between the practical people and the theoretical people. Systems people must learn some practicality and reactor engineers must become knowledgeable in systems theory in order to break the communications barrier that often exists.

Optimal Reactor Control

The term optimum is by no means new to the practicing reactor engineer. The designer is continuously trying to optimize such things as flux distribution and fuel loading. Indeed the practicing reactor-controls engineer often arrives at an intuitive "optimum" design by eyeballing a response while tweaking a pot setting or by examining various root loci. In the selection of such an optimum controller, various indexes of performance, such as response time, overshoot, damping, bandwidth and peaking, might be considered.

The optimal control considered in this article, however, is one that results from a more precise (although not necessarily more meaningful) mathematical problem. For example, the problem might be to vary reactivity in such a manner that reactor power is increased while some performance index,

$$J = \int_{t_0}^{t_1} L \, dt$$

is held to a minimum. Here t_0 is an initial time, t_1 is a terminal time, and L is the cost, which might be a function of power, temperature, reactivity, and other state or control variables. (State variables and state-space analysis are treated for the uninitiated reader in Refs. 1 and 2.) For certain commercial reactors, L may be an economic cost in dollars per hour of operation. In general, such problems have not been studied. The physical system further implies certain constraints on the allowable optimal control.

Optimal control problems have been solved by the maximum principle,[3,4] dynamic programming,[5–7] and extensions of the classical calculus of variations.[5,7] The reader is referred to the indicated textbooks for excellent treatments of the theory along with examples.

Minimal-time control of nuclear reactors probably has been analyzed in more detail than any other optimal reactor-control problem.[8–11] Time-optimal control is a maximum allowable effort type of process (in the simplest form, a bang-bang control). Roughly this means that, to increase power level in minimum time, reactivity is added as rapidly as possible until some maximum allowable limit is reached—the whole process within values that guarantee safe operation. Since the control is not inertialess, reactivity must be decreased at some predetermined time so that the re-

quired reactivity is attained at the desired terminal power level. Further, precursor levels have not yet reached equilibrium, and the required terminal reactivity is time variant so as to maintain a constant power level.

All this looks good on paper, but it does not work in practice. First, the model used to describe the system and used to arrive at the optimal process is always erroneous. Second, the required terminal control requires a precise measurement–estimation of precursor levels. Fortunately there are various approximations to the time-optimal process which may be synthesized in practical ways. For example, when the appropriate time (or reactor power) is reached, a fast-correcting closed-loop process can be utilized to control the desired terminal value. Such a closed-loop process can itself be designed optimally with a cost that is a quadratic function of power error and control. Another effective technique utilizes a dither (multiple bang-bang) process with certain control rods jittering about their theoretically required positions. The switching is determined by a small allowable dead zone in reactor power.[8]

STATE-SPACE CONSTRAINTS AND PRACTICAL SUBOPTIMAL CONTROL

Complications in the optimal process also result from certain constraints in such state variables as power level (possibly reactor period) and temperature. Although the computation of optimal processes with state-variable constraints is complicated by the presence of more Lagrange multipliers, it can be carried through with computers (as discussed in Refs. 8 and 12). Again the exact process is not too practical because of a lack of knowledge of the precise system dynamics and state. As would be expected, approximations can be used to synthesize a near optimal or suboptimal control system for the entire portion of the trajectory. A fast-acting closed-loop control can be utilized. Also, state-variable constraints and control constraints can be handled by the proper power-demand limits (and any other control-loop inputs) as well as by the physical limits imposed on control variables (e.g., rod-position demand limited). Another way to manage these constraints is to optimize the loop design with a performance index that implicitly includes constraints (e.g., as a certain quadratic performance index). For the nuclear rocket engine, a simple suboptimal control synthesized by cut-and-try methods with the aid of a computer simulation gives nearly optimal performance.[8,12] A more exact optimal design is obtained in Ref. 13 by optimizing the closed-loop control with respect to a quadratic performance index. In any event the optimization analysis provides a yardstick and paves the way even if more classic control is desired. Further, the closed-loop optimization analysis indicates that all state variables should generally be used in the synthesis.

Another approach to the approximately time-optimal closed-loop control problem is presented in Ref. 14. This technique utilizes the Hamilton–Jacobi equation. Time-optimal reactor control is also utilized as the optimal control of a nuclear rocket engine if propellant consumption is minimized.[12] For such a system, specific impulse (propellant temperature) is increased to its rated value as fast as possible while propellant flow is kept as low as allowable. Near the terminal temperature, flow is increased rapidly to the level for design thrust. Many constraints such as those due to core support thermal stresses and turbopump performance (stall and cavitation) must be considered. Also, it is readily seen that a maximum allowable effort control is a candidate for the optimal reactor process as long as the cost function L is, at most, linear in the control.

The practicing engineer might suggest that the above controls could have been synthesized by physical arguments. Indeed, intuitive arguments were used to arrive at a practical suboptimal bang-bang reactivity process discussed in Ref. 15. Current optimal control theory puts this type of work on a firmer foundation and leads to a more thorough understanding of the optimal process.

Above all, it should be realized that the engineer cannot drop his physical reasoning and classical control theory to rely on mathematics alone to generate optimal solutions. All are necessary design ingredients.

QUADRATIC PERFORMANCE INDEXES

Zero-power reactor control that minimizes a quadratic performance index involving reactivity and power for some desired trajectory is analyzed by dynamic programming in Refs. 16 and 17. The optimal control is found by making a nonlinear transformation of the neutron kinetics to a linear system discussed in Ref. 16. Shen and Haag[16] applied dynamic programming to find a fairly complicated control process. A quadratic performance index involving a variation from a desired neutron level and from a desired rate of change of neutron level has been investigated;[17] the analysis utilizes the maximum principle to arrive at a fairly complicated optimal control. As in Ref. 16, the optimal feedback control involves time-variant gains (hyperbolic functions). Such solutions, although optimal with respect to a quadratic performance index, would be suboptimal relative to a minimal-time trajectory.

Optimal control of a two-energy group neutronic model has been analyzed in Ref. 18. Here it is suggested that the optimal control really involves spatial variations, as well as time variations, in reactivity. This presents a host of challenging design problems.

XENON POISON AND SINGULAR SOLUTIONS

Reactor shutdown to minimize xenon peak production has been analyzed by dynamic programming[19,20] and the maximum principle.[21] Power pulsing (a bang-bang process) was shown to produce the optimal shut-

down. Roberts and Smith[22] considered minimal-time reactor shutdown with xenon concentration constrained by some maximum allowable value. For such a process the optimal power variation usually includes a single power pulse but is complicated by a continuous power variation to maintain the maximum allowable xenon concentration if such a value is reached. Also, a singular solution — a state trajectory that causes the switching function to be zero — can be part of the optimal trajectory. In other words the ideal optimal power usually would be zero until the xenon constraint value is reached, and then power is varied to maintain constant maximum allowable xenon until a certain minimal-time full-power trajectory is intercepted. The latter trajectory is optimal until the zero-power trajectory tangent to the maximum xenon line (in xenon–iodine state space) is reached. This new portion is then optimal to the terminal end (no poison). If the initial poison buildup is small, the required shutdown is merely zero power to the end. Both cases assume the singular condition is never reached. If the singular condition arises, it replaces a portion of the above trajectories.

Singular solutions were analyzed in Ref. 8 but were not time optimal for such problems. In most studies, however, singular solutions have been neglected. Such neglect can lead to erroneous answers, as in the case of xenon-poison consideration for shutdown.

Nonlinear Analysis

Neutron kinetics ordinarily are defined by a bilinear system of ordinary differential equations. In other words the system includes a $\rho(t)n(t)$ term and is linear in state and input (reactivity ρ) but not jointly linear in both. If reactivity is a time function, the system is linear and time variant. Generally, however, reactivity is a function of neutron level (via temperature coefficients and control), and the system is nonlinear.

Although heat-exchange processes are nonlinear, distributed, and often time variant, it is almost always assumed in the papers discussed below that the feedback systems are lumped, linear, and time invariant. Such assumptions are not always valid, but still the results can be useful if one realizes the conditions.

In the following papers, classical topological techniques[23] are sometimes utilized, but most of the recent work leans heavily on Liapunov's second (or direct) method.[24] Although the second method is most powerful, it yields only sufficient conditions that frequently give conservative estimates of stability. The technique involves generation of a particular type of function called a Liapunov function. Fortunately some techniques have been devised to bypass the trial and error involved in the generation of Liapunov functions.

Normally it is required that the reactor be stable — at least to the desired terminal state. Over certain portions of optimal trajectories, however, divergent modes might be acceptable. Such is the case for minimal-time startups. Only the most recent work with which I am acquainted is presented here. But first it should be noted that significant spadework appeared earlier by Welton, Weinberg, Ergen, Smets, Gyftopoulos, Popov, Akcasu, and DeVooght,[25–33] to mention a few.

Two recent papers[34,35] show that reactor stability without delayed neutrons does not always imply stability with delayed neutrons. Although delayed neutrons usually have a stabilizing effect, reactor engineers should be aware of a destabilizing possibility. Furthermore, Smets[34] shows that, if reactor-feedback elements exhibit a phase-lag frequency response, delayed neutrons are stabilizing.

Because the second method of Liapunov yields sufficient but not necessary conditions, the conclusions are often so conservative as to have little practical value. This is the case despite the fact that researchers continuously are reporting the latest, most nonrestrictive criteria such as have been claimed justly in Refs. 35 and 36. Also, Schultz[37] has shown that Lure's method yields smaller stability regions for reactors (and is thus less useful) than does the variable-gradient method.[38] The second method does allow a start for detailed computer studies in the selection of certain control-system parameters.

A useful detailed comparison of the Lure–Welton criterion,[31,33] Popov's criterion,[39] Aizerman's method,[33,40] Rosen's method,[41] a topological scheme, and a direct application of Liapunov's second method is presented in Ref. 42. Although a combination of techniques should usually be considered in practice, for the typical case shown in Ref. 42, a Liapunov function can be found directly that ensures stability over a significantly larger region of operation than do the other methods.

In some cases, analyses have been too specific; erroneous conclusions have resulted. For example, the conclusions reached in Ref. 34 indicate that stability for small perturbations without delayed neutrons does not imply stability for small variations with delayed neutrons as previously indicated.[32] Also, it has been shown in Ref. 30 that results reached in Ref. 26 are erroneous. That is, a reactor can even be asymptotically stable without delayed neutrons and unstable with delayed neutrons.

Another interesting conclusion is formulated by Lellouche[43]: for systems with more than one reactivity coefficient and with a prompt negative coefficient, a delayed positive coefficient is more stabilizing than a delayed negative coefficient. Also, Akcasu and Noble[44] show that, if a prompt negative reactivity exists, the reactor is stable if total reactivity-feedback transfer function (with respect to neutron level) has no positive real zeros and if the time integration of the nonprompt feedback-impulse response is negative for all positive time.

Chernick[45] and Shotkin[46] have made worthy contributions to nonlinear reactor theory for some time. In fact, Chernick[47] was probably one of the first to indicate that delayed neutrons do not always provide

damping. In a more recent paper, Garabedian and Lynch[48] analyze a two-energy-group multiregion neutron-kinetics model. Also, stability of coupled-core reactors (which might be economically feasible for nuclear rocket propulsion) with delay times is analyzed by Liapunov's second method in Ref. 49. Such coupled systems seem to want to work together.

Conclusions

Classical assumptions that are usually made (sometimes erroneously) include one or more of the following: zero-power reactor model, prompt-neutron kinetics, single-precursor model, linear time-invariant heat exchange, infinitely fast actuators, constant inputs, and point (space) dynamics. In the optimal control papers, singular solutions have been neglected in most cases. Also, optimality is usually assumed when only extremal solutions have been derived. These assumptions are sometimes valid, but in most cases many of them are invalid.

Undoubtedly, trial-and-error techniques with digital- and analog-computer simulations and classical linear-systems theory will continue to be useful with increasing help from modern techniques. Although we cannot hope to find analytical solutions to most practical reactor-control problems, intuitive arguments would often bridge the gap between theory and practice. This has been especially useful in showing that extremal solutions are sometimes indeed optimal.[8]

Because of the urgency involved, many studies of modern reactor-control theory have involved aerospace or military applications. On the other hand, it should be realized that the same sort of analysis is feasible for commercial reactor systems. For example, minimal-time control and xenon-poison considerations are significant for commercial reactors if maximum operational time for a given cost is of interest. Similarly, it is important to understand the effect of certain design parameters on stability of the nonlinear reactor, for safety reasons if nothing else. Undoubtedly there is a need for studies of cost effectiveness and optimization on commercial reactors and nonlinear dynamical analyses of more realistic commercial reactor models.

* * *

The author is grateful to the Sandia Corporation for support of research in this area. Also, some of the ideas presented here are based on the author's previous work at the Los Alamos Scientific Laboratory.

References

1. L. A. Zadeh and C. A. Desoer, *Linear System Theory*, McGraw-Hill Book Company, Inc., New York, 1963.
2. P. M. DeRusso et al., *State Variables for Engineers*, John Wiley & Sons, Inc., New York, 1965.
3. M. Athans and P. Falb, *Optimal Control*, McGraw-Hill Book Company, Inc., New York, 1966.
4. L. S. Pontryagin et al., *The Mathematical Theory of Optimal Processes*, Interscience Publishers, a division of John Wiley & Sons, Inc., New York, 1962.
5. S. E. Dreyfus, *Dynamic Programming and the Calculus of Variations*, Academic Press Inc., New York, 1965.
6. R. E. Bellman, *Dynamic Programming*, Princeton University Press, Princeton, N. J., 1957.
7. C. W. Merriam, *Optimization Theory and the Design of Feedback Control Systems*, McGraw-Hill Book Company, Inc., New York, 1964.
8. R. R. Mohler, Optimal Control of Nuclear Reactor Processes, USAEC Report LA-3257, Los Alamos Scientific Laboratory, March 1965.
9. R. R. Mohler, Optimal Control of Nuclear Reactor Systems, *Trans. Amer. Nucl. Soc.*, 7(1): 58-59 (June 1964).
10. I. Kliger, An Adaptive Automatic Control of a Nuclear Reactor for a Minimal Time Response, *Trans. Amer. Nucl. Soc.*, 1(1): 59-60 (June 1964).
11. I. Kliger, An Automatic Control of a Nuclear Reactor for Minimal Time Control, in Proceedings of the Third International Federation of Automatic Control Congress, London, 1966.
12. R. R. Mohler, Optimal Nuclear Rocket Engine Control, in *Neutron Dynamics and Control*, AEC Symposium Series, No. 7 (CONF-650413), Tucson, Ariz., May 1966.
13. P. A. Secker, and L. E. Weaver, Synthesis of Optimal Feedback Control for Nuclear-Rocket-Engine Start-Up, in *Neutron Dynamics and Control*, AEC Symposium Series, No. 7 (CONF-650413), Tucson, Ariz., May 1966.
14. J. L. Melsa, A Closed-Loop Approximately Time-Optimal Control Method, in *Neutron Dynamics and Control*, AEC Symposium Series, No. 7 (CONF-650413), Tucson, Ariz., May 1966.
15. T. P. Mulcahey, Time-Optimum Control of Nuclear Reactors with Velocity-Limited Control Devices, in *Reactor Kinetics and Control*, AEC Symposium Series, No. 2 (TID-7662, pp. 278-298), Tucson, Ariz., April 1964. Also, T. P. Mulcahey, Time-Optimum Control of Nuclear Reactors with Velocity-Limited Control Devices, USAEC Report ANL-6695, Argonne National Laboratory, October 1963.
16. C. N. Shen and F. G. Haag, Application of Optimum Control to Nuclear Reactor Startup, *IEEE (Inst. Elec. Electron. Eng.), Trans. Nucl. Sci.*, NS-11(2): 1-9 (April 1964).
17. I. Kliger, Synthesis of an Optimal Nuclear Reactor Control System, in *Neutron Dynamics and Control*, AEC Symposium Series, No. 7 (CONF-650413), Tucson, Ariz., May 1966.
18. C. N. Shen and T. C. Liu, The Control of Absorption Cross Section for a Nuclear Rocket, in *Neutron Dynamics and Control*, AEC Symposium Series, No. 7 (CONF-650413), Tucson, Ariz., May 1966.
19. M. Ash, R. Bellman, and R. Kalaba, On Control of Reactor Shut-Down Involving Minimal Xenon Poisoning, *Nucl. Sci. Eng.*, 6(2): 152-156 (August 1959).
20. M. Ash, *Optimal Shutdown Control of Nuclear Reactors*, Academic Press Inc., New York, 1966.
21. Z. R. Rosztoczy and L. E. Weaver, Optimal Reactor Shutdown Program for Minimum Xenon Buildup, *Nucl. Sci. Eng.*, 20(3): 318-323 (November 1964).
22. J. J. Roberts and H. P. Smith, Equivalence of the Time Optimal and Minimax Solutions to the Xenon Shutdown Problem, *Nucl. Sci. Eng.*, 23(4): 397-399 (December 1965).
23. W. J. Cunningham, *Nonlinear Analysis*, McGraw-Hill Book Company, Inc., New York, 1958.
24. J. LaSalle and S. Lefschetz, *Stability by Liapunov's Direct Method*, Academic Press Inc., New York, 1961.
25. W. K. Ergen and A. M. Weinberg, Some Aspects of Nonlinear Reactor Dynamics, *Physica*, 20: 413-426 (1954).
26. V. M. Popov, Notes on the Inherent Stability of Nuclear Reactors, in *Proceedings of the Second International Conference on the Peaceful Uses of Atomic Energy, Geneva, 1958*, Vol. 11, pp. 245-250, United Nations, New York, 1958.

27. W. K. Ergen, H. J. Lipkin, and J. A. Nohel, Application of Liapunov's Second Method to Reactor Dynamics, *J. Math. Phys.*, 36: 36-48 (1957).
28. H. B. Smets and E. P. Gyftopoulos, The Application of Topological Methods to the Kinetics of Homogeneous Reactors, *Nucl. Sci. Eng.*, 6(4): 341-349 (October 1959).
29. E. P. Gyftopoulos and J. DeVooght, Boundedness and Stability in Nonlinear Reactor Dynamics, *Nucl. Sci. Eng.*, 7(6): 533-540 (June 1960).
30. A. Z. Akcasu and A. Dalfes, A Study of Nonlinear Dynamics, *Nucl. Sci. Eng.*, 8(2): 89-94 (August 1960).
31. T. A. Welton, Kinetics of Stationary Reactor Systems, in *Proceedings of the International Conference on the Peaceful Uses of Atomic Energy, Geneva, 1955*, Vol. 5, pp. 377-389, United Nations, New York, 1956.
32. E. P. Gyftopoulos, Application of Geometric Theory to Nonlinear Reactor Dynamics, *Nucl. Sci. Eng.*, 10(3): 254-268 (July 1961).
33. H. B. Smets, *Problems in Nuclear Power Reactor Dynamics*, Presses Universitaires de Bruxelles, Brussels, Belgium, 1962.
34. H. B. Smets, On the Effect of Delayed Neutrons in Reactor Dynamics, *Nucl. Sci. Eng.*, 25(3): 236-241 (July 1966).
35. W. Baran and K. Meyer, Effect of Delayed Neutrons on the Stability of a Nuclear Power Reactor, *Nucl. Sci. Eng.*, 24(4): 356-361 (April 1966).
36. E. P. Gyftopoulos, Some Applications of Mathematical Methods to Nuclear Engineering at the Massachusetts Institute of Technology, in *Neutron Dynamics and Control*, AEC Symposium Series, No. 7 (CONF-650413), Tucson, Ariz., May 1966.
37. D. G. Schultz, Semiannual Status Report No. 1 on Research in and Application of Modern Automatic Control Theory to Nuclear Rocket Dynamics and Control, University of Arizona, 1964.
38. D. G. Schultz and J. E. Gibson, The Variable Gradient Method for Generating Liapunov Functions, *Trans. Amer. Inst. Elec. Engrs.*, 81(Pt. II): 203-210 (1962).
39. V. M. Popov, Absolute Stability of Nonlinear Systems of Automatic Control, *Automat. Remote Contr. (Engl. Trans.)*, 22(8): 857 (1962).
40. M. A. Aizerman and F. R. Gantmacher, *Absolute Stability of Regulator Systems*, Holden-Day, Inc., San Francisco, 1964.
41. J. B. Rosen, Stability and Bounds for Nonlinear Systems of Difference and Differential Equations, *J. Math. Anal. Appl.*, 2: 370-393 (1961).
42. J. DeVooght and H. B. Smets, Determination of Stability Domains in Reactor Dynamics, presented at EAES Meeting on Reactor Theory, Karlsruhe, June 1966 (to be published).
43. G. S. Lellouche, Reactor Kinetics Stability Criteria, *Nucl. Sci. Eng.*, 24(1): 72-76 (January 1966).
44. A. Z. Akcasu and L. D. Noble, Lagrange Stability in Reactors with Linear Feedback, *Nucl. Sci. Eng.*, 25(4): 427-429 (August 1966).
45. J. Chernick, Evolution of the Finite-Escape-Time Concept in Reactor Kinetics, in *Neutron Dynamics and Control*, AEC Symposium Series, No. 7 (CONF-650413), Tuscon, Ariz., May 1966.
46. L. M. Shotkin, Centers and Limit Cycles in Reactor Kinetics, in *Neutron Dynamics and Control*, AEC Symposium Series, No. 7 (CONF-650413), Tucson, Ariz., May 1966.
47. J. Chernick, A Review of Nonlinear Reactor Dynamics Problems, USAEC Report BNL-774, Brookhaven National Laboratory, July 1962.
48. H. L. Garabedian and R. E. Lynch, Nonlinear Reactor Kinetics Analysis, *Nucl. Sci. Eng.*, 21(4): 550-564 (April 1965).
49. H. S. Murray and D. G. Schultz, Stability of Nonlinear Coupled-Core Reactors, in *Neutron Dynamics and Control*, AEC Symposium Series, No. 7 (CONF-650413), Tucson, Ariz., May 1966.

Improved Design Predictions Through Liquid-Metal Heat-Transfer Research

By Ralph P. Stein

One of the more frequently occurring objectives of basic research in heat transfer is to find prediction methods that will be useful for the design and analysis of systems in which there is technological interest. For convection heat transfer, the pertinent fundamentals are fairly well developed. These fundamentals include the familiar conservation laws related to mass, energy, and momentum together with relations describing their local rates of transport. Direct application of these fundamentals to specific situations usually results in complicated mathematical formulations that, for engineering purposes, would better be avoided if possible. As a result, research in this area has centered about application of these fundamentals to general situations so as to discover prediction methods that will be more convenient for engineering use.

To use a deceptively simple and certainly familiar example, consider the relation

$$q = h(t_s - t) \qquad (1)$$

where q is the local rate of heat flow per unit area of and from a surface at temperature t_s to a fluid with a suitably defined average temperature t. This equation defines the heat-transfer coefficient h. When h can be considered a constant, or treated as some appropriate average value, use of this equation is much simpler than the use of the mathematical formulation of fundamentals it replaces. Basic research studies discovered best definitions of t for several general classes of applications. The heat-transfer coefficient could then be considered independent of q and $(t_s - t)$ and easily related to other variables without destroying the simplicity of Eq. 1, thereby supporting its practical usefulness.

Similar potentially useful results of basic research pertaining to liquid-metal heat transfer will be reviewed here. These include improved methods for predicting surface temperatures in reactor coolant channels and heat-transfer rates in heat exchangers. They derive from applications of fundamentals to analytical investigations of liquid-metal forced-convection heat transfer.[1,2]

COEFFICIENTS FOR LIQUID METALS

With turbulent forced-convection heat transfer of nonmetallic fluids in ducts, the "heat-transfer-coefficient concept,"—namely, that it is possible and beneficial to consider q proportional to $(t_s - t)$—has proved to be both accurate and convenient in most situations of engineering interest. With liquid metals, however, the situation is more complicated because, unlike the situation with nonmetallic fluids, heat-transfer coefficients are affected significantly by the actual heat-transfer boundary conditions, such as heat-flux or temperature distributions at the duct surfaces.

Although the sensitivity of liquid-metal heat-transfer coefficients to boundary conditions is well known, satisfactory prediction methods that account for this sensitivity with engineering computations have not been firmly established. The implication of current practice is that Eq. 1 is still to be used, but with the complication that the heat-transfer coefficients must be appropriate to the specific boundary condition of the application. However, the many possible boundary conditions of interest cause much of the convenience and apparent simplicity of Eq. 1 to be lost. Further, in many cases determination of appropriate heat-transfer coefficients—for example, by application of fundamentals or experiment—is equivalent to "solving" the problem, after which application of Eq. 1 is no longer necessary. Thus basic research in liquid-metal convection heat transfer would search for prediction methods that can account for the effect of boundary conditions, as well as for other possible

effects, in more convenient forms than implied by a consistent use of Eq. 1.

HOW IMPORTANT?

How important is this type of basic research to current liquid-metal technology? In many design applications of Eq. 1 to systems involving liquid-metal heat transfer, the effects of boundary conditions on appropriate values of h are mostly ignored. This can be justified by expediency — why bother complicating a situation in which, when the entire system is considered, other aspects may be more important and cannot be accounted for accurately?

For example, because of the excellent thermal properties of liquid metals, predictions of temperatures and heat-transfer rates for most design problems in existing or proposed liquid-metal-cooled reactor systems are not greatly influenced by the accuracy with which liquid-metal heat transfer can be predicted. In typical liquid-metal-cooled reactors, because of the relatively poor thermal properties of present fuel materials, temperature differences between the surface of a coolant channel and the center of the fuel material are roughly an order of magnitude larger than temperature differences associated with convection of the coolant. Moreover, the pertinent physical properties of these fuel materials are not known very accurately. In current liquid-metal heat exchangers and liquid-metal-heated steam generators, structural and safety considerations usually result in large thermal resistance to heat transfer through the exchanger walls. As a result, inaccurate values of h for application of Eq. 1 have little effect on the overall design. Also, with steam generators, steam-side heat-transfer predictions are highly uncertain.

However, with the interest in liquid metals as industrial coolants[3] as well as working fluids in fast reactors and in space power plants, refinements in design soon may require improved accuracy in predicting liquid-metal heat transfer. How soon will depend on the future direction and interest of the related technology.

Improved Prediction Methods

Three examples of the results of basic research in liquid-metal heat transfer illustrate potentially useful design prediction methods. The first example is related to appropriate forms of Eq. 1 when applied to fuel-coolant channels idealized as annular spaces with unequal heat fluxes on opposite sides; it has its origins in a paper by Seban[4] in 1950. It was also discussed in the 1952 edition of the *Liquid Metals Handbook*[5] and reformulated in somewhat more generalized terms[6] in 1956. Even so, there are indications that communication of the results of basic research have not been effectively communicated for this particular example. This is evidenced by the contents of several recent surveys of liquid-metal heat transfer for design.

The second example suggests an extension of Eq. 1 that accounts for the effect of nonuniform axial heat-flux distributions. The third example refers to improvements in predictions of heat-transfer rates in liquid-metal-to-liquid-metal heat exchangers for which indiscriminate applications of Eq. 1 can lead to inaccurate designs.

UNIFORMLY HEATED ANNULAR SPACES

Let subscripts 1 and 2 identify quantities associated with the inner and outer walls of an annular space. Then Eq. 1 as applied to the inner wall can be written as

$$q_1 = h_1(t_{s,1} - t) \tag{2}$$

with t the bulk or heat-content mean temperature of the fluid. When q_1 and q_2 are known, the bulk temperature is computed easily by simple heat balance. But what is the proper value for the heat-transfer coefficient h_1 so that the surface temperature $t_{s,1}$ can be predicted? For liquid metals, h_1 is influenced[6] strongly by the ratio of the heat fluxes q_2/q_1. Let this ratio be represented by y, and consider the heat-transfer coefficient to be a function of y — that is, $h_1(y)$. Then Ref. 6 shows that

$$h_1(0)/h_1(y) = 1 = a_1 y \tag{3}$$

where a_1 is a positive number which depends on the Peclet and Prandtl numbers of the fluid, on the diameter ratio of the annular space, and, when the heat transfer is not "fully developed," on duct axial position also but which is independent of y. Using Eq. 3, we can rewrite Eq. 2 as

$$q_1 - a_1 q_2 = h_1(0)\ (t_{s,1} - t) \tag{4}$$

from which, with a_1 and $h_1(0)$ known, $t_{s,1}$ can be computed easily. For fully developed heat transfer, $h_1(0)$, the heat-transfer coefficient for an internally heated annulus can be obtained from existing correlations[7]; a_1 can be obtained from the detailed computations of Kays and Leung[8] over wide ranges of Peclet and Prandtl numbers and diameter ratios.[1] Alternately, a_1 can be obtained from existing correlations for fully developed heat-transfer coefficients in symmetrically heated annular spaces — that is, from $h_1(1)$ — since

$$a_1 = [h_1(1) - h_1(0)]/h_1(1) \tag{5}$$

from Eq. 3. By use of Eq. 5, another form of Eq. 4 can be written as

$$(q_1 - q_2)/h_1(0) + q_2/h_1(1) = t_{s,1} - t \tag{6}$$

which, with existing correlations for fully developed values of $h_1(0)$ and $h_2(1)$, may be the most convenient form for predicting $t_{s,1}$ for design purposes.

The appropriate form of Eq. 3 for the outer wall of the annular space is

$$h_2(0)/h_2(y) = 1 - a_2 y \tag{7}$$

where now $y = q_1/q_2$. Similar algebraic manipulation leads to

$$(q_2 - q_1)/h_2(0) + q_1/h_2(1) = t_{s,2} - t \tag{8}$$

for predicting the surface temperature of the outer wall of the annular space, $t_{s,2}$. Correlations of fully developed values for $h_2(0)$ and $h_2(1)$ are also available.[7,9] Note that Eqs. 6 and 8 give simple expressions for predicting $t_{s,1}$ when $q_1 = 0$ and for $t_{s,2}$ when $q_2 = 0$.

Relations similar to these are given in Refs. 5 and 10.

NONUNIFORM AXIAL HEAT FLUX

Equation 1—as applied to liquid-metal heat transfer with q a function of axial position l measured from the duct inlet—results in h being a function of the flux distribution and of the axial position (except for certain special cases). In fact, for simple "unchopped" cosine flux distributions, h—when defined by Eq. 1—will always be zero at the fuel-channel outlet. As a result the customary definition of h as given by Eq. 1, with t the usual bulk temperature, becomes cumbersome to use because then h must be determined in advance as a function of the flux distribution and of the axial position.

A recently suggested[1] extension of Eq. 1 avoids this difficulty but involves the use of higher ordered dimensionless thermal-resistance coefficients R_n, associated with successive derivatives of q with respect to l. The coefficients R_n are functions of Peclet (or Reynolds) and Prandtl numbers and duct shape but are independent of the flux distribution and, for sufficiently large l, are also independent of axial position. This extension of Eq. 1 for sufficiently large l can be written as

$$q + \sum_{n=1}^{\infty} R_n (d^n q/dx^n) = h(t_s - t) \tag{9}$$

where $x = l/D$ (D is the duct hydraulic equivalent diameter) and h is the fully developed heat-transfer coefficient for uniform heat-flux distribution for a circular tube, an internally or externally heated annular space, or an annular space with equal heat fluxes from both sides. Equation 9 is a dimensional form of Eq. 49 in Ref. 1. Note that when q is uniform—that is, independent of x—Eq. 9 reduces to Eq. 1.

The coefficients R_n decrease rapidly with increasing n, so that in most cases only a few terms of the infinite series need be retained. In other cases the higher order derivatives may be zero. For example, a reasonable approximation of $q(x)$ for many reactor applications is

$$q = (4q_{\max.})(D/L)^2(L/D - x)_x \tag{10}$$

where L is the fuel-coolant-channel length. Then Eq. 9 is simple to use to predict maximum fuel or channel surface temperatures because only the coefficients R_1 and R_2 are required.

For the coolant channel idealized as the space between infinitely wide parallel planes, the coefficients R_n can be computed from

$$R_n = (-1)^n \, (\mathrm{Nu}/2) \, (\mathrm{Pe}/4)^n \sum_{k=1}^{\infty} C_k/\lambda_k^{2n} \tag{11}$$

where Nu is the appropriate fully developed Nusselt number corresponding to the fully developed heat-transfer coefficient for uniform heat-flux distribution h used in Eq. 9 and Pe is the Peclet number. Representative values of C_k and λ_k^2 are given in Tables 1 and 2 as functions of Reynolds and Prandtl numbers. These values were computed from the "Fundamental Eigenvalues Problem"[1] related to liquid-metal heat transfer in heated parallel-plane ducts.[11] The computations were based on use of von Kármán's universal velocity profile with eddy diffusivities for

Table 1 VALUES OF C_k AS A FUNCTION OF REYNOLDS AND PRANDTL NUMBERS

Prandtl number	Reynolds number	C_k for Eq. 11				
		C_1	C_2	C_3	C_4	C_5
0.003	30,000	0.1798	0.0509	0.0232	0.0134	0.0086
	100,000	0.1619	0.0485	0.0219	0.0129	0.0082
	300,000	0.1280	0.0413	0.0183	0.0110	0.0070
	1,000,000	0.0802	0.0269	0.0119	0.0075	0.0049
0.01	30,000	0.1538	0.0463	0.0205	0.0117	0.0072
	100,000	0.1181	0.0388	0.0170	0.0102	0.0065
	300,000	0.0753	0.0255	0.0113	0.0072	0.0047
	1,000,000	0.0340	0.0199	0.0056	0.0038	0.0026
0.03	30,000	0.1127	0.0363	0.0149	0.0082	0.0045
	100,000	0.0694	0.0236	0.0103	0.0064	0.0040
	300,000	0.0336	0.0119	0.0055	0.0037	0.0025
	1,000,000	0.0120	0.0046	0.0023	0.0017	0.0012

Table 2 VALUES OF λ_k^2 AS A FUNCTION OF REYNOLDS AND PRANDTL NUMBERS

Prandtl number	Reynolds number	λ_k^2 for Eq. 11				
		λ_1^2	λ_2^2	λ_3^2	λ_4^2	λ_5^2
0.003	30,000	11.67	44.92	100.84	178.42	278.56
	100,000	13.16	51.24	116.08	206.54	322.96
	300,000	16.91	68.66	158.91	284.79	446.08
	1,000,000	26.63	121.16	290.52	523.80	819.36
0.01	30,000	13.87	53.84	121.96	216.96	339.36
	100,000	18.42	75.34	175.05	314.10	491.98
	300,000	28.18	129.58	311.83	562.13	879.13
	1,000,000	52.75	295.50	733.46	1320.98	2056.17
0.03	30,000	19.20	77.79	180.43	323.34	506.69
	100,000	30.38	140.43	338.16	609.74	953.43
	300,000	53.32	297.39	736.65	1327.76	2067.21
	1,000,000	116.24	785.12	1977.85	3551.05	5501.29

heat transfer taken equal to those for momentum transfer and assumed to be uniform and equal to their maximum values at the duct center. Computations by other methods will not give significantly different results, except possibly for large Peclet numbers where very accurate values of the coefficients R_n are not needed.

Reference 1 shows that, for cosine heat-flux distributions, when

$$(\pi/4)\ (\mathrm{Pe}\,D/L) \ll \lambda_1^2 \tag{12}$$

Eq. 9 reduces to the very simple form

$$q + R_1\ (dq/dx) = h(t_s - t) \tag{13}$$

Further computations[12] indicated that

$$(\pi/4)\ (\mathrm{Pe}D/L) \lesssim 0.05\lambda_1^2 \tag{14}$$

is usually sufficient to justify the use of Eq. 13. Applications of Eq. 13 to predict maximum fuel and surface temperatures for typical liquid-metal-cooled fast reactor designs revealed that neglecting the second term on the left side of Eq. 13 gave values that were less than 10°F too low. Thus, for practical design purposes, and with h taken equal to fully developed heat-transfer coefficients for uniform flux distributions, Eq. 13 will be sufficiently accurate for application to cosine heat-flux distributions when Eq. 14 is satisfied. Accurate predictions at the channel outlet, or in general with larger heat fluxes than those allowed in current designs, will require full use of Eq. 13.

Reference 1 also discusses the cosine heat-flux case when Eq. 14 is not satisfied, generalizations of Eqs. 6 and 8 for nonuniform heat-flux distributions, and cases for which the heat transfer is not fully developed. Tables 1 and 2 give the values of C_k and λ_k^2 (which were not available when Ref. 1 was written); they will be found useful for analyses of these special cases as applied to fuel-coolant channels idealized as the space between infinitely wide parallel planes.

PREDICTING RATES IN HEAT EXCHANGERS

The necessity of obtaining alternate or extended forms of Eq. 1 in the previous two examples is related to the sensitivity of liquid-metal heat-transfer coefficients — as defined by Eq. 1 — to the duct heat-flux boundary conditions. With heat exchangers, these boundary conditions depend on the operating conditions of the exchanger and, except for special limiting cases, cannot be specified in advance. The situation is further complicated with liquid metals because a significant portion of the overall heat-transfer rate occurs along the entrance regions of the exchanger where heat-transfer coefficients are very large and vary with duct axial position — i.e., along regions where the heat transfer is not fully developed. These considerations suggest that the design of liquid-metal-to-liquid-metal heat exchangers based on the traditional applications of Eq. 1, as used for the turbulent flow of nonmetallic fluids, can lead to important inaccuracies.

Current basic research on simple double-pipe heat exchangers[1,2] has shown that traditional methods of heat-exchanger design, when applied to heat transfer between liquid metals, leads to inaccurate predictions in certain operating ranges — although in other ranges inaccuracies are not too important. When these inaccuracies are serious, oversized heat exchangers result.

The practical significance of this research is seen in Tables 3 and 4, which compare predictions of concentric-tube countercurrent-flow heat-exchanger lengths (or heat-transfer areas) required for various specified overall heat-transfer rates. Heat-exchanger lengths were computed by simple applications of Eq. 1, with h assumed to be independent of axial position and equal to values corresponding to the boundary condition of uniform heat flux; these are compared with accurate predictions by a detailed analysis based on fundamentals.[1,2] The detailed analyses show that the operating conditions of the exchanger are characterized by the three dimensionless parameters H, K, and K_w, so that these parameters must be defined before the comparisons can be understood.

Table 3 ERRORS IN PREDICTING HEAT-EXCHANGER* LENGTHS

Specified efficiency	Error in predicted length, %		
	$H = 0.1$	$H = 0.5$	$H = 1.0$
0.3	202		56.9
0.4	178		39.2
0.5	167	65.0	27.3
0.6	154	55.4	16.9
0.7	143	46.0	11.4
0.8	136	36.9	8.0
0.9	122	30.9	2.6

*Countercurrent flow; $K = 0.1$, $K_w = 0.05$.

Table 4 ERRORS IN PREDICTING HEAT-EXCHANGER* LENGTHS

Specified efficiency	Errors in predicted length, %		
	$K_w = 0$	$K_w = 0.05$	$K_w = 0.1$
0.3	206		
0.4	155		
0.5	115	65	46
0.6	87	55.4	38.1
0.7	71.2	46.0	31.2
0.8	55.6	36.9	25.8
0.9	53.2	30.9	20.0

*Countercurrent flow; $K = 0.1$, $H = 0.5$.

The parameter H is the heat-capacity flow-rate ratio defined by

$$H = c_2 W_2 / c_1 W_1 \tag{15}$$

where c is the fluid specific heat, W is the mass rate of flow, and subscripts 1 and 2 refer to the tube and annulus sides of the exchanger. The parameter K is the relative thermal resistance of the fluid in the annular space and is defined as

$$K = (k_1 k_1^+ / k_2 k_2^+)(1 - R)/R \qquad (16)$$

where k is the fluid thermal conductivity, R is the diameter ratio of the annular space, and k^+ accounts for the contribution of turbulent flow to the heat transfer with satisfactory accuracy when Peclet numbers are less than 1000.[1] For the tube side of the exchanger

$$k_1 \approx 0.875 + 0.00312(\mathrm{Pe}_1)^{0.8} \qquad (17)$$

For the annulus side with R close to unity — that is, when the annular space is narrow,

$$k_2^+ \approx 0.965 + 0.00333(\mathrm{Pe}_2)^{0.8} \qquad (18)$$

The parameter K_u is the relative thermal resistance of the tube wall which, when the wall is thin, is defined by

$$K_u = (k_1 k_1^+ / k)(b/r_1) \qquad b/r_1 \ll 1 \qquad (19)$$

where k_u is the thermal conductivity of the wall material, b is the wall thickness, and r_1 is the tube radius. The computations assume R is close to unity, and thus K will be a very small number. The parameter K_w will usually be a small number also. A value of K of 0.1 and a range of values of K_u from 0 to 0.1 were chosen as reasonable representations of liquid-metal-to-liquid-metal concentric-tube exchangers with narrow annular spaces.

In Tables 3 and 4 the specified overall heat-transfer rate is shown as an "efficiency," defined as the ratio of the actual heat-transfer rate to the rate obtainable for an exchanger with infinite heat-transfer area at the same operating conditions. The length (or heat-transfer area) comparisons, shown as percent errors of the length predicted by use of Eq. 1 for three values of H, are always larger than the lengths computed by the accurate detailed analysis. The errors are extremely large for values of H of 0.1 but negligibly small for $H = 1$ with moderate to high efficiencies.

Errors in predicted lengths result from two effects: (1) the sensitivity of liquid-metal heat-transfer coefficients to heat-flux boundary conditions and (2) the high rates of heat transfer in the entrance regions of the exchanger. For the not unusual case of $H = 1$ and a sufficiently long exchanger (equivalent to a high efficiency), heat fluxes along the central regions of the exchanger become independent of axial position — so fully developed heat-transfer coefficients correspond to the boundary condition of uniform heat flux, as used when applying Eq. 1; thus errors are small. The increase in percent errors of predicted length with decreasing efficiency for the case of $H = 1$ reflects the importance of the entrance regions of the exchanger where heat fluxes are significantly higher than those in the central regions. For values of K_w significantly larger than 0.1, the wall thermal resistance begins to control the local heat-transfer rates; as a result the local heat-flux distributions and overall heat-transfer coefficient approach uniformity, so that the traditional applications of Eq. 1 become sufficiently accurate.

The computations of the detailed analysis based on fundamentals are complex and require the use of a large digital computer.[2] Simpler computational procedures are preferred for engineering applications, especially when heat-exchanger performance must be predicted over large ranges of conditions when the operation of a complete power-plant cycle is explored. Improved design and performance relations, based on extensions of the familiar effectiveness (or efficiency) vs. NTU types of equations,[13] have been suggested as part of the basic research investigations.[1,2] These extensions introduce two correction factors: η, which is the ratio of the actual fully developed overall heat-transfer coefficient to the fully developed overall heat-transfer coefficient based on uniform heat-flux boundary conditions, and ϕ, called the "effectiveness coefficient," which accounts for the high local heat-transfer rates in the entrance regions of the exchanger by multiplying the exponential terms in the usual effectiveness vs. NTU equations.

Both η and ϕ depend on H, K, and K_w, but ϕ also depends on the heat-exchanger length (or, equivalently, the heat-exchanger efficiency). However, for sufficiently large efficiencies, ϕ becomes independent of length and is called the "fully developed effectiveness coefficient." Table 5, an extension of a similar table in Ref. 2, shows typical values of these correction factors for the circular-tube countercurrent flow heat exchanger with a narrow annular space. The "fully developed effectiveness coefficient" is denoted by $\phi(\infty)$ and applies for values of the heat-exchanger

Table 5 CORRECTION FACTORS FOR THE CONCENTRIC-TUBE COUNTERCURRENT-FLOW HEAT EXCHANGER

		$K_w = 0$		$K_w = 0.05$		$K_w = 0.1$	
K	H	$\phi(\infty)$	η	$\phi(\infty)$	η	$\phi(\infty)$	η
0.01	0.1	0.6	4.74	0.8	2.39	0.8	1.851
	0.5	0.78	1.468	0.85	1.229	0.88	1.160
	0.9	0.966	1.037	0.976	1.025	0.982	1.018
	1.1	0.971	0.971	0.979	0.979	0.985	0.985
	2.0	0.85	0.851	0.881	0.890	0.91	0.916
0.05	0.1	0.63	3.50	0.8	2.18	0.82	1.767
	0.5	0.792	1.318	0.856	1.206	0.892	1.147
	0.9	0.968	1.033	0.978	1.023	0.983	1.017
	1.1	0.973	0.974	0.981	0.981	0.986	0.986
	2.0	0.86	0.863	0.888	0.898	0.914	0.922
	10.0	0.7	0.770	0.79	0.823	0.83	0.861
0.10	0.1	0.67	2.76	0.8	1.990	0.827	1.678
	0.5	0.811	1.269	0.867	1.181	0.899	1.133
	0.9	0.971	1.029	0.979	1.021	0.984	1.016
	1.1	0.975	0.977	0.982	0.983	0.986	0.987
	2.0	0.86	0.878	0.894	0.908	0.918	0.929
	10.0	0.75	0.795	0.79	0.842	0.83	0.876

efficiency larger than 0.7. The values of $\phi(\infty)$ may also apply for much smaller efficiencies, but further investigations are required to verify this possibility.[2] Most of the results shown in Tables 3 and 4 can be reproduced with satisfactory accuracy by the values of η and $\phi(\infty)$ in Table 5 and by noting that $\eta = 1$ and $\phi(\infty) = 1$ correspond to the traditional applications of Eq. 1 for heat-exchanger design as used with nonmetallic fluids in turbulent flow.

CONCLUDING REMARKS

These three examples of contributions of basic research to design are based on fundamental studies of relatively simple models. However, actual liquid-metal-cooled reactor fuel channels are not usually simple annular spaces or circular tubes — and actual heat exchangers rarely have simple double-pipe configurations. Even so, the research suggests general principles that often can be made applicable to more complex systems. For example, procedures for applying the results of basic research on simple annular spaces to fuel-element rod bundles or heat-exchanger tube-in-shell configurations have been suggested[14] and have been,[15] and continue to be, tested by experiment.

References

1. R. P. Stein, Liquid Metal Heat Transfer, in *Advances in Heat Transfer*, Vol. 3, pp. 101-174, Academic Press Inc., New York, 1966.
2. R. P. Stein, Mathematical and Practical Aspects of Heat Transfer in Double Pipe Heat Exchangers, in *Proceedings of the Third International Heat Transfer Conference*, Chicago, Ill., August 7–12, 1966, Vol. I. pp. 139-148, American Institute of Chemical Engineers, New York, 1966.
3. L. Rosenblum, Liquid Metal Technology, in Conference on New Technology, Lewis Research Center, Cleveland, Ohio, June 4–5, 1964, Report NASA-SP-5015 (CONF-640601), National Aeronautics and Space Administration, 1964.
4. R. A. Seban, Heat Transfer to a Fluid Flowing Turbulently Between Parallel Walls with Asymmetric Wall Temperatures, *Trans. ASME*, 72: 789 (1950).
5. R. N. Lyon, (Ed.), *Liquid-Metals Handbook*, 2nd ed., NAVEXOS P-733(Rev.), U. S. Atomic Energy Commission and Department of the Navy, Superintendent of Documents, U. S. Government Printing Office, Washington, June 1952.
6. R. P. Stein, The Dependence of Heat Transfer Coefficient on the Ratio of the Heat Fluxes from the Walls of Parallel Plane Channels, in Reactor Heat Transfer Conference of 1956, USAEC Report TID-7529(Pt.1)(Bk.2), November 1957.
7. O. E. Dwyer and P. S. Tu, Unilateral Heat Transfer to Liquid Metals Flowing in Annuli, *Nucl. Sci. Eng.*, 15(1): 58-68 (1963).
8. W. M. Kays and E. Y. Leung, Heat Transfer in Annular Passages — Hydrodynamically Developed Turbulent Flow with Arbitrary Prescribed Heat Flux, *Int. J. Mass Trans.*, 6(7): 537-557 (July 1963).
9. O. E. Dwyer, Heat Transfer to Liquid Metals Flowing Turbulently Between Parallel Plates, *Nucl. Sci. Eng.*, 21(1): 79-89 (1965).
10. C. F. Bonilla, Annuli and Parallel Plates, Sec. 2.1 of Chap. 2, Heat Transfer, in *Reactor Handbook*, 2nd ed., Vol. 4, *Engineering*, p. 49, S. McLain and J. H. Martens (Eds.), Interscience Publishers, New York, 1964.
11. J. M. Nichols, M. Chu, and R. N. Rice, The Fundamental Eigenvalue Problem Related to Liquid Metal Heat Transfer in Heated Ducts, AMU–ANL Summer Engineering Practice School Report, July 2, 1965.
12. J. S. Philbin, M. H. Richardson, and H. J. Weaver, Fuel Surface Temperatures in Liquid Metal Cooled Nuclear Reactors, AMU–ANL Summer Engineering Practice School Report, Sept. 3, 1965.
13. W. M. Kays and A. L. London, *Compact Heat Exchangers*, p. 11, The National Press, Palo Alto, Calif., 1955.
14. O. E. Dwyer and P. S. Tu, Analytical Study of Heat Transfer Rates for Parallel Flow of Liquid Metals Through Tube Bundles, in Chemical Engineering Progress Symposium Series, No. 30, pp. 183-193, American Institute of Chemical Engineers, New York, 1960.
15. A. J. Friedland et al., Heat Transfer to Mercury in Parallel Flow Through Bundles of Circular Rods, in *1961 International Heat Transfer Conference, International Developments in Heat Transfer*, Part 3, p. 526, American Society of Mechanical Engineers, New York, 1961.

NPD Performance Indicates Merit of On-Power Refueling

By Karl K. Brown

With enriched-uranium fuel, reactors can be designed to be refueled during plant shutdowns that coincide with annual turbine-generator overhauls. But when the fuel is natural uranium, power reactors must be refueled at least every 6 months to maintain reactivity. In Canada, where D_2O-moderated natural-uranium-fueled pressure-tube reactors[1] are favored, there is strong economic motivation to refuel while the reactor is operating at power so as to achieve high burnup and low fuel cost (Table 1). With successful on-line refueling comes the bonus of higher plant availability.

Canadian experience in refueling the 20-Mw(e) NPD plant (abridged in Ref. 2) is significant not only to their plants and to competing systems but also to related designs such as the U. S. Heavy Water Organic Cooled Reactor[3] (HWOCR) which also are to have on-line refueling. All committed Canadian nuclear power plants — the two 500-Mw(e) CANDU type units at Pickering, Ontario, scheduled for operation in 1970 and 1971, and the 250-Mw(e) CANDU-BLW, also scheduled for 1971 — will refuel at power.

On-power refueling machines are already installed in the new 200-Mw(e) CANDU reactor at Douglas Point, in the 20-Mw(e) NPD (Figs. 1 and 2), and also in a research reactor — the NRU. Operation of the NRU on-power refueling equipment began in 1957, although serious design consideration dates back to 1949. The more than 2 years of experience with on-power refueling machines on the NPD power reactor are statistically inadequate, but the prognosis is for high unit availability and low forced-outage rates. Plant unavailability resulting from refueling-machine problems at NPD amounted to only 2.44%

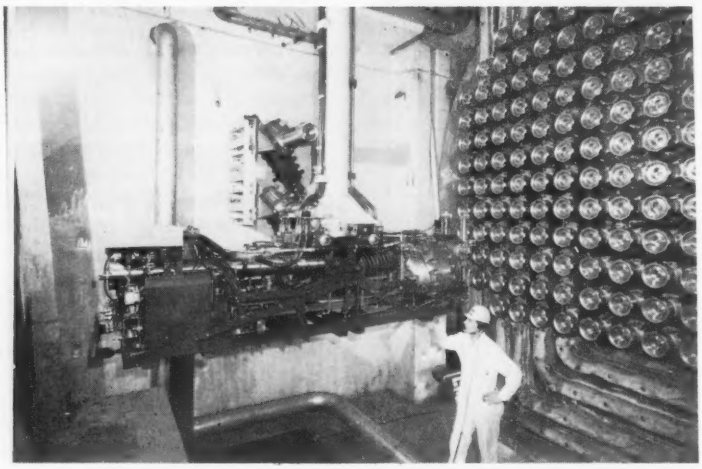

Fig. 1 NPD on-power refueling machine during commissioning in 1962.

Why Refuel at Power?

Natural uranium is an essential feature in the Canadian approach to nuclear power. In effect, they choose to enrich the moderator rather than the fuel.[4] With this choice, however, reactivity requirements commit them to refuel the reactor no less frequently than semiannually. Utility energy demands, the cost of shutdowns, and fueling costs make it desirable to refuel while the reactor continues producing power.

Table 1 shows comparative power costs for the first pair of 500-Mw(e) units in the Pickering generating station. These estimates are for conditions in Canada and are based on long-term Ontario Hydro finance criteria. Capital and operating costs of on-power refueling are included and are based on a burnup of 223 Mw-hr per kilogram of uranium, a net unit efficiency of 29.7%, and a unit fuel cost of (Canadian) $50 per kilogram of uranium. The low fuel cost of 0.75 mill/kw-hr can only be achieved with on-power refueling. In the Ontario Hydro power system, the difference in incremental operating costs between coal and nuclear generation is ~2 mills/kw-hr in favor of nuclear with on-power refueling.

Table 1 ESTIMATED POWER COST*
WITH REFUELING ON-POWER VS. OFF-POWER

Category	With on-power refueling	With off-power refueling		
		Two times per year	Three times per year	Four times per year
Capital charges	2.18	2.24	2.30	2.36
Operations and maintenance	0.42	0.43	0.44	0.45
Fuel	0.75	2.10	1.50	1.40
Total	3.35	4.77	4.24	4.21
Relative	100% (Reference)	143%	127%	126%

*Expressed as Canadian mills per kilowatt-hour and assuming 5.25% interest, 30-year life, 80% capactiy factor, and 6.69% fixed charges for the Pickering generating station with two 500-Mw(e) net units.

If off-power refueling is employed, the reactivity-limited achievable burnup raises fuel cost and, thus, power cost. For instance, with semiannual off-power refueling, which is barely possible from a reactivity point of view, burnup is only 79 Mw-hr per kilogram of uranium and the complete core change triples the fuel cost from 0.75 mill/kw-hr to 2.1 mills/kw-hr. With off-power refueling three times annually, burnup can reach 110 Mw-hr per kilogram of uranium and the fuel cost is only approximately doubled to 1.5 mills/kw-hr. Quarterly refueling, which is unacceptable owing to seasonal peak-power requirements, would increase burnup to 120 Mw-hr/kg.

It can be assumed that one off-power refueling could coincide with an annual shutdown; others would cause shutdowns. The cost of unavailability is interdependent with the cost of fuel and also depends on both design concept and hardware. For infrequent off-power refueling, each additional shutdown reduces the annual availability by ~2% —which effectively increases the energy unit cost due to capital and operation (fixed charges) by 2% for each shutdown.

Cost of the entire on-power refueling system for a large station (e.g., Pickering) is estimated at <3% of total plant capital cost. It is unlikely that the cost of off-power refueling systems would be less. In fact, to secure high reactor availability, a faster machine would be desired; so machine cost might actually increase.

during the 26-month period ending Mar. 1, 1966. As refueling-machine performance improves, fuel-scheduling experience should also improve.

NPD Refueling Concept

The NPD overall refueling system is shown in Fig. 3. After an operator loads a new fuel bundle into the machine port and the machine automatically positions it in the machine "head," the machine traverses to the reactor, clamps (leaktight) onto the proper pressure-tube end fitting (Fig. 4), removes the seal plug (Fig. 5), and sets it aside within the head. Concurrently, a discharge machine similarly clamps onto the end fitting at the other end of the reactor pressure tube and removes the seal plug there.

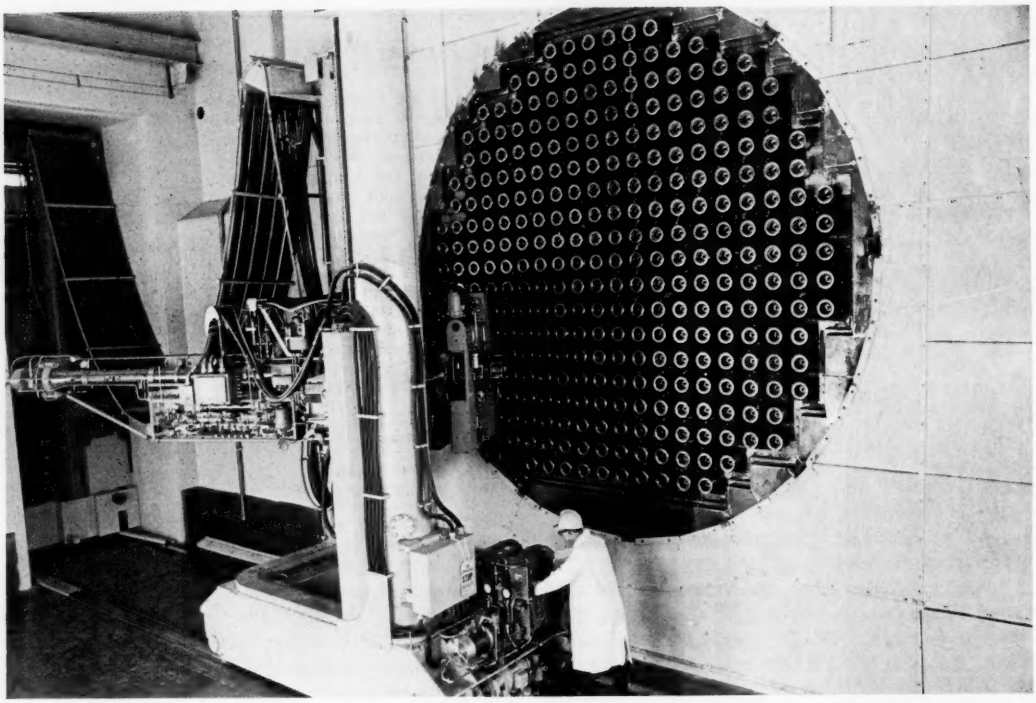

Fig. 2 Douglas Point on-power refueling machine during recent commissioning. This and later designs provide shutdown shielding between reactor and refueling machines.

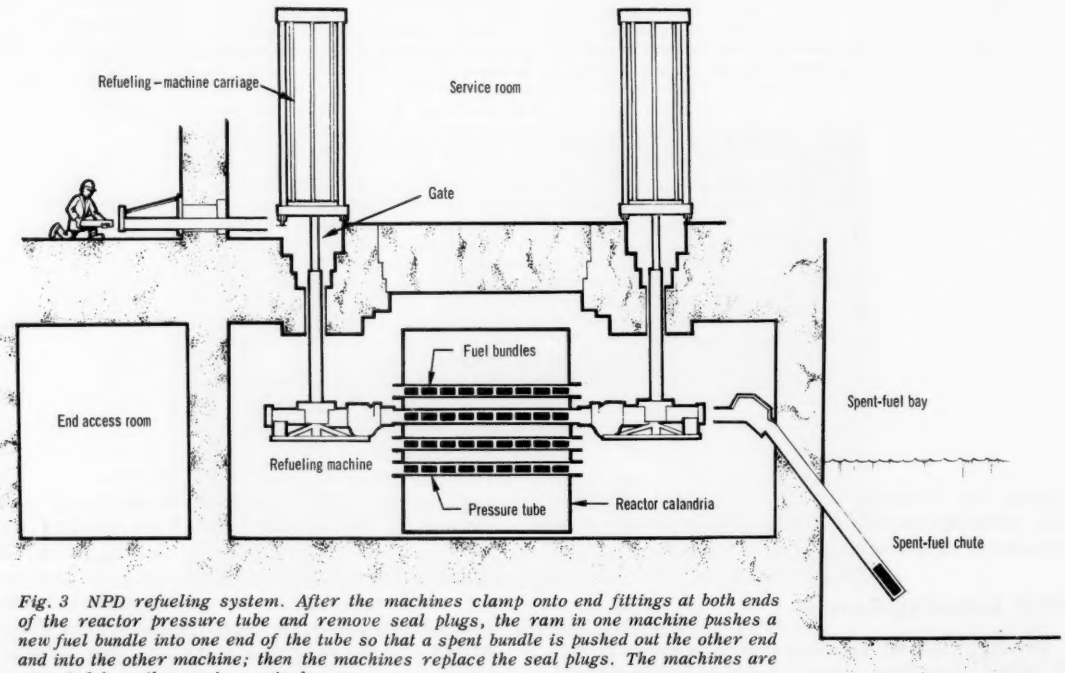

Fig. 3 NPD refueling system. After the machines clamp onto end fittings at both ends of the reactor pressure tube and remove seal plugs, the ram in one machine pushes a new fuel bundle into one end of the tube so that a spent bundle is pushed out the other end and into the other machine; then the machines replace the seal plugs. The machines are operated from the reactor control room.

Then the charging machine rams the new fuel into the pressure tube, pushing a spent-fuel bundle into the discharge machine, the machines replace the seal plugs in the end fittings, and the machines unclamp. Adjacent pressure tubes are refueled from opposite ends to balance power generation within the core.

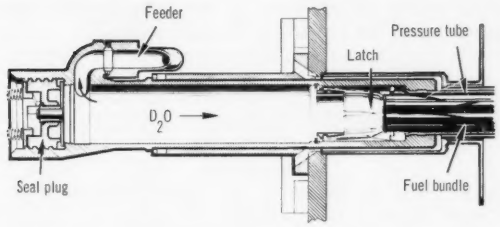

Fig. 4 End fitting of stainless steel on each end of Zircaloy-2 reactor pressure tube has seal plug that refueling machine removes for access to fuel bundles.

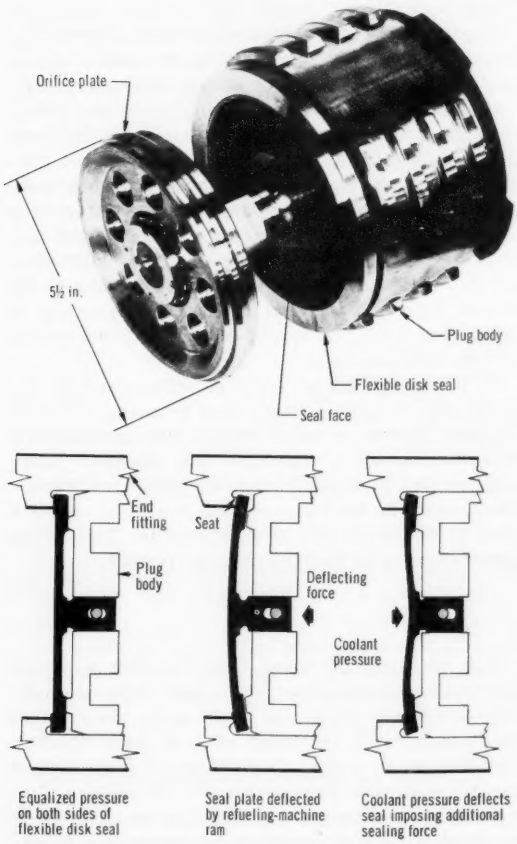

Fig. 5 Seal plug has flexible-disk seal (stainless steel) on which reactor-coolant pressure acts to tighten disk against sealing faces.

Refueling-Machine Performance

When the refueling machines were first conceived, several obstacles were obvious: (1) leakage at the end fittings could cause high D_2O losses, (2) radioactivated equipment would complicate maintenance, and (3) sticking of fuel, seal plugs, and clamps could require plant shutdown for repairs. How well the design has overcome these obstacles can be seen from consideration of refueling-machine performance.

COMPONENTS

Figure 4 shows the NPD end fittings, which contain D_2O at 1050 psig, 530°F. Although several hundreds of tests were performed in the laboratory on the NPD design, a major leak occurred in the reactor in December 1962 when an elastomer seal extruded through a sealing face because of inadequate clamping forces. Since correction of this deficiency, 452 routine on-power fueling operations have been carried out (904 clampings) without further trouble (as of Mar. 1, 1966).

Seal plugs (Fig. 5) in the 264 end fittings in NPD must be routinely removed and replaced during refueling without serious chronic D_2O loss. This requirement is met in two ways: (1) development and use of a long-life self-energizing seal and (2) continued recovery of any escaped steam or liquid from the reactor-vault atmosphere or floor.

LEAKAGE

Low-leakage seal plugs are required whether fuel is changed under on-power or off-power conditions. To prove that each plug is leaktight, the machine automatically tests it before the machine seal is unclamped. Spare seal plugs are carried in the machine magazines and can be installed on the pressure tubes while the reactor is at power. There have been no outages or deratings due to seal-plug leakage.

The average chronic escape rate of heavy water into the reactor vault for all reasons during 1964 and 1965 was 280 g/hr. The average recovery rate was 262 g/hr during the same period, so the average loss rate was 18 g/hr, or ~1 lb/day.

RADIATION LEVELS

The refueling-machine heads and associated equipment in the reactor vault are subjected to high radiation levels. Although no outages or failures have resulted from radiation degradation, electrical wiring, hoses, and internal-machine elastomers have been replaced. Neoprene hoses lined with Buna-N rubber are now used to achieve good thermal stability.

MAINTENANCE

Maintenance of the refueling-machine heads results in personnel exposure to radiation produced by

direct neutron activation of surface contaminants as well as from corrosion products, fission products, and tritium. Although there has never been a case where a person has exceeded the allowable exposure of 5 rems/year, maintenance and modification of the refueling machines during 1964 and 1965 caused a total of 27 man-rems/year exposure. The present goal is <6 man-rems/year per unit (two machines).

Because the reactor vault is inaccessible to personnel and the machine could stick on an end fitting, the design permits manual emergency operations through openings in a rotating shield at the end of the reactor vault. Two machine outages have required the use of these openings at NPD. A special cone-shaped bung was inserted manually into the reactor pressure tube after the machine was detached. This has proved to be a relatively simple and straightforward operation.

In the Douglas Point and Pickering designs, this problem has been further reduced by placing shutdown shielding between the reactor and the refueling machine.

Emergency provisions were also made at NPD to permit a refueling-machine head containing jammed fuel to be transferred and immersed in the spent-fuel canal remotely. Although fuel has jammed in the head on two occasions, the emergency provisions proved unnecessary because radiation levels were much lower than indicated by the conservative calculations on which the design was based. Thus these events were handled with relative ease and caused no outages.

NPD Refueling-System Results

The NPD has operated with on-power refueling routinely since Jan. 1, 1964—the data presented here cover experience from then until March 1966. Clearly, 2 years of data for one unit during a period of plant immaturity are insufficient for firm conclusions. Early problems are still being identified, and development is in progress, so performance should improve.

STATION OPERATION

During the entire year 1964 and the first half of 1965, NPD was run to provide base load. From July to November 1965, numerous planned training and modification outages and some forced and maintenance outages occurred. During the 1965–1966 winter peak (December to February), the unit was base loaded with no planned outages.

No attempt is made here to discuss the overall unit statistics, nor have any attempts been made to adjust the records for tests, modifications, etc. The overall values are presented solely for the purpose of providing perspective for the refueling-machine statistics.

OUTAGES

Table 2 shows the unavailability of NPD for all reasons, together with unavailability caused by the refueling system. Although the refueling system caused three outages during 1964 and four during 1965, it caused no outages during January or February 1966. The average outage lasted 66 hr. Two limit-switch deficiencies on the refueling-machine heads accounted for 75% of the lost time.

Table 2 UNAVAILABILITY HISTORY FOR NPD STATION

Period	Station unavailability for all* reasons, %	Caused by refueling system	
		Unavailability, %	No. of outages
1964	14.14	0.63	3
1965	23.30	4.67	4
1966 (January and February)	0.06	0.00	0
Average per year	17.26	2.44	3.2

*All includes experiments, tests, modifications, maintenance, and all other events that caused NPD to be unable to produce electricity.

The forced-outage rate for the winter period is a vital statistic in the Ontario Hydro system and is particularly important in planning reserve capacity. The 1964–1965 2-month base-load run was during December and January; in the winter of 1965–1966, the base-load peak was during a 3-month run, December to February. During these two runs there were no outages caused by the refueling system. The perfect performance during this period is not statistically reliable, of course, and NPD will suffer forced outages caused by the refueling system in the future. However, by careful planning they expect to achieve a very low forced-outage rate during the system seasonal peaks.

The achievement of 2.44% refueling-machine unavailability might be interpreted as adequate or acceptable performance. However, the unavailability data can be, and in this case are, completely misleading. Unavailability cannot substitute for forced-outage rate in assessing system reserves and is a poor yardstick for economic evaluation. Perhaps its greatest virtue is the ease of measurement.

CAPABILITY

For economic purposes, unavailability is a poor yardstick because it does not include derating or energy consumed during outages and is too awkward for sophisticated treatment of coincident troubles. Accordingly, "capability" is defined as a measure of ability to produce net energy. Its complement, "incapability," is a measure of unit imperfection. Where availability uses a time base, capability uses an energy base.

Table 3 represents NPD capability data during the on-power experience period; it also shows the plant

Table 3 NPD STATION CAPABILITY STATISTICS

Period	Operating policy	Station factor, %		Station incapability, %						
				For all reasons			Caused by refueling system			
		Capacity*	Capability†	Outage	Derating	Total	Direct Outage	Indirect outage	Derating	Total
1964	Base load	82.6	82.9	14.93	2.14	17.07	0.8	2.5	0.2	3.5
1965	Modification and training	70.3	71.3	25.00	3.70	28.70	5.4	1.4	1.5	8.3
1966 (January and February)	Base load	99.9	99.9	00.07	0.00	0.07	0.0	0.0	0.0	0.0
Average annual		78.2	78.9	18.40	2.70	21.10	2.87	1.80	0.79	4.05

*Capacity factor = $\frac{\text{actual net energy produced} \times 100}{\text{net energy with perfect continuous operation at full capacity}}$.

†Capability factor = $\frac{\text{net energy unit capable of producing} \times 100}{\text{net energy with perfect continuous operation at full capacity}}$.

incapability caused by refueling-system troubles. For the latter the major difference between the average plant unavailability, 2.44%, and the average plant incapability, 4.05%, corresponds to energy consumed during shutdown, indirect outages, startup losses, derating during xenon buildup after outages, and derating as a result of refueling-machine trouble.

During 1965 the incapability rose to 8.3% for two reasons: (1) two limit-switch problems on the refueling machine increased direct-outage incapability to 5.4% (development work was required to correct the problems) and (2) equilibrium-fuel operation in 1965 was more representative of normal conditions and caused the derating incapability caused by refueling-system trouble to increase to 1.5%. Modifications made in late 1965 and improved maintenance were expected to yield a major improvement in refueling-system performance during 1966.

Table 4 gives present performance targets. Although these targets are not vital to the economics of this concept, they are desirable to minimize energy cost. The real balance is reached where increased performance is offset by increased capital and operating costs for each variable. McConnell concludes[2] that "although we are very pleased with the average fueling-system incapability experience of 4.05%, we are confident of achieving 1% in NPD."

Table 4 PERFORMANCE GOALS FOR MATURE STATIONS AND REFUELING SYSTEMS

Station	Station performance for all reasons					Station performance caused by refueling system			
	Lifetime capacity factor, %	Winter-peak forced-outage rate, %	Incapability, %			Winter-peak forced-outage rate, %	Incapability, %		
			Outage	Derating	Total		Outage	Derating	Total
NPD-2		1.50				0.33	0.85	0.15	1.00
Douglas Point-1	80	3.30	6.50	0.70	7.20	0.56	1.11	0.18	1.29
Pickering-1	80	4.70	9.00	1.00	10.00	0.55	1.06	0.25	1.31

Fuel-Scheduling Experience at NPD

The payoff for on-power refueling with the equipment described comes when it performs to help achieve design burnups on an equilibrium basis and to increase station availability. Fuel-scheduling experience so far, as reported by Fanjoy[5] and summarized here, covers the time from reactor startup to near-equilibrium burnup. (Equilibrium occurs when core-average burnup reaches a constant value with specified burnup profiles.) Figure 6, the actual core-average burnup, shows that NPD is approaching equilibrium — although the burnup profiles are not yet quite as had been specified. At equilibrium, twice the asymptotic value is the discharge burnup; thus the extrapolated value from this curve will be ~10% over the design discharge burnup (152 Mw-hr per kilogram of uranium).

In the ideal natural-fuel schedule, fuel is simply shifted from channel to channel until equilibrium (1200×10^3 Mw-hr) is reached. Then new fuel is added at the equilibrium rate (Fig. 7), and there is no further shifting of bundles among channels. However, the ideal schedule cannot be achieved in practice because of physical limitations of the system — mainly fuel movement, maximum burnup, and flux distribution. Furthermore, NPD scheduling was also complicated by our use of depleted fuel in the core center to compensate for the excess reactivity caused by the new fuel in the initial loading. Thus Fig. 7 also shows the schedule calculated[6] for adding new fuel bundles on the basis of the depleted-fuel effect and practical shift rules. (Fuel bundles are kept within the design burnup by shifting the bundles removed with low burnups to alternate channels and discharging the others.)

THE ACTUAL SCHEDULE

Figure 7 also shows the actual numbers of bundles shifted between channels and the number replaced by new bundles. Decisions on whether and where to move

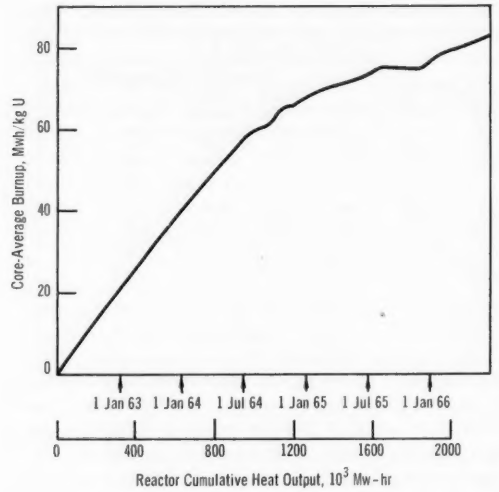

Fig. 6 Actual core-average burnup is approaching equilibrium value; discharge burnup is twice the asymptotic value.

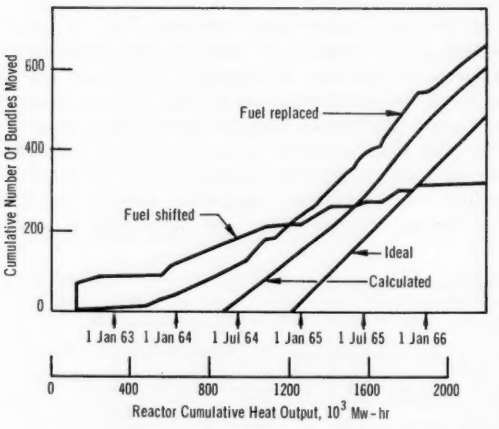

Fig. 7 Refueling schedules—theoretical ideal, calculated,[6] and actual—during the time from reactor startup with all-new fuel to the achievement of near-equilibrium burnup. Note actual refueling upsurge to prepare for winter 1965–1966 peak-demand period.

fuel were made in the following order: (1) fuel was moved only when the reactor needed reactivity, (2) channels with the highest burnup were refueled first, (3) problems unrelated directly to the fuel were considered, and (4) flux profile was checked. The flux profile did not cause much difficulty because the conservativeness of the reactor design allowed sufficient maneuvering room.

There are not yet quantitative data to explain the difference between the calculated and the actual schedules in Fig. 7; however, the difference is caused by (1) optimistic refueling rules in the calculated case; (2) imperfect refueling-maching operation [resulting in increased use of enriched booster (93% enriched UAl), more shutdown fueling than desired, premature discharge of fuel, and some preferential fueling of the core center to maximize reactivity gain]; (3) the experimental program resulting in more discharge than demanded by the schedule; (4) mechanical difficulties requiring that specific channels be left untouched; and (5) one accidental addition of light water—approximately 1000 gal—that reduced moderator purity from 99.8 to 99.1% D_2O. Continued refueling-machine development may eliminate most of these difficulties.

FOR THE FUTURE

Experience with NPD indicates that, during the period before equilibrium, on-power refueling of a large power reactor must be scheduled with the aid of a sophisticated computer program that calculates the flux profile and the burnup in individual channels. But after equilibrium is achieved, much of the computer work can be eliminated because the flux profile will be relatively static. Then refueling can be decided on the basis of (1) bundle burnups calculated with static flux profiles or (2) decreased coolant temperature at a pressure-tube outlet as an indication of burnup of fuel bundles in that tube.

* * *

This article has been prepared with the cooperation and assistance of Messrs. McConnell, Fanjoy, and Elston of the Hydro-Electric Power Commission of Ontario.

References

1. Heavy-Water-Moderated Pressure Tube Reactors, *Power Reactor Technol.*, 8(1): 35-46 (Winter 1964–1965).
2. L. G. McConnell, Canadian On-Power Fueling Experience, *Trans. Amer. Nucl. Soc.*, 9(1): 220 (June 1966).
3. W. B. Murray, Availability Assurance for the Heavy-Water Organic Cooled Reactor (HWOCR), *Trans. Amer. Nucl. Soc.*, 9(1): 219 (June 1966).
4. J. O. Holt, Canadian HWR Economic Assessment, *Nucl. Eng.*, 11(121): 461-463 (June 1966).
5. G. R. Fanjoy, Fuel Scheduling Experience at NPD, *Trans. Amer. Nucl. Soc.*, 9(2): 535 (October–November 1966).
6. W. M. Barss, A Computer Study of Reactor Fueling, Canadian Report AECL-1528, May 1962.

Recent Developments in Liquid-Metal MHD Power Systems

By Michael Petrick

The growing interest in magnetohydrodynamic (MHD) generation of electric power stems from the potential 15 to 25% increase in power-station overall efficiency possible with an MHD generator in a topping cycle on a steam plant.[1] However, the modest temperatures achievable with economic central-station reactors likely to be available in the relatively near future make MHD generators of earlier interest for space applications. Recent developments in magnetohydrodynamic technology, as described in the more than 200 papers presented in the third International Symposium on Magnetohydrodynamic Electrical Power Generation,[2-4] focus attention on defining both the promise and the specific problems of the various types of MHD systems. This article summarizes recent significant advances in liquid-metal MHD cycles, which were discussed in detail for the first time at the third symposium.

Future articles will similarly review other closed-cycle MHD systems and open-cycle MHD systems. Closed-cycle developments involved system experiments, nonequilibrium theory and measurements, conformal mapping of the potential field and electrical leakage between electrodes. Discussions of open-cycle MHD concentrated on magnet and materials problems, striated flows, and combustion plasma physics. General MHD problems, such as diagnostics, shock tubes, flow and field distributions, auxiliary ionization, and relaxation, were also discussed at the symposium.

ROLE OF REACTORS

The future of MHD power generation is very closely related to the direction and rate of development of nuclear power reactors.

Closed-cycle MHD systems can become successful only if high-temperature reactors or equivalent heat sources can be developed. Reactors for closed-cycle gas plasma systems must operate at ~3000°F, whereas liquid-metal cycles require reactor temperatures 1000 to 1500°F less. For either system the temperature imposes specialized requirements on reactor design and development.

On the other hand, and perhaps most important, the economic justification for MHD will be affected by the impact nuclear power is having on power costs. If nuclear fuel costs continue to decline as they are now doing, then the incentive for improving power-plant efficiency by means of MHD or other topping cycles will diminish.

Status of Liquid-Metal MHD

The feasibility of liquid-metal MHD conversion systems has been demonstrated. On the basis of the indicated performance of known fluid-flow devices (nozzles, separators, etc.), practical cycle efficiency of ~6% can be achieved. Such efficiency appears adequate for space power—and the general consensus is that liquid-metal MHD will probably be used initially in various space applications. In fact, liquid-metal MHD power cycles could be available for use in space before turboelectric systems.

There is considerable doubt, however, concerning the adaptability of liquid-metal MHD power cycles to commercial power systems. Minimum MHD topping-cycle efficiencies of 12 to 15% will be required to gain an economic incentive. It is not clear that such efficiencies can, in fact, be realized because of extensive friction losses in various system components—especially in the 1100 to 1600°F range, which appears to be a reasonable extrapolation of today's state of the art in reactor and materials technology.

The most crucial area where additional work is necessary in liquid-metal MHD is in the development of efficient liquid accelerators for converting the thermal energy of the fluid emerging from the heat source to kinetic energy (or stagnation head) of the

fluid before it enters the MHD generator. The basic MHD cycles differ essentially in the method chosen for accomplishing this transformation. Generator development has proceeded more rapidly and is closer to resolution. There is little fundamentally new or different in liquid-metal MHD generators; the problem is to tailor the generator to the cycle and achieve acceptable performance. As with the cycle, generator performance is also friction limited. A complete small-scale liquid-metal MHD power cycle could be operating at temperature within the next 5 years.

Progress in liquid-metal MHD during the past 2 years has been very substantial. The symposium called attention to the fact that liquid-metal MHD has emerged from its embryonic stage of development and is now a bona fide area of magnetohydrodynamics which is sparking considerable and increasing interest.

The major areas of liquid-metal MHD which have received and are continuing to receive the most intensive study are: (1) generator performance, (2) methods for liquid acceleration, and (3) cycles.

Generators

Impressive progress has been made toward the development of liquid-metal MHD generators. Most of this has concerned either the induction generator operating with single-phase flow or the conduction generator operating with two-phase flow.

A-C INDUCTION GENERATORS

Progress has perhaps been greatest with induction-generator development. An induction generator, such as is shown in Fig. 1, is a linear version of the conventional induction machine.[5] A traveling magnetic field is produced by polyphase windings, and, for the machine to run as a generator, the fluid velocity v must exceed the wave velocity v_s, or the slip, defined as $s = (v_s - v)/v_s$, must be negative. Two phases are shown in Fig. 1, but a three-phase winding would probably be used, as in conventional machines.

Sequence. Significant events in the development of induction generators occurred in the following sequence. In the spring of 1964 the first induction generator was tested at the Massachusetts Institute of Technology (MIT) by Jackson, Pierson, and Porter.[6] In August of 1965 a 350-cps 10-pole-pair flat-channel constant-fluid-velocity induction generator was tested by Prem of Atomics International on a NaK blowdown facility at Jet Propulsion Laboratory.[7] Net power of 1840 watts at 215 volts was generated with an electrical efficiency of 36%. Because operation was on a blowdown facility, the experiment ran for less than a minute. Evaluation of these tests shows that a sinusoidal magnetic field and induced current and voltage can be produced. Extrapolation of these data to a large-scale generator led the author to conclude that efficiencies as high as 70% could be obtained.

The next induction generator was run in early 1966 by Radebold and coworkers[8] at the Technical University of Berlin. This generator produced a net power of 1 kw at 50 cps and 210 volts; the excitation power required was 9.5 kva. This generator, which ran for ~½ hr under steady-state conditions, was designed primarily to produce basic data that could be compared to theory, not to demonstrate high efficiency.

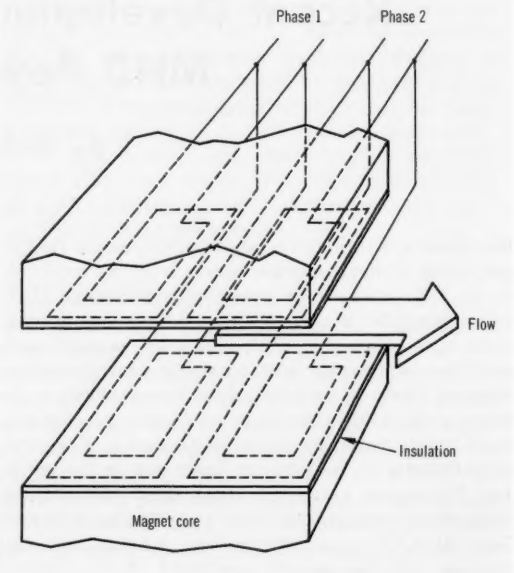

Fig. 1 Linear a-c induction MHD generator.[5]

Immediately preceding the symposium another significant development occurred which was not reported in a symposium paper. The author had the opportunity of witnessing the startup of a generator from a capacitor bank at the Technical University of Berlin. This successful experiment was also carried out by the AEG (Allgemeine Elektricitäts-Gesellschaft) group in collaboration with W. D. Jackson.

Perhaps the most significant development in regard to induction generators was reported by Elliott and coworkers[9]—the development of a short (1 to 2) wavelength machine with compensation poles at the generator entrance and exit to reduce end losses. Generator development in the past progressed toward long-, many-wavelength machines to eliminate end effects. However, performance suffered because of extreme friction losses. The solution to the problem as proposed in Ref. 9 is to try to make an electrically short generator appear like a 1-wavelength section of an infinite generator. Analyses indicate that, with compensation poles, efficiencies up to 70% are attainable if the generator has a length/gap ratio of no

more than 70 (for low friction loss) and an electrical length of no more than 1 or 2 wavelengths (for low winding loss). A 1-wavelength generator has been built (Fig. 2) and is being tested at Jet Propulsion Laboratory.[9]

Increasing Current Density. A way is being investigated to overcome the potentially serious problem of generator performance being limited by the current density in the generator windings.[10] In MHD-generator configurations the windings system consists of a conventional multiphase system like that used for the conventional asynchronous machine. But, unlike these, the gap between iron cores is increased to a channel height generally 20 to 30 times greater. Therefore the reactance of the machine and the inductive component of the current become large, which in turn give the machine a small power factor. Compensation is made by an increase in the current density of the primary windings to about 20 to 30 times that in the conventional asynchronous machine. This is only possible by use of a cryogenically cooled primary winding system. An MHD converter utilizing windings cryogenically cooled with liquid nitrogen and employing mercury as the working fluid is now being run to study the predicted performance and the technological problems involved.

Materials Considerations. The generator channel must be able to withstand >1100 to 1600°F liquid metals flowing at several hundred feet per second with negligible corrosion or erosion.[11] Refractory metals such as niobium and its alloys, which are good electrical and thermal conductors, are envisioned as candidates. The protection of the magnetic core and windings from excessive temperatures would require thermal insulation between the hot liquid metal and the field structure. Even so, to minimize insulation thickness and refrigeration power required for space applications, the magnetic core should be operated at the highest temperature consistent with high permeability and low loss. Thus the authors discussed feasible operating temperatures for magnetic and excitation-winding materials, as well as cooling methods for the field structure.

In considering design-engineering aspects, the authors extended MHD induction-generator theory to include both the conducting channel walls and the thermal insulation. Although the thermal insulation would have only a small effect on machine electrical

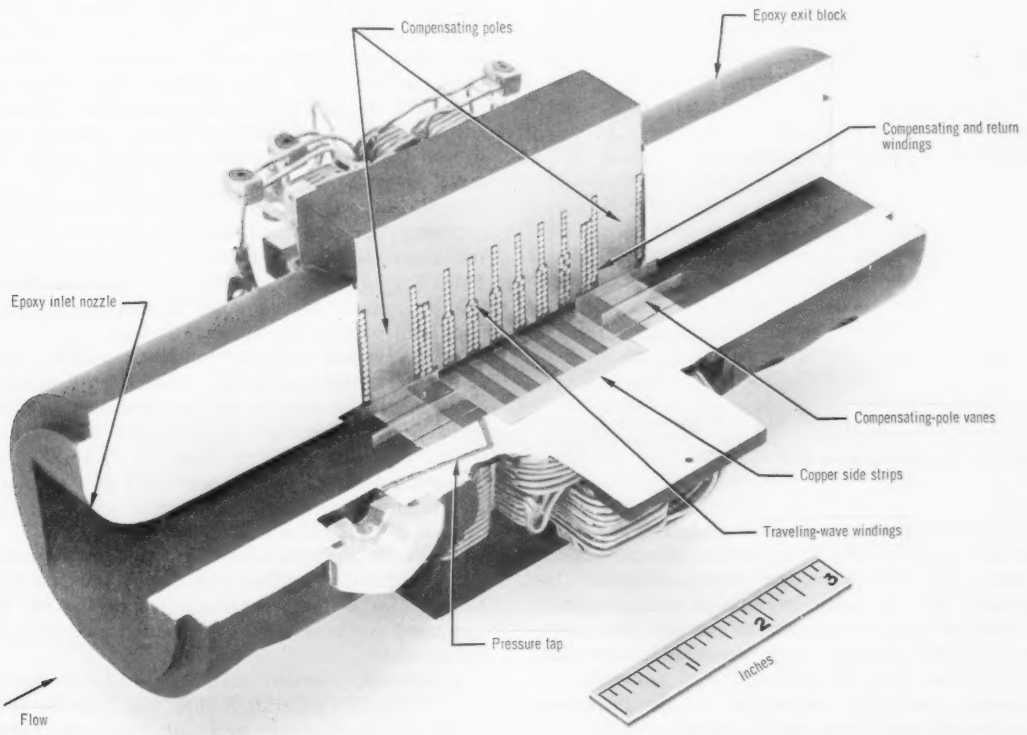

Fig. 2 Experimental 1-wavelength generator is being tested at Jet Propulsion Laboratory.[9]

performance, the channel wall thickness required (on the basis of pressure-vessel codes) to contain pressures of several hundred pounds per square inch would cause excessive electrical losses if conventional construction methods were employed. Thus novel construction schemes are suggested along with practical materials questions. (Some cycles do not involve generator-channel pressures requiring thick walls; for instance, the concept being pursued at Atomics International has 1- to 5-psi channel pressure.)

D-C CONDUCTION GENERATORS

The possibility of operating conduction generators on two-phase mixtures was discussed in Refs. 12 and 13. Initial performance data on both a film-flow and a two-phase-flow conduction generator indicate that there are limited parameter areas of operation which are feasible.[12] As shown in Fig. 3, data obtained from a two-phase ($NaK-N_2$)-flow generator indicate that, as the mixture quality and void-volume fraction are increased, generator efficiency decreases. The efficiency decrease is gradual until a mixture void fraction of ~0.85 is reached, then power and efficiency suddenly drop to virtually zero. The performance drop-off was attributed to rapidly decreasing electrical conductivity of the two-phase mixture with increasing void fraction.

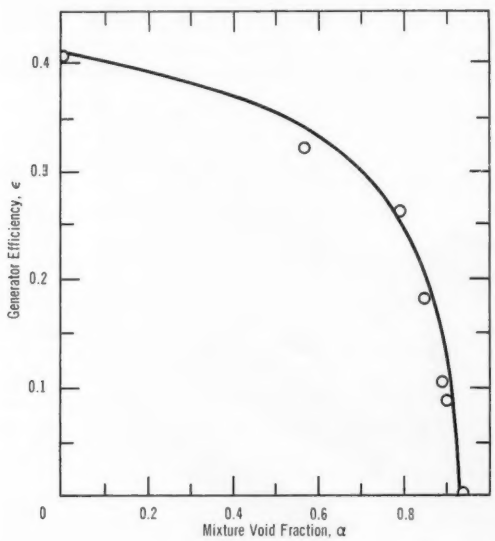

Fig. 3 Efficiency decreases in a two-phase-flow generator as mixture quality and void-volume fraction increase. Magnetic field was 4900 to 5500 gauss.[15]

The problem of defining the conductivity of two-phase mixtures remains unsettled, as evidenced by newly reported data for potassium mixtures at elevated temperatures.[13] Experiments carried out with potassium mixtures (vapor content varied from 2 to 95%) at 1100°F indicated substantial electrical conductivity. The authors hypothesize that the emission of electrons from the surface of the liquid droplets — and not the influence of the liquid film — is the cause of the enhanced electrical conductivity.

Preliminary film-flow-generator data were taken on a small-scale generator;[12] the maximum measured power achieved was 237 watts. Performance was poor at very low liquid flow rates and magnetic fields but increased with increasing values of these parameters. The limited data presented indicate that a film-flow generator apparently is feasible and stable in operation. However, many unanswered questions remain in regard to efficiency, range of stability, etc.

REDUCING END LOSSES

The end-loss problem has been analyzed for both a-c induction generators[9,14] and d-c conduction generators.[15] End losses in a generator usually arise from the large gradients of magnetic field at the inlet and outlet of the generator channel.

Methods were investigated for reducing the end losses in conduction generators, in both constant- and variable-area channels, by employing insulating vanes parallel to the flow.[15] In an initial attempt to determine optimum vane configuration, considering both electrical and viscous losses, a number of channel vane configurations were studied. The author was also able to extend the method of Sutton, Hurwitz, and Poritsky[16] to channels of linearly variable area with the assumption of large Reynolds number and small magnetic Reynolds number. Under those conditions, and with the use of an "equivalent channel geometry," a conformal-mapping technique permits the exact calculation of the net electrode current. For a 2:1 aspect-ratio channel with which no attempt has been made to use vanes to reduce end losses, maximum possible generator efficiency is 40.4%. If simple vanes are used, they must be very long, which means large viscous losses. Thus, with long vanes down the center line of the previous duct (both upstream and downstream so that the aspect ratio becomes 4:1), top efficiency rises to only 52.1%. Short but more complex vanes could yield 66% efficiency in the most promising configuration with a 2:1 aspect ratio or 74% in a 4:1 channel.

The scheme[9] proposed for resolving the a-c induction generator end-effect problem by using compensating poles at the generator entrance and exit was discussed in the section on induction-generator developments.

In addition, previous analyses[17,18] of end losses in linear induction generators have been extended to include circle diagrams depicting real and reactive currents.[14] The two-dimensional induction MHD generator of finite length is treated as a boundary-value problem by a two-sided Laplace transform.

MHD Cycles and Acceleration Methods

Because of detailed analyses by numerous investigators, there is more general agreement on the predicted efficiencies of the various proposed cycles than has ever existed in the past. All the papers on this topic dealt with three basic cycles, namely, the separator cycle, condensing injector cycle, and the two-phase generator cycle. The first two have been discussed and described in detail in the literature,[19] whereas the latter was discussed in detail for the first time at this symposium.[20,21] The two-phase generator cycle was discussed initially in a preliminary manner at a previous symposium[19] and in Ref. 22.

TWO-PHASE GENERATOR CYCLE

This cycle can operate with either one- or two-component fluids (Fig. 4). In the one-component fluid cycle, the two-phase mixture generated in the heat source passes directly through the MHD generator to a condenser–diffuser and back to the heat source. In the two-component flow cycle, additional components needed are the mixer and separator.

If the fluid is expanded through the MHD generator directly, the separate nozzle or stagnation head generator can be eliminated. In a sense, the MHD generator behaves as an expansion engine and produces electrical energy as the expanding conductive fluid interacts with the magnetic field. The two-phase flow generator behaves in a manner analogous to that of the plasma flow generator.

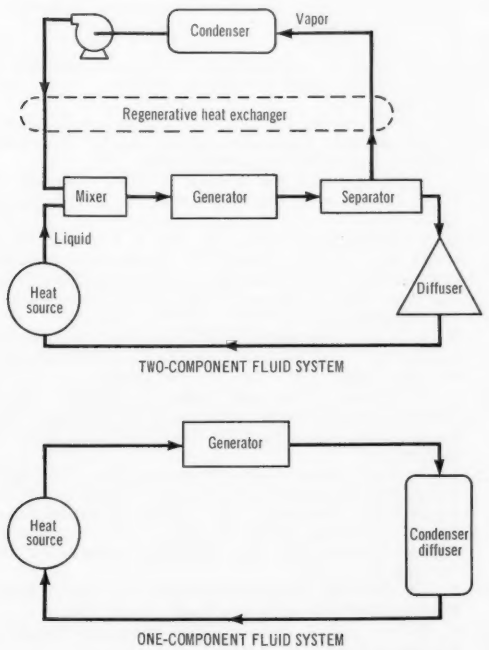

Fig. 4 Two-phase generator cycle variations can be either two-component system (above) or one-component system (below).

The efficiency of a two-phase generator cycle is potentially higher because power can be extracted under controlled velocity conditions to minimize friction—and the two-component mixture then can be separated at a lower energy and with lower losses. The potentially attractive performance of the cycle was discussed by Hammitt.[20] He showed that higher cycle efficiencies are obtainable if a high gas-to-liquid volume flow ratio can be tolerated in the generator without undue loss in efficiency; under this condition, cycles that can use successfully a high volume flow ratio appear best. However, if the generator efficiency decreases seriously with volume flow ratios, this conclusion is reversed.

A novel two-phase generator cycle was also proposed by Bidard and Sterlini.[21] The cycle features an MHD pump instead of a diffuser to return the fluid to the high-pressure end of the cycle. Another unique feature of this proposed cycle is that the entire apparatus would be enclosed within a magnet so that end effects in the pump and generator could be eliminated.

CONDENSING-INJECTOR CYCLE

Several new variations of the condensing-injector cycle were also proposed. Both Prem[7] and Radebold[8] stress the possibility of minimizing the losses associated with mixing fluids of different velocities by the use of a multistage concept in which the injected-fluid velocity would be matched stepwise with the flow velocity in the nozzle. The theoretical thermodynamic efficiency of such a cycle was reported to be 60% of the Carnot efficiency,[7] although no numerical analysis was presented to corroborate quantitatively the improved performance claimed. Present and planned studies will determine the conversion of a liquid into a foglike two-phase flow in the heat source, dispersion of the liquid injected in the different steps of the transformation, and condensation of the fog flow.

Because of the potential for considerably higher internal efficiency, the two-component cycle was perhaps the most important variation of the condensing injector analyzed.[23,24] With lithium as the subcooled injection stream and cesium or potassium as the vaporized stream, the losses due to the acceleration of the injection stream would be reduced because of the high heat-sink capacity (and thus lower injection flow rate) of lithium. For a cycle with lithium–cesium as the two-component working fluid, vapor–liquid internal efficiency may approach 80% and cycle thermal efficiency could reach 30% with a 1200°K maximum cycle temperature. There is an optimum vapor quality that gives maximum injector and cycle performance; lower mixing-chamber pressure reduces injector efficiency but raises overall efficiency; increased inlet liquid velocity diminishes

performance. Because the results presented in both studies are based solely on thermodynamic considerations and no losses are accounted for, the results represent the maximum thermodynamic performance that can be achieved. Although the results are comparable to those presented previously for other fluids and cycles,[25–27] these studies underscore the possible gains that might be obtained through the use of two fluids in the cycle.

Additional experimental data[28] on the performance of the condensing injector for space power show exit pressures greater than both liquid and vapor inlet pressures. The data, which are encouraging in terms of predictability and efficiency performance, also indicate that detailed knowledge of the mixing process is needed to design high-performance condensing injectors. The highest efficiencies occur when the velocity ratio between vapor and liquid is maximum and the flow ratio of liquid to vapor is minimized.

Progress Expected in Next 2 Years

The greatest effort in the next 2 years will probably be directed toward building and testing an efficient induction generator. As rapporteur, W. D. Jackson stated in his analysis of the state of the art of generator development, "A quick calculation of the relevant magnetic Reynolds number and a comparison of it with what rotating machine designers call the reactance to the distance ratio allowable in solid rotor induction machines shows that the results presented for the operation of these generators, their self-excitation, their steady running, and so on, was never really seriously in doubt. The basic issue remains one of realizing an induction generator of acceptable real efficiency within the limitations imposed by systems and materials considerations."

Another major question that is expected to be resolved in this time period will be the feasibility and performance of the condensing-injector cycle. The geometries, fluids, and parameters of interest to liquid-metal power cycles have not been studied experimentally thus far. However, studies under way at MIT and Argonne National Laboratory and elsewhere will remove the uncertainty concerning injector performance.

References

Except for Refs. 1 to 6, 16 to 19, 22, and 25 to 27, all references are papers presented at the Symposium on Magnetohydrodynamic Electrical Power Generation, jointly sponsored by the International Atomic Energy Agency and the European Nuclear Energy Agency, (OECD), held in Salzburg, Austria, July 4–8, 1966. Volume 1 of the proceedings, *Electricity from MHD*, is now available in the United States through the National Agency for International Publications, Inc., 319 E. 34th Street, New York, N. Y. 10016.

1. M. Petrick, Liquid-Metal MHD Topping Cycles, *Power Reactor Technol.*, 8(4): 199-209 (Fall 1965).
2. Proceedings of Third Symposium on Magnetohydrodynamic Electrical Power Generation, Salzburg, Austria, July 4–8, 1966, to be published.
3. *Magnetohydrodynamic Electrical Power Generation*, Symposium Proceedings, Paris, July 1964, Vols. 1 to 4, European Nuclear Energy Agency, Organization for Economic Cooperation and Development, 1964.
4. *Magnetoplasmadynamic Electrical Power Generation*, Symposium Proceedings, Newcastle-on-Tyne, England, 1962, The Institution of Electrical Engineers, London, 1963.
5. W. D. Jackson, Magnetohydrodynamic Power Generation—A Status Report, *Electron. Power*, 10: 258-263 (August 1964).
6. W. D. Jackson, E. S. Pierson, and R. P. Porter, Design Considerations for MHD Induction Generators, in *Magnetohydrodynamic Electrical Power Generation*, Symposium Proceedings, Paris, July 1964, Paper 61, European Nuclear Energy Agency, Organization for Economic Cooperation and Development, 1964.
7. L. L. Prem, Analytical and Experimental Results of the Fluid Metal MHD Power Conversion Programme, Paper SM-74/184.
8. R. Radebold, H. Lang, T. Schultz, H. Weh, E. Klein, and K. H. Wagner, Energy Conversion with Liquid Metal Working Fluids in MHD-Staustrahlrohr, Paper SM-74/30.
9. D. G. Elliott, D. J. Cerini, L. G. Hays, and E. Weinberg, Theoretical and Experimental Investigation of Liquid-Metal MHD Power Generation, Paper SM-74/177.
10. W. Peschka, C. Carpetis, A. Gann, and B. Tries, Some Aspects of the Use of a Cryogenically-Cooled Primary Windings System for an A.C. MHD Generator, Paper SM-74/196.
11. W. D. Jackson and E. S. Pierson, Material Limitations in the MHD Induction Generator, Paper SM-74/161.
12. M. Petrick, MHD Generators Operating with Two-Phase Liquid Metal Flows, Paper SM-74/196.
13. P. L. Kirillov, V. I. Subbotin, I. P. Stakhanov, and N. M. Turchin, Measuring the Electrical Conductivity of a Liquid-Vapour Potassium Mixture, Paper SM-74/106.
14. F. Engeln and W. Peschka, End Effects on the Linear Induction MHD Generator Calculated by Two-Sided Laplace Transform, Paper SM-74/93.
15. J. R. Moszynski, End Losses in MHD Channels of Variable Cross-Section and Their Reduction, Paper SM-74/194.
16. G. W. Sutton, H. Hurwitz, Jr., and H. Poritsky, Electrical and Pressure Losses in a Magnetohydrodynamic Channel Due to End Current Loops, *IEEE (Inst. Elec. Electron. Eng.) Trans. Commun. Electron.*, 80(58): 687-695 (1961).
17. R. N. Sudan, Interaction of a Conducting Fluid Stream with a Traveling Wave of Magnetic Field of Finite Extension, *J. Appl. Phys.*, 34: 641-650 (1963).
18. E. S. Pierson, The MHD Induction Machine, Sc. D. Thesis, Massachusetts Institute of Technology, September 1964; also Report AFAPL-TR-65-107, Chap. 6, August 1965.
19. M. Petrick, Performance Characteristics of a Liquid Metal MHD Generator, in *Magnetohydrodynamic Electrical Power Generation*, Symposium Proceedings, Paris, July 1964, Paper 62, European Nuclear Energy Agency, Organization for Economic Cooperation and Development, 1964.
20. A. G. Hammitt, Magnetohydrodynamic Liquid Metal Power Conversion Systems, Paper SM-74/193.
21. R. Bidard and J. Sterlini, MHD Generator Using an Emulsion, Paper SM-74/108.
22. W. F. Wade and M. B. Moffett, The Bubble-Flow Magnetofluid-Mechanical Energy Conversion System for Space Power, Report ER-5978, Thompson Ramo Wooldridge Inc., May 18, 1964.

23. S. N. Basov, P. L. Kirillov, V. I. Subbotin, and N. M. Turchin, Injection of Liquid Metals in MHD Converters, Paper SM-74/107.
24. K. A. Yakimovich, E. E. Shpilrain, and Yu. M. Syaskin, Thermodynamics of a Two-Component Liquid-Metal Power MHD Assembly with Injector, Paper SM-74/218.
25. K. S. Lee, Analysis of an MHD Power Generation System for Liquid Metals, S.M. Thesis, Massachusetts Institute of Technology, January 1964.
26. G. A. Brown and K. S. Lee, A Liquid Metal MHD Power Generation Cycle Using a Condensing Ejector, in *Magnetohydrodynamic Electrical Power Generation*, Symposium Proceedings, Paris, July 1964, Paper 60, European Nuclear Energy Agency, Organization for Economic Cooperation and Development, 1964.
27. M. Petrick and K. Y. Lee, Liquid MHD Power Cycle Studies, USAEC Report ANL-6954, Argonne National Laboratory, June 1965.
28. G. A. Brown and E. K. Levy, Liquid-Metal Magnetohydrodynamic Power Generation with Condensing Ejector Cycles, Paper SM-74/171.
29. K. I. Dmitriev, Yu. M. Mikhailov, and V. S. Presnyakov, Experimental Investigation of the Magnetohydrodynamic Flow of a Liquid Metal in a Rectangular Duct with Conducting Walls, Paper SM-74/93.
30. I. B. Stechkina and F. R. Ulinich, Hydrodynamics of Flow Two-Component Mixtures in Nozzles, Paper SM-74/100.
31. T. Sekiguchi, M. Katsurai, and K. Yokoyama, An MHD Rotating Machine — A New Type of A.C. Magnetohydrodynamic Power Generator and Turbine, Paper SM-74/137.
32. R. R. Barthelemy and C. E. Oberly, Optimum Magnets for MHD Generators, Paper SM-74/167.
33. L. D. Nichols, Criteria for Use of Rankine–MHD Systems in Space, Paper SM-74/190.
34. A. Maciulaitis, A. L. Loeffler, Jr., and P. J. Calcanes, Experimental Investigation of MHD Flows Through Circular Pipes at High Hartmann and Reynolds Numbers, Paper SM-74/195.
35. Ya. Ya. Lielpeter, Applicability of the Electrodynamic Approximation in the Theory of Liquid-Metal Induction MHD Converters, Paper SM-74/240.
36. L. A. Vulis and V. T. Yaglenko, Observations of Mercury Flowing Along a Trough in a Transverse Magnetic Field, Paper SM-74/249.

Component Development: Key to Rankine-Cycle Space Applications

By Edward J. Croke

The development of reactor and isotope heat sources, combined with projected requirements for compact, lightweight electric-power generators for space and undersea application, has given rise to extensive turboelectric-power development programs intended to exploit the potentially high efficiency of the Rankine cycle. Experience in these system development programs has spotlighted the importance of improving the technology of high-performance components capable of long-time unattended operation.

In terms of practical engineering, a great deal of Rankine-cycle component development has taken place in recent years. Much of it has been based on very pragmatic developmental methods. At present, bearing wear, boiler conditioning, and turbine erosion are the most significant problems in achieving reliable Rankine cycles. Fabrication techniques for longer life bearings and higher temperature turbines, more efficient pumps, and less vulnerable radiators are being developed. Heat-transfer properties of useful liquid metals are being investigated in several research facilities. Nevertheless, for the long term, the work done so far indicates that additional basic research is needed in the areas of heat transfer, materials, and structural mechanics. The situation is illustrated by consideration of the status of the four major Rankine-cycle programs and the component experience discussed in this article.

Rankine-System Development Programs

The four major Rankine-system development programs include the mercury Rankine program sponsored by the U. S. Atomic Energy Commission (AEC),[1] the SNAP-8 Program of the AEC and the National Aeronautics and Space Administration (NASA),[2] the SNAP-50/SPUR Program of the AEC and the U. S. Air Force,[3] and the Organic Working Fluid Rankine Cycle Programs of the U. S. Navy, Air Force, and AEC.[4] There also have been associated component studies and development efforts at various government and industrial facilities.

The early history of Rankine-system development parallels the growth of the national space program. Initially, mission requirements were not well defined, and, with a premature sense of optimism, full-scale systems were projected before the problems of building a component technology were fully evident. When experience spotlighted the component problems, and as mission requirements were seen to change rapidly, most of the systems programs evolved into component and technology programs that will permit development of a range of Rankine systems that can supply power for a variety of anticipated space missions.

MERCURY RANKINE PROGRAM

Development of the AEC's SNAP-2 system began in 1957 with the objective of producing a flyable 3-kw(e) reactor-powered mercury Rankine system (Fig. 1) capable of operating for 1 year (Ref. 5). With changes in mission requirements, the SNAP-2 program evolved into the mercury Rankine program—whose initial objectives were to develop system technology and qualify components (exclusive of the reactor or isotope heat source) for a space power plant with 3- to 5-kw(e) power-conversion modules so that the plant could be adapted to supply 3 to 25 kw(e) for 2500 hr of operation in space.[1] The ultimate goal was to achieve reliable performance for 10,000 hr. The mercury Rankine program is now in the process of being phased out, with only two combined-rotating-unit turbomachinery tests to be completed.

Component Tests. Development tests of the components at Atomics International, the prime contractor, indicated that the required operating life

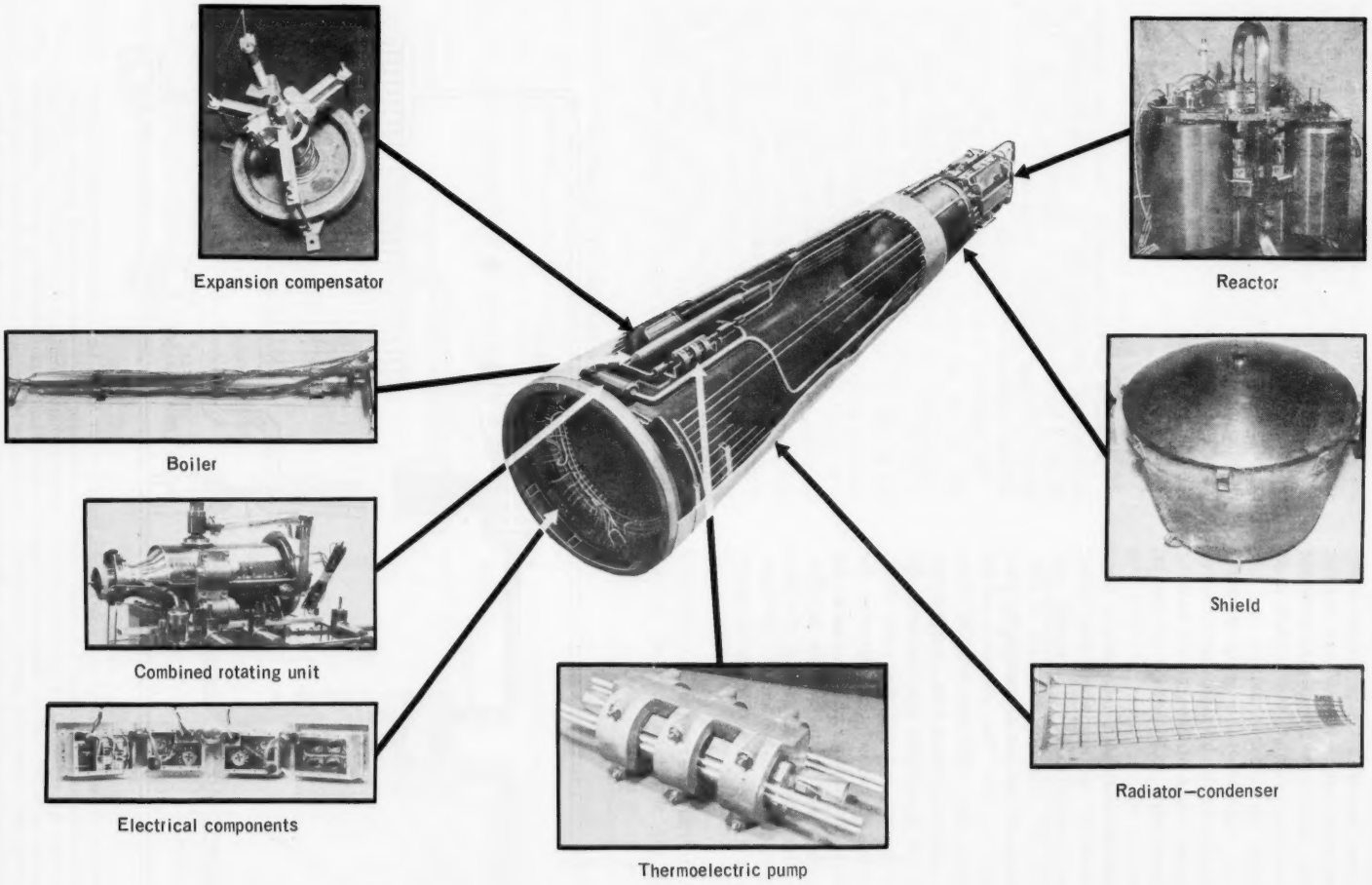

Fig. 1 Mercury Rankine-cycle turboelectric system, as envisioned by Atomics International, would develop 3 to 5 kw(e) at 120 volts and 1800 cycles/sec. Compact reactor heats NaK in primary loop, which circulates NaK into a boiler, where it evaporates and superheats mercury. Mercury vapor drives a turbine that powers a permanent-magnet alternator and a mercury pump, all three of which are mounted on a single mercury-lubricated shaft to form a combined rotating unit. From the turbine the mercury passes through a radiator–condenser and then is pumped back to the boiler to complete the cycle. The NaK is pumped by a thermoelectric direct-current conduction pump that uses the NaK as the hot junction and the mercury as the cold junction for the thermoelements.[1]

could be achieved. System performance, orbital start-up capability, and structural integrity have been verified in system-test facilities.[1] Although one combined rotating unit was tested for 7000 hr without major damage, the major developmental problem has been journal-bearing erosion, which could limit the life of the mercury rotating machinery.

The previously experienced bearing erosion–cavitation has been decreased by almost an order of magnitude by reducing loads and increasing bearing pressure. Life capabilities well beyond 10,000 hr now seem feasible.

Other components demonstrated satisfactory performance. The model-5C boiler, which was tested for 38,000 hr, has proved to be structurally and thermally acceptable for long-life operation if protected from exposure to air and contaminants such as trace quantities of oil. The adequacy of the thermoelectric pump was demonstrated by many hours of testing. Several pumps have operated for >20,000 hr. Both the honeycomb and aluminum-fin radiator–condensers have demonstrated good structural and operational characteristics, although the process for bonding aluminum radiator fins to the Haynes 25 condenser tubes caused some developmental problems. The startup components (pressure regulator and injection tanks) posed no problems more serious than the fabrication of the metal starting bellows.

System Startup. Orbital (zero-gravity) transient characteristics of the integrated Rankine system have been simulated successfully, and automatic startup has been accomplished with a nonnuclear installation. Although the simulated system achieved stable operation, long operating lifetimes remain to be demonstrated—and performance degradation, control interactions, mercury corrosion, metallurgical-processing effectiveness, and long-term exposure to vacuum must be evaluated to qualify the system for flight operation. Multiple-restart capability has also been demonstrated.

SNAP-8 SYSTEM

The NASA Lewis Research Center has project-management responsibility for the development of SNAP-8 power-conversion equipment, and the AEC Space Nuclear Systems Division is charged with nuclear-systems development.

The mercury Rankine turboelectric-power system (Fig. 2) for the SNAP-8 Program, which was based considerably on technology developed under the SNAP-2 program, has had a history somewhat similar to that of the SNAP-2 Program and the mercury Rankine program. The initial objective of developing a 35-kw(e) reactor-powered system for 10,000 hr of operation in space after a remote-controlled startup has remained more or less intact from program inception in 1960 to the present. However, limitations of the state of the art of liquid-metal-systems technology in 1962 resulted in a major redesign of the prototype system. With system-level development curtailment in 1965, actual development was limited

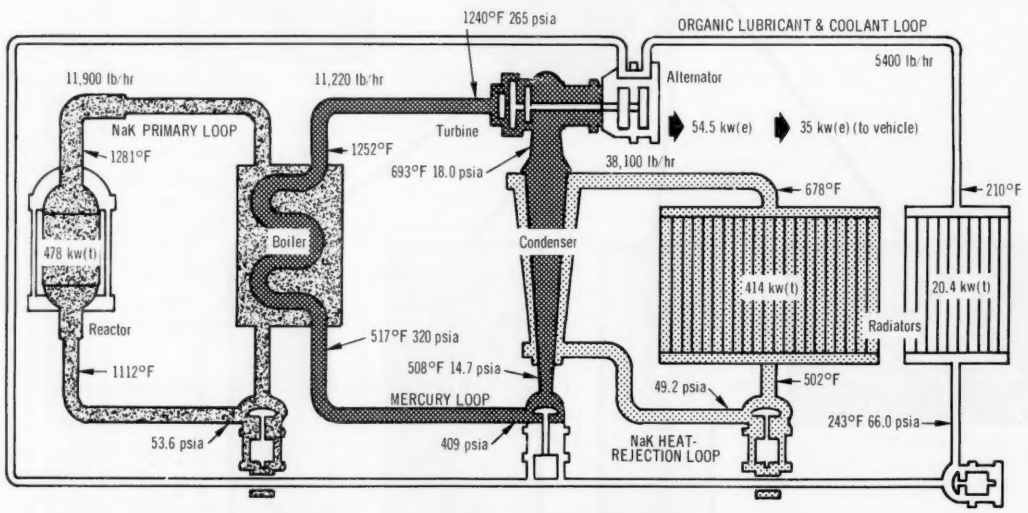

Fig. 2 The SNAP-8 mercury Rankine-cycle system, developed for NASA Lewis Research Center by Aerojet-General Corporation, consists of a compact uranium–zirconium fueled-and-moderated reactor (developed by Atomics International), a boiler, condenser, turboalternator, radiator–condenser, mercury and NaK pumps, and a control system. These are arranged in three liquid-metal circulating loops: A NaK primary loop cools the reactor and powers the mercury Rankine-cycle secondary loop; the tertiary NaK loop transfers heat from the mercury condenser to the radiator–condenser, where the heat is rejected to space. In a fourth loop an organic fluid circulates to lubricate bearings and to cool the alternator, electric motors, and controls.[2]

to an attempt to qualify the first power-conversion test system for 10,000 hr of operation.

Reactor Tests. The SNAP-8 test reactor went critical in June 1963 and later demonstrated sustained power operation and static and dynamic stability. The longest continuous test run was 5000 hr; the reactor and test facility were shut down as planned in April 1965 after accumulating a total of 12,000 test hours that included 100 days of operation at 600 kw(t) with a NaK exit temperature of 1300°F. Design has been completed, and fabrication is under way for the second SNAP-8DR reactor test.

Component Tests. Although the boiler designed for SNAP-8 proved generally satisfactory, it was plagued with inconsistent boiler conditioning (scouring of scale oxides and contaminants from the heat-transfer surface). The mercury condenser performed generally well in preliminary tests. The 51.6-kw(e) turboalternator performed satisfactorily in more than 830 hr of tests at approximately design conditions. The NaK pump-motor assemblies accumulated more than 1000 hr of operation in >1100°F NaK; the mercury pump-motor assemblies completed >120 hr of operation at an inlet temperature of 500°F; a Thompson Ramo Wooldridge Inc. lubricant–coolant pump-motor assembly achieved >1000 hr of operation at rated conditions without performance degradation (seven of these units accumulated a total of more than 4300 hr of operation). The start system, voltage regulator, speed controller, and related electrical subsystems demonstrated satisfactory performance.

Although the mercury boiler, turbine, condenser, and pump demonstrated satisfactory combined performance for 837 hr in a multiple-component test loop, the entire nonnuclear four-loop system has not yet been operated as an integral unit. Such a test of the first power-conversion system is scheduled for early 1967 as part of the component qualification program.

SNAP-50/SPUR SYSTEM

Little information is available on this program, but AiResearch Mfg. Co. (a division of the Garrett Corp.) indicates that turbine-rotor bearing materials, lubrication, and stability may be among the foremost problems.[6] Blade erosion and associated turbine-life limitations are no longer expected to loom large among development difficulties. Experience with these components will be considered in greater detail in the Rankine Component Technology subsection of this article.

ORGANIC RANKINE-CYCLE SYSTEM

This 1.5-kw(e) Rankine system, whose combined rotating unit was being developed by Sundstrand Corp. for the U. S. Air Force, would have been heated either by a ^{210}Po source or by solar energy concentrated by a mirror. The Dowtherm A working fluid reaches a maximum temperature of ~700°F, and so the high-temperature problems of the liquid-metal Rankine systems are avoided. The organic Rankine system (Fig. 3) consists of a boiler, a combined rotating unit (including turboalternator and Pitot pump), a radiator–condenser, a regenerator, and the control system. The thermodynamic cycle is shown in Fig. 4.

The combined rotating unit accumulated more than 2000 hr of successful tests; a single set of bearings has served for more than 600 hr of cumulative running time with more than 100 restarts. Although these tests have shown good performance, long-endurance

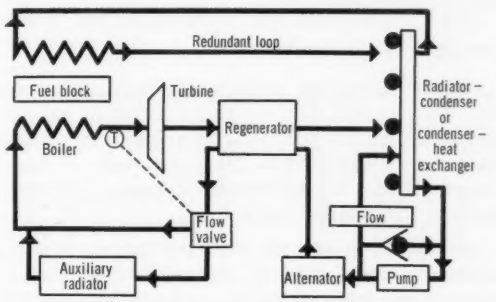

Fig. 3 Organic Rankine-cycle turboelectric system for Apollo type mission would have a 17.5% overall cycle efficiency (including losses and control power) with 750°F 157-psia Dowtherm A working fluid and ^{210}Po as fuel. The system would provide 1.5 kw(e) for a 14-day mission plus a 30-day hold. Fuel block and shielding would weigh 250 lb, and redundant conversion equipment would weigh 280 lb (Ref. 4).

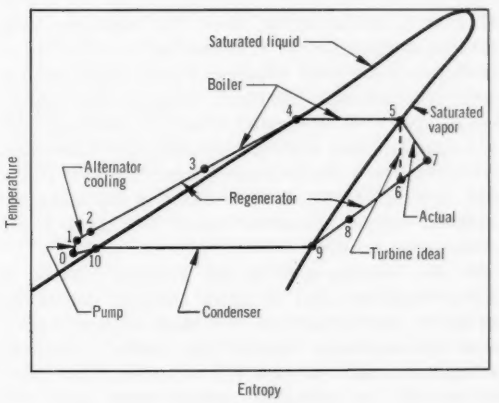

Fig. 4 Temperature–entropy diagram for Dowtherm A Rankine cycle. Dowtherm A has a composition of 26.5% by weight $(C_6H_5)_2$ and 73.5% $(C_6H_5)_2O$, molecular weight of 165.65, freezing point of 53.6°F, and vapor pressure of 0.63 psia at 300°F and 106.81 at 700°F. Corresponding characteristics of biphenyl, another organic fluid, are $(C_6H_5)_2$ composition, 154.20 molecular weight, 158°F freezing point, and vapor pressure of 0.68 psia at 300°F and 109.0 psia at 700°F (Ref. 4).

system capability equivalent to 10,000 hr of unattended operation in space remains to be demonstrated. Because the thermal stability of the working fluid may limit system life, AEC programs are evaluating this uncertainty.

Rankine Component Technology

Each major component of a high-temperature Rankine system has its own developmental and operational problems. Thus it is worthwhile to consider and compare components developed in the various Rankine programs. In general, parallel and essentially independent solutions seem characteristic of Rankine technology.

PUMPS

Notable among the pumps under development are the mercury and NaK pumps for SNAP-8, the NaK pumps for the mercury Rankine program, the potassium pumps operated at Oak Ridge National Laboratory (ORNL), and those being developed by General Electric Company for NASA.

Mercury Pumps for SNAP-8. The duty cycle of the mercury pump in SNAP-8 includes 10,000 hr of unattended operation in a radiation environment of 10^{13} neutrons/cm^2 at a speed of 8000 rpm and with an inlet suction temperature of 405°F. Pump flow rate is 1.775 gal/min at a nominal head of 10.5 psi (Ref. 2).

A jet pump at the inlet of the main pump housing overcomes potential cavitation difficulties at the rather low specified pump suction head. The mercury pump is a single-shaft overhung system with an impeller at one extremity (upstream of the jet pump) and a drive motor at the other. The semiopen-vane centrifugal impeller is ball-bearing mounted in a housing that has been designed to minimize bearing loads. The bearing lubricant, organic 4P3E (polyphenyl ether), is separated from the mercury flow by a dynamic seal system consisting of a viscopump that maintains a stable liquid–vapor interface in the fluid. Leakage of the fluid to space is minimized by a helical thread molecular pump that has a 3-mil rotating clearance.

On the bearing side of the rotating system, a similar dynamic seal is used; however, additional low-speed (6000 rpm) and stationary sealing is provided by stationary carbon face seals; a bellows arrangement lifts the carbon face seals off the bearing surface at rotational speeds > 6000 rpm. The central housing of the pump supports two angular contact end bearings of M-50 tool steel. Between these end bearings is a rotating "slinger" seal and a molecular pump. The pump motor has silicon-steel laminae and is a 400-cycle induction unit cooled with 4P3E. At the ends of the motor, the terminals are hermetically sealed. Between the motor and one end bearing is a scavenging seal; at the other end of the pump, there is a face seal. The prospect of running the pump flooded was considered, but the system temperature rise caused by viscous effects proved to be excessive, and hence the end scavenger was provided.

The test pump weighs ~186 lb in the fully instrumented state. Much of this weight is in the 9% chronium–1% molybdenum steel housings hogged from solid forgings. A realistic flight weight for the system would be ~110 lb.

Tests have been conducted on both the subassembly and system levels. The cavitation performance of the jet pump has been tested with mercury, and the sealing system has been tested for 1000 hr in vacuum. Extrapolation of the results of these tests shows that the mercury loss to space will be ~1.75 lb per 10,000 hr and that 0.1 lb of 4P3E will be lost in this same time. The motor has been tested for over 20,000 hr immersed in 4P3E, and, although the coolant temperature reached 350°F during the tests, no compatibility problems were evident.

Three pump assemblies were built. Two were retained at Aerojet-General Nucleonics and one was sent to NASA Lewis Research Center for testing. More than 140 starts were accumulated on these units, of which 72 starts were on one pump. Except for two failures of the space-seal lift-off bellows, all tests were successful. However, some degree of cavitation was detected near the end of the tests.

The cavitation limit of the assembly was imposed by the centrifugal impeller, which is provided with a 2-ft head by the jet pump. The minimum net positive suction head ranged from 0.1 ft at 0.5 gal/min to 0.75 ft at 2.25 gal/min. Overall efficiency of the pump was found to be ~13%.

NaK Pumps for SNAP-8. In the primary and tertiary NaK loops of the SNAP-8 system, each pump is a self-contained hermetically sealed unit with a single-shaft connecting motor (208-volt induction, rated at 1530 rpm) and an impeller. The type 410 stainless-steel impeller, a semiopen-vane unit with 90° backvanes, has a rated specific speed of 1600 rpm and is enclosed in a double volute housing of type 304 stainless steel. It is designed for use with 1170°F fluid.[7]

The pump has been tested in a loop containing a heat-exchanger cold trap, an economizer, and a 5-μ NaK filter. The fluid discharged at 350°F into the economizer, where it was cooled to 320°F and sent to the heat-exchanger cold trap and cooled to 290°F. It then entered a canister containing stainless-steel wire mesh (to trap oxides) and returned to the economizer, where it was heated to 300°F and filtered. (Reheating prevents the filter from becoming an oxide trap since it is not permitted to become the coldest part of the system.)

Considerable testing of this design also has been done on the subassembly level. The motor has been dynamometer checked in air, and the bearings have

been run in both oil and NaK to determine the minimum allowable bearing thickness as a function of bearing load. The capability of the cold trap to keep the oxide level below 20 ppm was tested and verified, and water tests have determined the heat-exchanger heat-transfer characteristics.

A major development problem was NaK leakage (at temperatures above 500°F) through inclusions in the original type 347 stainless-steel pump housing. This design was successfully fabricated in type 304 stainless steel. Another problem was rotor sticking, caused by flat bearing pads; this situation was corrected by grinding a radial taper on the bearings to obtain a line contact.

Eight pumps were built and tested at fluid temperatures up to 1200°F. One unit was run for 2040 hr. The design is reported to have met or exceeded all requirements with a demonstrated efficiency of 35 to 40%. (The significant NaK pump losses are frictional.)

Thermoelectric-Powered NaK Pump. The Atomics International electromagnetic pump (Fig. 5) is an unusual device in that the 3.5 kw(e) required for its operation is generated thermoelectrically from the waste heat of the primary loop.[8] Rated for a flow of 12 gal/min at 1200°F, the pump has a pressure head of 1 psi. The design has been optimized in terms of weight vs. thermoelectric thickness, weight vs. throat height, and weight vs. magnetic-field strength.

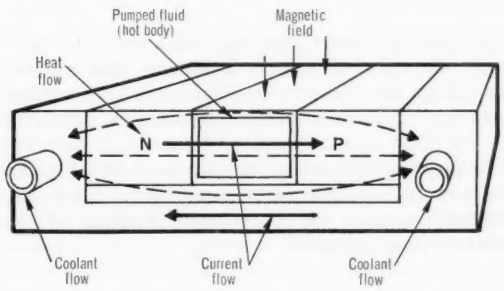

Fig. 5 Schematic of SNAP-2 thermoelectric-powered electromagnetic NaK pump.[8]

An electrically heated test loop was constructed for this direct-current induction pump. Four test series were devised: (1) flight-operation duty cycle, (2) startup transient tests, (3) steady-state performance evaluation, and (4) endurance testing. Of the 12 pumps built, 10 have been tested at rated conditions. About 20,000 hr have been accumulated on each of three units; two tests were terminated after 5000 hr of operation each.

The maximum temperature transient encountered was 363°F/sec — well above the specification limit of 50°F/sec — but no adverse results were reported. Maximum observed degradation in performance was associated with a 16% flow decrease after 5000 hr of operation on one unit and a 10% flow decrease after 5000 hr on another. Two units, tested in a vacuum environment for 800 to 1000 hr, showed no significant performance degradation; test units subjected to thermal cycling evidenced leakage only after 3000 to 5000 hr. Magnet degradation caused by nuclear radiation at operating levels appeared negligible over the time considered.

Potassium Pumps with Turbine Drives. A program was established at ORNL to accumulate experience with liquid-metal turbopumps by fabricating and testing several machines of typical performance and behavior.[9] High reliability was found to depend on bearing design and materials, minimization of turbine-bucket damage, and minimization of pump cavitation.

The turbopump developed at ORNL (Fig. 6) used bearings of tungsten carbide with 12% cobalt binder. Because the coefficient of thermal expansion of this material differs significantly from that of the austenitic steel casing, TZM bearing housings were chosen. Radial thermal expansion was accommodated by cantilever-mounting the bearings to obtain radially soft but axially stiff behavior. Journal bearings were lubricated with potassium. Axial loads were carried by two flat-plate thrust bearings.

The turbine shown in Fig. 6 is 2.75 in. in diameter, and the impeller is 1.0 in. in diameter. Turbine speed is 24,000 rpm, and the design inlet temperature is 1540°F. Eight of these units were fabricated, and seven were successfully tested to failure for periods ranging from 0.5 to 327 hr. One continuous run was 140 hr, and total accumulated operating time was >540 hr. More than 125 starts were recorded. In these tests, termination was caused by such failures as bearing-sleeve fractures, seizing of the journal bearings of the turbine or impeller, impeller rubbing against the pump housing, or filter clogging. Figure 7 shows pump performance.

Fabrication of two larger pumps was contracted to Aeronutronic/Philco. The first of these, Mark I (Fig. 8), had a 6-in.-diameter turbine wheel and a 2.75-in.-diameter impeller; the second model, Mark II, was similar but was rated for a higher flow and had a more massive casing. Other improvements in the Mark II included (1) carburizing all TZM surfaces to eliminate galling, (2) nitriding all stainless-steel surfaces to reduce corrosion, (3) mounting the WC bearing housings on conical surfaces to compensate partially for differential thermal expansion, and (4) lengthening certain bearings. The Mark I turbine used convergent–divergent nozzles, but the Mark II turbine used only convergent nozzles.

Characteristics and performance of three turbopumps are shown in Table 1. Although one of these pumps was run to 75% of theoretical cavitation conditions, cavitation damage was not found. The low

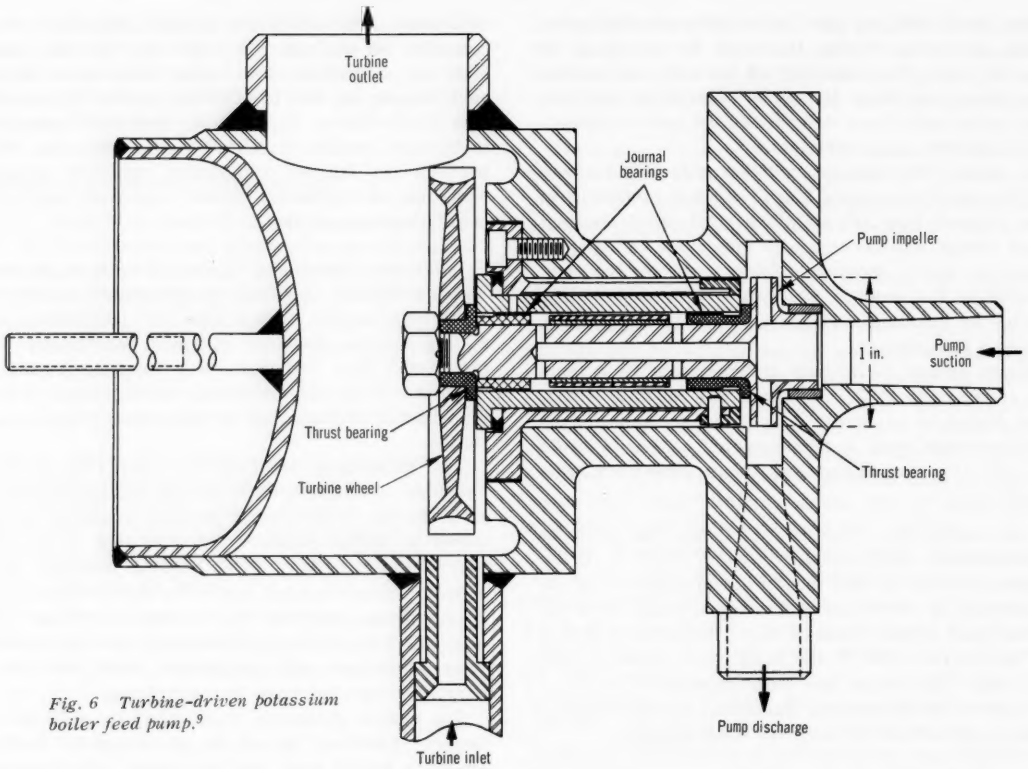

Fig. 6 Turbine-driven potassium boiler feed pump.[9]

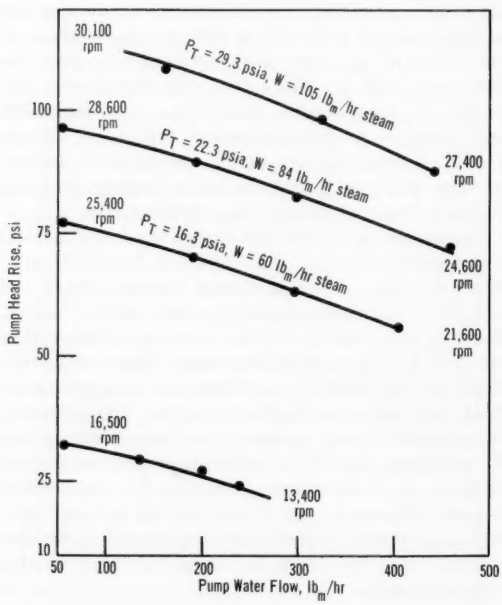

Fig. 7 Turbine-driven-pump performance characteristics on steam and water. P_T is turbine inlet pressure, W is turbine vapor flow; turbine outlet pressure is ~2 psia for all runs.[9]

velocities and short runs may have prevented damage, but there is reason to believe that extreme cavitation need be no more damaging to a machine than mild cavitation—depending upon the properties of the fluid and the degree of subcooling involved. The quality of the turbine exhaust was ~ 95% for these units. Little erosion was detected under these conditions, in which the condensated consisted of very finely divided particles.

BOILERS

A principal factor limiting Rankine-system boiler design has been a lack of precise liquid-metal heat-transfer data. A better design basis has been established by studies with mercury, potassium, and sodium.

MRP Mercury Boiler. Considerable test experience has been achieved with the mercury Rankine program compact boiler; three design models have accumulated a total of 38,000 hr. Major problems have been with the mercury corrosion and boiling heat-transfer conditioning of the Haynes 25 tubing. The mercury corrosion rate is diffusion controlled, decaying with time such that the generated "crud" products can be adequately trapped or filtered to assure at least 1 year of operation. The boiler deconditioning appears to be controllable if precautions

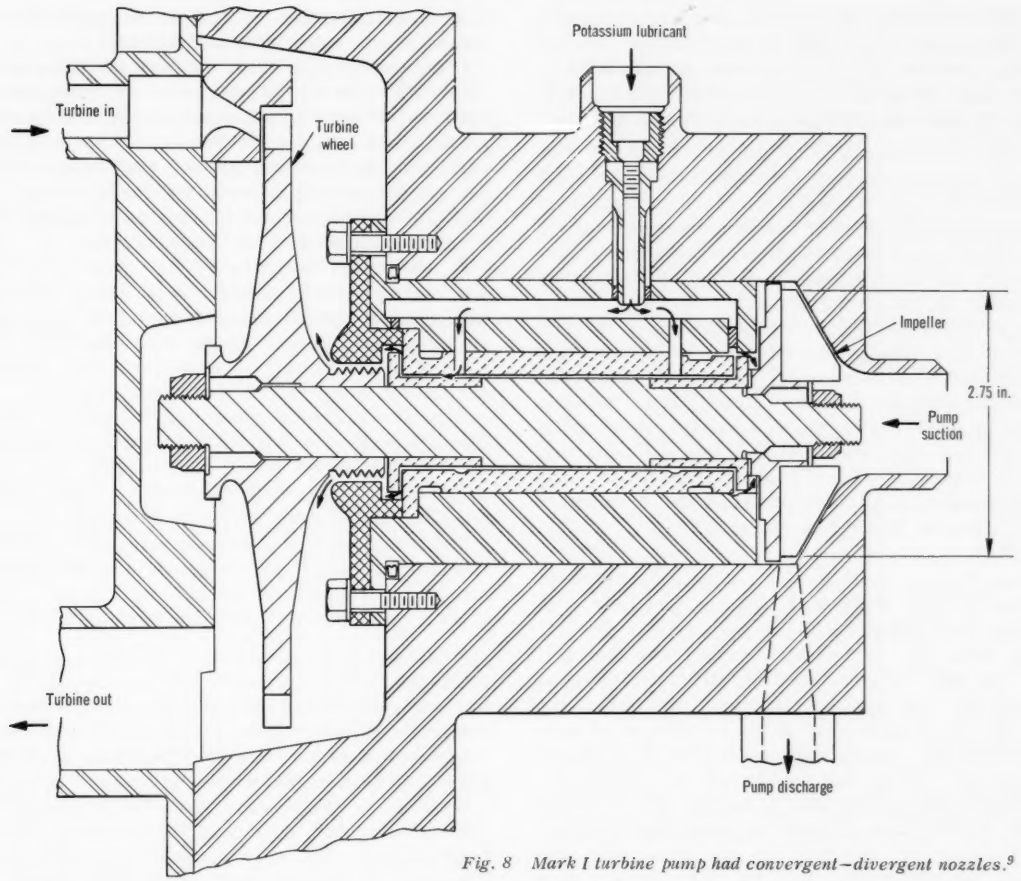

Fig. 8 Mark I turbine pump had convergent–divergent nozzles.[9]

are taken with respect to cleanliness, air inclusion, and surface treatment. Even with some degree of boiler deconditioning, the power from the model-V combined rotating unit was generally adequate. The endurance experience of various boiler tests indicates generally that conditioning characteristics improve with time with a leaktight system.

Mercury Boiler for SNAP-8. Considerable boiler test experience was accumulated during the SNAP-8 development effort.[10] A 480-kw(t) forced-convection one-pass mercury boiler heated by NaK (with a gas-fired heater) was extensively tested. The NaK enters this tube-in-shell boiler at 1280 to 1330°F. Mercury enters (0.3 ft/sec) the double spiral helical coils surrounding the NaK shell at 320 psia and 517°F, and, at rated operation, exits at 1252°F. The helical tubes are 9% chromium–1% molybdenum steel, chosen for its corrosion resistance, and the NaK shell is of type 315 stainless steel. Over 1600 test hours were accumulated on this configuration—1400 hr were on a single unit.

Table 1 TURBINE-DRIVEN POTASSIUM BOILER FEED PUMPS[9]

	Pump		
	ORNL	Mark I	Mark II
Speed, rpm	25,000	8,000	8,400
Inlet temp., °F	1,540	1,540	1,540
Turbine inlet pressure, psi	30	30	30
Turbine exhaust temp., °F	1,050	1,050	1,140
Turbine exhaust pressure, psi	1.5	1.5	3.0
Flow, gal/min	1.5	1.5	3.0
Suction temp., °F	1,050	1,050	1,050
Suction pressure, psi	1.5	1–4	1–4
Pump discharge pressure, psi	70	50	60
Accumulated run time, hr	327	1,500	

These boilers are rated for 11,000 lb/hr flow and have mass velocities of 200 lb/(sec)(sq ft). Instability was 4 to 6 cycles/min or ~200 psi. Predictions of pressure drops and heat transfer were made with the Martinelli correlation.

Boiler conditioning proved to have a major influence on performance. The first unit tested required ~100 hr of operation to become wetted and to achieve rated performance. When conditioning was complete, the pressure drop and the exit temperature stabilized near the predicted values for a wetted system. A second boiler operated for ~20 hr in a

derated condition with an exit temperature of ~900°F rather than the rated 1252°F. Exit quality was only ~70%, and the pressure drop was correspondingly low. After 20 hr the exit temperature stabilized at 1200°F, and near rated performance was achieved.

Later tests revealed that the addition of ~20 ppm liquid rubidium (to serve as a wetting agent) rapidly raised the exit temperature of an unconditioned boiler from 800 to 1200°F with a corresponding increase of pressure drop. After boiler shutdown and restart, further rubidium injection was required—probably because of consumption as oxides during the shutdown period. Because rubidium does form oxides that cause unpredictable alteration of the heat-transfer properties of the mercury, this conditioning technique was not favored for the SNAP-8 system. After 200 hr of operation with rubidium, the boiler was shut down, cleaned out, and restarted; rated performance was attained immediately. Rubidium appears to have promoted the cleaning of scale from the boiler-tube surfaces.

Heat Transfer in Mercury Boilers. Four basic modes of heat transfer in mercury flow have been defined: (1) contact boiling in the liquid regime, (2) slug flow, (3) intermediate contact (semiboiling), and (4) film boiling. The first, third, and fourth of these flow regimes are fairly well understood, but the second, slug flow, is neither well known nor easy to investigate. Liquid slugs form at low flow velocities (~0.5 ft/sec) and tend to use up considerable boiling length without significant heat transfer. High flow velocities are required to avoid slug flow in a heat exchanger; however, the associated pressure drops are frequently prohibitive. To achieve a high pressure drop and flow velocity in a test boiler at Aerojet-General Nucleonics, workers fabricated several inlet plugs that would provide high flow velocities.[11] These were constructed in two sections, a high-velocity section that gave 0.9 to 6 ft/sec with some preheating of the fluid and a two-phase section with a swirl inducer. Each plug consisted of a cylindrical core spirally wrapped with wire. The amount of flow constriction was such as to initiate boiling at the exit of the first section of the plug since, if boiling were not in progress at the plug exit, the high velocities achieved would not be maintained downstream of the plug, and slug flow might ensue.

A plug designed for an exit velocity of 0.9 ft/sec was installed in a helically wound NaK–mercury boiler fabricated from type 315 stainless-steel tubing. Tests with this plug indicated that the boiler remained unconditioned over most of its length even after extended operation. With a 6 ft/sec plug, significant conditioning was observed after 4 hr and nearly complete conditioning was observed after 20 hr of operation. Subsequent tests with a 4.5 ft/sec plug and with a 0.9 ft/sec plug indicated full conditioning. From these tests was drawn the rather obvious conclusion that a fully conditioned boiler is free of slug flow and needs no inlet plug.

Contaminated fluid tests run with the same set of plugs, but with the addition of oil (contaminant) to the fluid, proved more interesting. When the conditioned boiler with the 0.9 ft/sec plug was contaminated with oil, no deconditioning was observed until the system was shut down. When restart was attempted, the boiler was found to be deconditioned; no amount of running would recondition it.

A conditioned boiler was then fitted with the 4.5 ft/sec plug. The addition of oil caused deconditioning, but reconditioning began after continued operation. Regression was observed after shutdown, but full reconditioning was achieved after restart and 75 hr of operation. In the next test the boiler was fitted with the 6.5 ft/sec plug, and oil was added. Deconditioning occurred, but reconditioning was complete in only 25 hr. Higher plug velocities promoted corrosion and erosion in the systems. (Each of the test plugs was designed for 30% exit quality.)

Deconditioning inevitably occurred after boiler shutdown in these tests. Thompson Ramo Wooldridge reported that hydrogen bright annealing of boilers tends to minimize or to eliminate this effect.

Potassium Boiler for SNAP-50/SPUR. A multitube potassium boiler, designed to test overall heat-transfer performance against theoretical predictions and to verify the results of Freon tests, was fabricated at AiResearch Mfg. Co.[3] The unit, a 19-tube Haynes 25 tube-in-shell boiler, is counterflow heated by sodium in the primary loop. The outer shell is semicircular; the inner 0.25-in.-OD tubes contain twisted tape inserts diffusion bonded to the tube walls. Potassium is circulated by an induction pump; an auxiliary heater at the boiler inlet assures the desired fluid inlet temperature.

The design flow was 5 to 15 lb/min at a mass velocity of 10 to 30 lb/(sec)(sq ft). Exit conditions of up to 150°F superheat were anticipated. Tests indicated that system performance was correlated well by means of the Martinelli equation incremented by 30% to correct for the twisted tape inserts. For fluid exit qualities as low as 40%, the overall measured heat-transfer coefficient was lower than the predicted value, as for low flow rates (~5 lb/sec), where data scatter was considerable.

Operation of the boiler was stable at all times, and boiling was easily initiated by providing sodium at only ~10°F above the potassium saturation temperature. Superheating up to 150°F was readily attained. The achievement of a pressure drop sufficient to ensure two-phase flow was achieved with inlet orificing.

High-Performance Potassium Boiling. A 300-kw Haynes 25 potassium boiler was fabricated by General Electric Company in Evendale, Ohio. This unit employs a gas-fired sodium loop as the heat source and features an air-cooled condenser. The test sec-

tion is illustrated in Fig. 9. A series of tests measured local heat-transfer coefficients over the entire series of flow regimes from the subcooled liquid to the superheated vapor states. Local heat-transfer data were evaluated in the nucleate-boiling, critical-heat-flux, transition-boiling, and superheated vapor phases. The tests also produced average heat-transfer data and pressure-drop measurements.[12]

Data runs included tests in which subcooled heating, nucleate boiling, transition-zone boiling, and superheating occurred simultaneously in the flow channel. Local heat fluxes and heat-transfer coefficients were measured in each zone. Figures 10 to 12 are typical of the results obtained. This information should be useful in the design of potassium boilers over a wide range of operating conditions.

Additional nucleate-boiling data were taken at a power level of 100 kw. The effect of vapor quality on heat transfer was not observed to be significant, but the magnitude of the total heat flux did influence the heat-transfer coefficient.

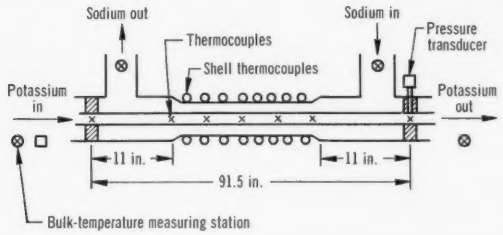

Fig. 9 Instrumentation of 300-kw test facility that includes Haynes 25 potassium boiler.[12]

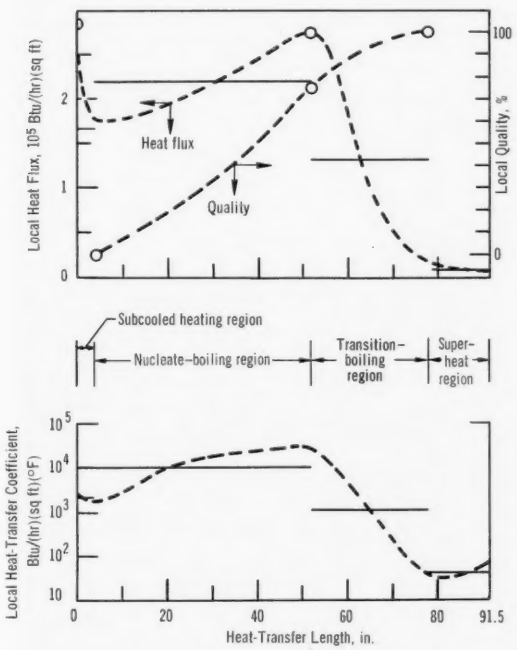

Fig. 10 Results of a typical once-through boiling run with P/D = 6 insert in the 300-kw facility shown in Fig. 9. Data points show calculated or known values; solid lines show average values; dashed lines show estimated values.[12]

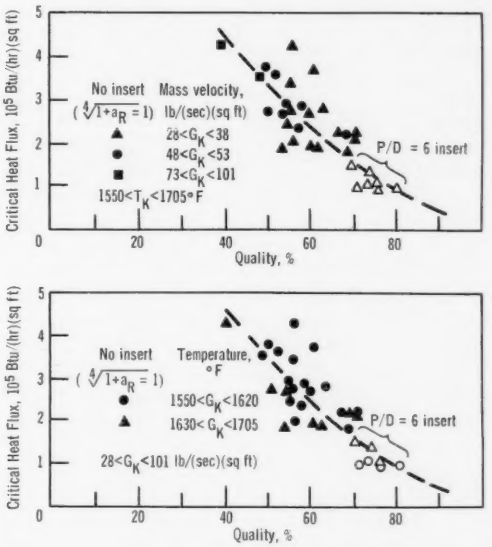

Fig. 11 Critical-heat-flux results for a 0.67-in.-ID boiler tube, showing (top) the effect of mass velocity and (bottom) the effect of temperature.[12]

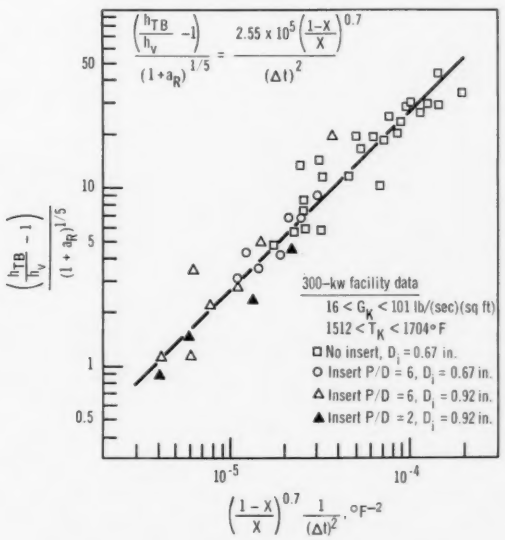
300-kw facility data
16 < G_K < 101 lb/(sec)(sq ft)
1512 < T_K < 1704°F
No insert, D_i = 0.67 in.
Insert P/D = 6, D_i = 0.67 in.
Insert P/D = 6, D_i = 0.92 in.
Insert P/D = 2, D_i = 0.92 in.

Fig. 12 Potassium transition-boiling data plotted in terms of the empirical correlation given.[12]

Pressure-drop data for boiling potassium were taken at 300 kw (Fig. 13); fairly good agreement was established with the Martinelli correlation. It appeared that the variation of the overall heat-transfer coefficient could be predicted with reasonable accuracy for flow conditions which were not very different from those set up for the tests, but, for flow conditions which differ significantly from those tested, local heat-transfer coefficients must be employed. A homogeneous flow model usually predicts a lower heat-transfer coefficient than is actually the case.

Forced-Flow Boiling of Sodium. A high-temperature test loop was assembled at NASA Lewis Research Center to study the heat-transfer characteristics of boiling sodium.[13] All components, including the 4-ft-long single-pass tube-in-shell heat exchanger, which were expected to operate above 1500°F, were constructed of niobium–1% zirconium alloy. The primary fluid, sodium or potassium, was electrically heated. Maximum oxygen partial pressure of $\sim 10^{-6}$ torr was maintained by baking out the system at 1400 to 2000°F with temperature cycling and by exposing the system to vacuum to ensure that all niobium components had completely outgassed.

Boiling was difficult to achieve with this apparatus, and, when obtained, was unstable. Two distinct boiling regimes were observed: (1) a low-heat-flux mode with relatively large oscillations in flow, pressure drop, and fluid temperature with low (<10%) quality and considerable superheating; (2) a high-heat-flux [$\sim 10^6$ Btu/(hr)(sq ft)] mode that was associated with relatively high quality (>35%) and little superheating. Although these two conditions were repeatable over a series of tests, no explanation of the reason for two coexistent flow regimes was evident. Apparently some source cavities for boiling that were dormant in the low-heat-flux regime were activated at elevated temperatures.

The test series was conducted with shell Peclet numbers ranging from 50 to 350, and the overall heat-transfer coefficients for the boiler were found to be between those predicted for constant-temperature and constant-heat-flux surfaces. The heat-transfer coefficient and vapor quality were obtained as functions of flow rate, and pressure-drop data were taken. Temperatures >1920°F were attained, and over 400 hr of running time at >1500°F were accumulated. Flow rates were ~1000 lb/hr, and the temperature differential across the heat exchanger was ~250°F. Flow oscillations up to 50% were observed in the first boiling mode (probably amplified by the condenser).

TURBOELECTRIC COMPONENTS

Turboelectric design involves the development of lightweight machinery, usually turboalternators, operable at rotational speeds from 12,000 to 36,000 rpm and at turbine inlet temperatures from 650 to 1800°F. Temperature gradients of 600 to 700°F across a few inches are encountered, and close

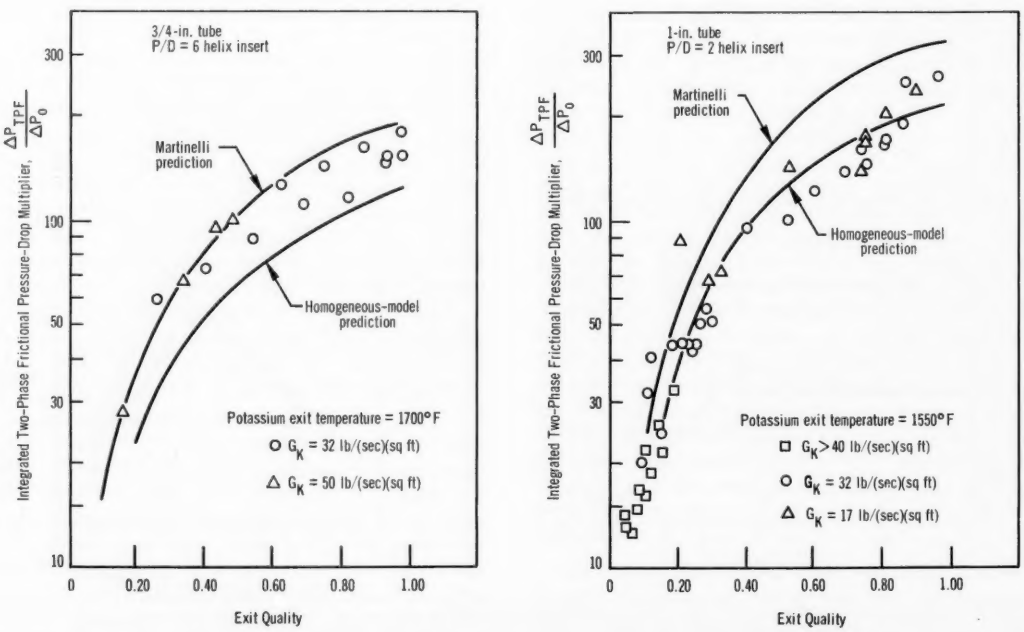
3/4-in. tube
P/D = 6 helix insert
Martinelli prediction
Homogeneous-model prediction
Potassium exit temperature = 1700°F
G_K = 32 lb/(sec)(sq ft)
G_K = 50 lb/(sec)(sq ft)
Integrated Two-Phase Frictional Pressure-Drop Multiplier, $\frac{\Delta P_{TPF}}{\Delta P_0}$
Exit Quality
1-in. tube
P/D = 2 helix insert
Martinelli prediction
Homogeneous-model prediction
Potassium exit temperature = 1550°F
G_K > 40 lb/(sec)(sq ft)
G_K = 32 lb/(sec)(sq ft)
G_K = 17 lb/(sec)(sq ft)
Integrated Two-Phase Frictional Pressure-Drop Multiplier, $\frac{\Delta P_{TPF}}{\Delta P_0}$
Exit Quality

Fig. 13 Typical two-phase boiling-potassium pressure-drop data.[12]

clearances and manufacturing tolerances are mandatory. Material creep and coefficient-of-expansion data for liquid-metal turbine operation up to and beyond 10,000 hr at high temperatures are not abundant for the materials of interest; turbine design technique is pressing the limits of metallurgical technology.

Turboalternator for SNAP-2. The model-V combined rotating unit (Table 2) developed by Thompson Ramo Wooldridge for the SNAP-2 system (Fig. 14) and the Mercury Rankine Power Conversion Program has a mercury-vapor-driven turbine, a pump, and an alternator on a common shaft.[5] These rotating components of the mercury loop are also lubricated by mercury. Figure 15 shows the bearings for possible use in this system.

The 4.1-kw alternator is an 1800-cycle unit with a design efficiency of 87%. This three-phase device has a four-wire Y-connected circuit that is externally grounded neutral.

The two-stage turbine consists of a subsonic impulse type first stage with 30% admission and a transonic impulse-reaction second stage with full admission.

Two sets of impellers were tested for the centrifugal mercury pump. The first set has five vanes with a 10° inlet angle and a 31° discharge angle, and the second set has six vanes with a 45° discharge angle. Pump efficiency of 30% was obtained in tests at 45 lb/min flow.

Table 2 SPECIFICATIONS FOR THE COMBINED ROTATING UNIT IN SNAP-2 (REF. 5)

Speed, rpm	36,000
Turbine	
Inlet pressure, psia	115
Inlet temperature, °F	1150
Discharge pressure, psia	9
Discharge temperature, °F	628
Efficiency, % (min)	55
Flow rate, lb/min	20
Alternator	
Frequency, cycles/sec	1800
Voltage, volts	
Line-to-neutral	63 ± 9.5
Line-to-line	110 ± 16.5
Output power, kw	4.1
Power factor	1.0 to 0.8
Duty cycle	Continuous
Efficiency at gross power, %	87
Mercury pump	
Inlet pressure to jets, psia (min)	5.9
Inlet temperature, °F (max.)	443
Discharge pressure, psia	525 ± 25
Flow, lb/min	50 ± 5
Efficiency (with dynamic seal), %	41
Bearings	Three-pad
Power consumption, watts	
Alternator	210
Turbine	210
Thrust	100
Flow rate, lb/min	
Alternator	8–10
Turbine	8–10
Thrust	7–8

The combined rotating units have been subjected to design-verification tests, including endurance, shock, and vibration testing. Five units have accumulated a total of >30,000 hr of running time with more than 100 starts. Unit endurance-run times were 6637, 2558, 2049, 861, 3159, 1277, 760, 863,

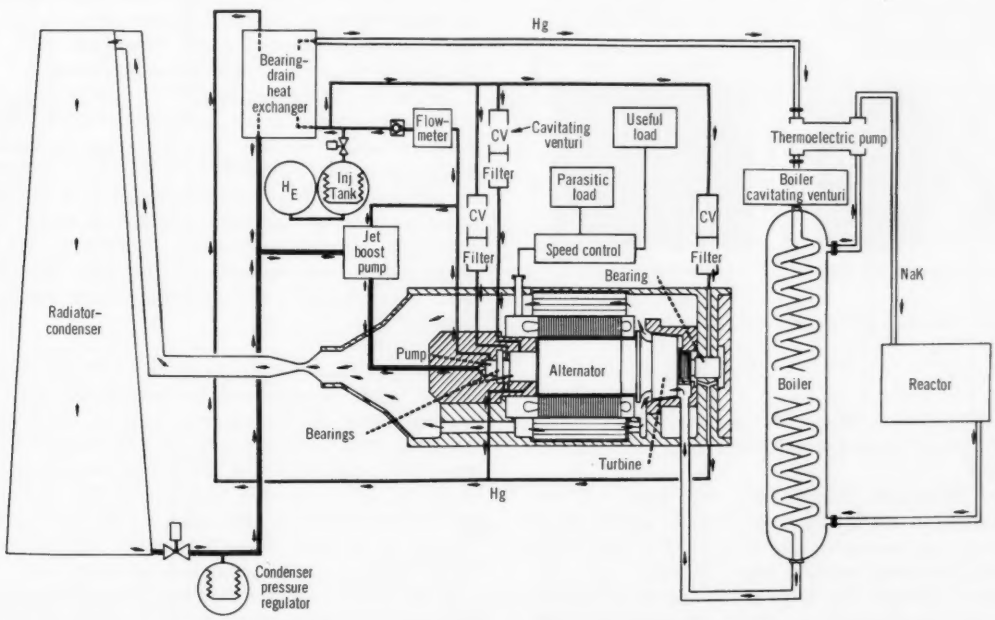

Fig. 14 Combined rotating unit in SNAP-2 (Ref. 5).

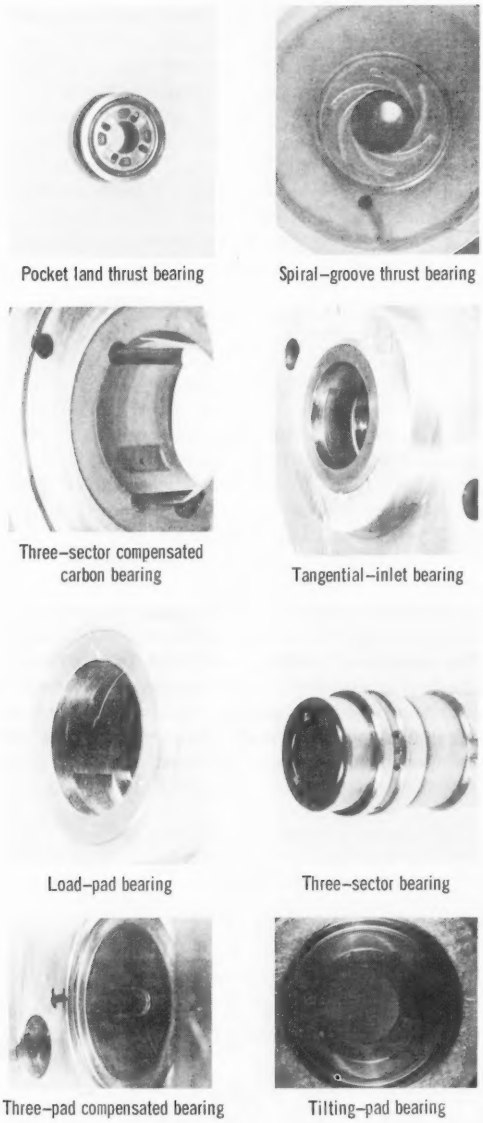

Fig. 15 Mercury-lubricated bearings for the SNAP-2 combined rotating unit.[5]

2500, 4767, and > 900 hr, for a total of ~25,000 hr. Degradation during the endurance runs has been very slight.

The combined rotating unit has been run with preheating to 400°F with no detrimental effects noted; however, a preheating level of 200°F apparently resulted in some bearing wear. At near rated conditions, 4.2 kw(e) has been generated at a maximum mercury temperature of 1150°F. The unit has demonstrated its capability of operating for 2500 hr and has passed all dynamic and performance tests, except that zero-gravity operation has not been verified.

Turboalternator for SNAP-8. The SNAP-8 turbine is a four-stage axial-flow impulse machine with a rotational speed of 12,000 rpm. The first two stages have 38% admission, whereas the latter two stages have full admission. The turbine wheels are of Haynes Stellite 6B, and the inner housing is type 316 stainless steel. Inlet temperature and pressure are 1260°F and 265 psi; exit conditions are 265°F and 16.5 psia. Turbine measured efficiency is 54% (the dry-gas efficiency is 58%). The turbine and alternator operate with separate but connected shafts. Overall efficiency is ~49.4% (Ref. 14).

The turbine bearings are angle-contact preloaded units of iron–silicon–bronze, mounted in a back-to-back configuration. They are lubricated with 4P3E and include dynamic slingers so that flooded operation is avoided. A portion of the turbine shaft is vented to space to prevent bearing lubricant from leaking into the mercury working fluid.

The alternator is a one-piece straddle-mounted rotor with angle contact bearings lubricated with 4P3E, which also cools the windings. This unit has been operated successfully up to a power level of 53 kw(e) and has an efficiency of 87%. In testing, the turboalternator has run 830 hr and had 45 starts prior to the failure of a spiral-wound snap ring in one of the turbine-shaft labyrinth seals. The Stellite 6B in the nozzle diaphragm and turbine wheel proved to be notch sensitive, and cracks were observed in these components. During operation the grain structure of the Stellite 6B changed. Redesign eliminated all sharp corners and the separate blade shroud. A type 316 stainless-steel nozzle block was used, and Stellite 6B blades were inserted in the wheel.

During test runs totaling 830 hr, the Stellite 6B blades did not erode, but performance for 10,000 hr has not been verified. Bearing-wear and space-sealing problems remain to be solved for the 10,000-hr duty cycle. Turbine critical speed is 20,000 rpm; however, the unit has been operated at 19,000 rpm with no significant increase in vibration. In general, performance requirements for this unit have been met, but endurance and reliability have yet to be achieved.

Turbogenerator for SNAP-50/SPUR. The turbogenerator under development by AiResearch Mfg. Co. for the SNAP-50 system was intended to produce 350 kw(e). The turbine design, Fig. 16, was for a six-stage 50% reaction device with a final stage diameter of 8.5 in. and a speed of 24,000 rpm. The final stage has an exit quality of 86% (Ref. 6). A single journal bearing is provided at each end of the turbine, and a thrust bearing is installed at the discharge end.

A problem is the development of suitable bearings (Fig. 17). A single-stage Inconel X impulse turbine with supersonic nozzles and an efficiency of 50% was

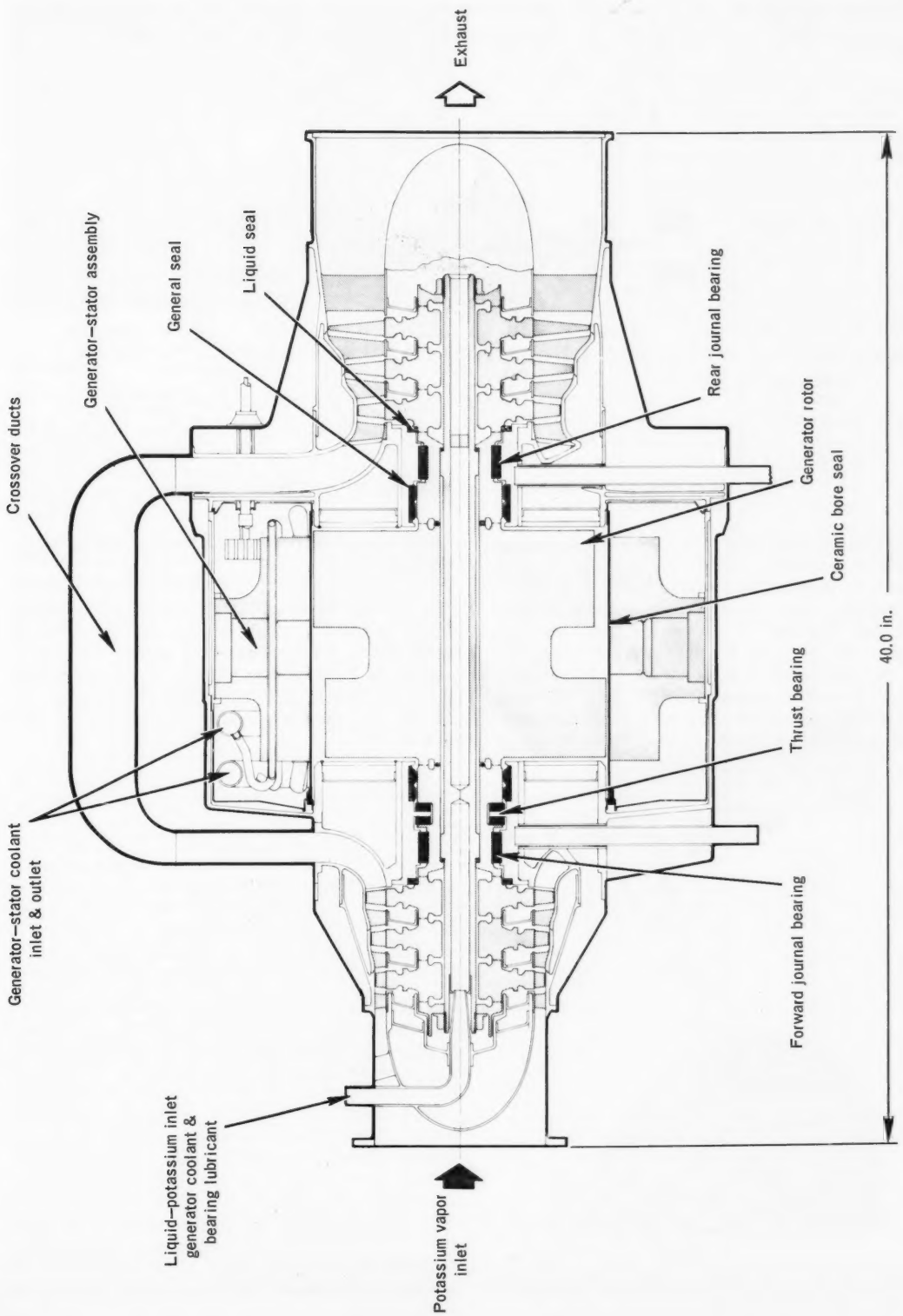

Fig. 16 Potassium turbogenerator for SNAP-50/SPUR (Ref. 6).

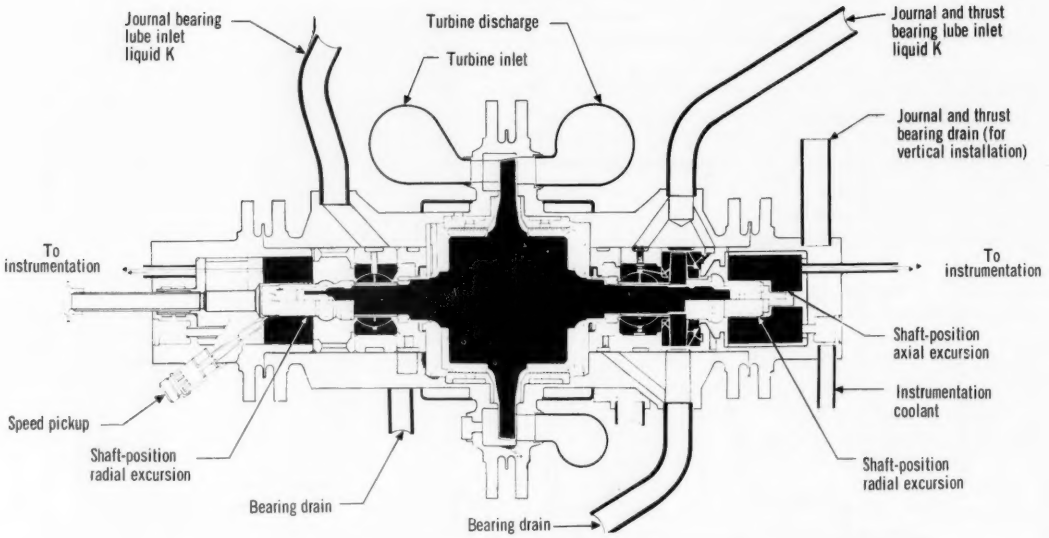

Fig. 17 Dynamic bearing test rig uses a single-stage Inconel X impulse turbine.[6]

employed in bearing tests. This wheel was lubricated by 550°F potassium, which was supplied through grooves in the bearing sleeves. Excellent bearing-test results were obtained with tungsten carbide tilting-pad bearings in a type 316 stainless-steel housing. The tungsten bearings were run for over 1000 hr continuously without evidence of wear, and, although subsequent restarts resulted in journal wear (as a result of retaining-ring movement), the lubricated bearings continued to operate smoothly at 24,000 rpm. Table 3 summarizes the bearing-wear-test experience.

A 200-Hp Two-Stage Potassium-Vapor Turbine. Under a NASA contract General Electric Company developed a 200-hp potassium turbine that represented the third and fourth stages of a Rankine-cycle turbogenerator (Fig. 18) (Ref. 15). Turbine speed was 19,200 rpm, and it operated with a pressure ratio of 2.95.

Table 3 FRICTION AND WEAR* OF BEARING MATERIALS IN 500°F POTASSIUM

Materials,† rotor/shoe	Starting torque, in.-lb	Running torque, av. in.-lb	Calculated coefficient of friction	Weight change, mg	Remarks‡
K94/Mo−0.5 Ti	18.3	13.1	0.266/0.190	+0.6/−4.0	Poor
K601/Mo−0.5 Ti	17.4	10.9	0.253/0.159	−1.1/−3.7	Poor
TZM/K94	>26	Shutdown	0.380/	−40.0/−9.2	Very poor
K94/TZM	17.0	10.9	0.247/0.159	+1.0/−5.0	Poor
K601/TZM	28.4	Fractured	0.410/		
TZM/K94	26.2	14.0	0.381/0.204	−59.0/−0.5	Poor
Mo−0.5 Ti/K94	24.0	17.4	0.350/0.253	−69.8/+0.2	Poor
K601/TZM	28.4	Fractured	0.410/		
TZM/W	>35.0	Shutdown	0.510/	−108.4/−14.0	Very poor
W/TZM	22.7	17.4	0.333/0.253	−15.4/−0.5	Poor
K94/K94	15.3	13.0	0.222/0.189	−0.2/−0.4	Excellent
K94/W	26.2	19.6	0.381/0.285	−666.3/−288.6	Poor
W/TZM	4.3	4.0	0.062/0.058	−5.5/−0.7	Poor
Mo−0.5 Ti/W	2.1		0.03/	−50.0/+5.0	Poor
K96/K96	8.3	1.75	0.121/0.025	−1.1/−0.1	Excellent
K11/K11	4.36	2.18	0.063/0.052	−0.8/−0.3	Excellent
K94/K94	4.36	4.36	0.063/0.063	+0.2/+0.2	Excellent
K701/K701	2.18	3.9	0.032/0.057	−0.6/−0.2	Excellent
K701/K11	3.06	2.62	0.045/0.039	−0.5/−0.2	Excellent
K11/K701	4.36	3.92	0.063/0.057	−0.9/−0.1	Excellent

*50 in./sec; 0_2 < 50 ppm.

†TZM: Mo−0.5% Ti−0.1% Zr−0.02% C; Mo−0.5 Ti: Mo−0.5 Ti−0.02 C; W: pure arc-cast W; K11: WC−3 Co−0.1 TiC; K94: WC−12 Co−2(Ta, Cb)C; K96: WC−12 Co−2(Ta, Cb)C; K701: WC−9.5 Co−0.1 TiC−4.0 Cr_3C_2; and K601: 84.5 W−10 Ta−5.5 C, no limit.

‡Excellent: Negligible wear, no material transfer, and polish both specimens. Poor: Excessive wear, surface roughened, material transfer, and high friction. Very poor: Test not completed due to excessive wear, friction, material roughening, and transfer.

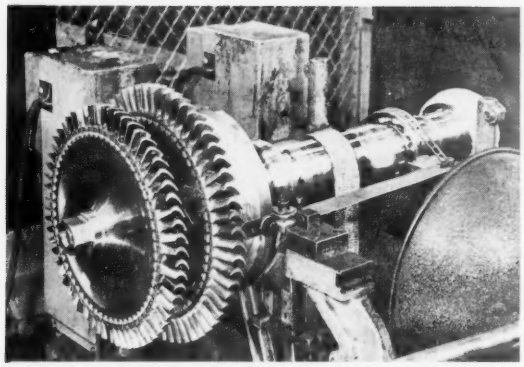

Fig. 18 Saturated-vapor test turbine designed for 1600°F potassium at 92% inlet quality.[15]

One attempt was made to simulate the wet conditions of the latter turbine stages by spraying liquid into the inlet stream. This was not successful because of the inability to obtain the fine droplets that would be present in an actual machine.

Oil-lubricated bearings were employed during the tests to separate blade-erosion investigation from the equally important problem of bearing wear. Heat was supplied by a gas-fired boiler. Test conditions are shown in Table 4.

Table 4 POTASSIUM–TURBINE TEST CONDITIONS[15]

Inlet temperature, °F	1450–1580
Turbine speed, rpm	15,400–21,000
Pressure ratio	1.4–4.4
Flow rate, lb/sec	1.6–2.1
Efficiency, %	40–70
Inlet quality, %	99

Subsequent to the successful completion of performance tests, an endurance run was begun, and a total of 5000 hr (two runs) was logged.

There was no visible second-stage blade erosion. A three-stage machine is being built for tests at higher last-stage moistures.

Organic Working-Fluid System. A relatively low temperature Rankine turbine developed by Sundstrand uses Dowtherm as the working fluid.[4] This system consists of a boiler, turboalternator, regenerator, condenser, and pump in which the maximum fluid temperature attained is 653°F. The working-fluid serves as the lubricant for all rotating components.

The shrouded, single-stage, Inconel X, radial-impulse turbine (Fig. 19) has a wheel radius of 3 in. and rotates at 24,000 rpm. It uses four supersonic (Mach 3) nozzles with a pressure ratio of 100 at an inlet pressure and temperature of 75 psi and ~650°F. Turbine efficiency of 54 to 61% has been attained. Because the expansion of the Dowtherm through the turbine is a superheated process, no condensation problems are encountered. The turbine nozzles are set at a fixed tangential angle of 17°; power output is varied by changing nozzle size.

A Pitot pump was employed since a minimum-leakage design was required for the very low (0.06 lb/sec) flows associated with this system. At 24,000 rpm the pump exit pressure is 95 psi. Only partially successful, this design attained the specified pressure ratio but not the specified flow rate, a deficiency attributed to inlet cavitation effects. Net pump efficiency achieved was ~26%.

The homopolar alternator consists of a main alternator and a parasitic unit that provides for load variation with constant turbine output. This 120- to 280-volt three-phase 3200-cycle unit was initially intended to produce 1.5 kw(e) but later was redesigned to yield 4 kw(e). Design efficiency of the alternator is 85%.

The bearings of the combined rotating unit, which consists of turbine, pump, and alternator, were tested with dry-start spin-ups to 24,000 rpm. Over 137 starts and 905 hr of operation were accumulated on one set of bearings, and the feasibility of startup with dry bearings was verified. The turbine and alternator employed in these tests accumulated > 2200 hr of operation.

The system was designed for flight use with a solar heat source. Therefore component weights are

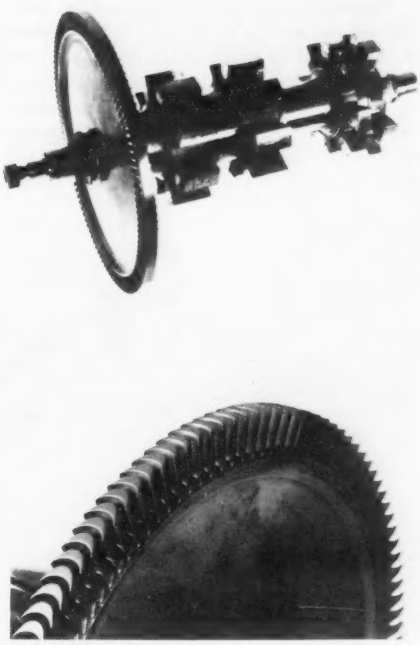

Fig 19 Organic Rankine-cycle impulse turbine wheel uses 115 electrochemically machined Inconel X blades.[4]

minimal (Table 5). Further testing and modification of this system are in progress at Sundstrand.

Follow-on programs have been initiated. One of the key problems in the long-term operation of an organic system is the stability of the working fluid with time and temperature. The AEC-sponsored programs at Sundstrand, Philco, and the National Bureau of Standards are investigating the long-term behavior of several candidate working fluids in simulated power-conversion loops. Under Air Force sponsorship, Sundstrand is investigating the feasibility of a 2- to 10-kw(e) combined rotating unit.

Table 5 DOWTHERM RANKINE-CYCLE COMPONENT WEIGHTS[4]

Component	Weight, lb
Alternator housing and windings	32
Alternator rotor	6.5
Nozzle housing	7.5
Pump housing	1.75
Rear bearing housing	2.25
Pump and bearings	1.25
Total	51.25

RADIATOR–CONDENSERS

A number of designs have been tested and appear to be satisfactory. As with boilers, the limiting factor is precise heat-transfer data. Radiator-tube vulnerability to meteors has also been studied briefly.

Condensing Mercury in Low-Gravity Environments. Two mercury-vapor-condensation test systems have been set up at the NASA Lewis Research Center. The first of these (Fig. 20) was a nitrogen-cooled tapered-glass-tube apparatus that was tested in both 0- and 1-g environments. Glass tubes were selected to permit photography and to promote nonwetting flow for the tests. Test results included 4000 frame/sec records of the condensing flow pattern.[16]

Pressure drops were correlated with the Martinelli parameter over flow rates from 0.028 to 0.049 lb/sec. The Martinelli correlation proved effective for high-quality flow (a low value of the two-phase flow modulus) but gave results significantly lower than the measured value for low-quality flow. The presence or absence of gravity had little effect on the measured pressure drops.

Tests were made with both wetting and nonwetting flow conditions (Fig. 21), and it was found that, at the lower flow rates, the pressure drop was only slightly affected by wetting. At higher flow rates the nonwetting pressure drop was lower than the wetted-tube pressure drop.

A second series of tests was conducted with a NaK-cooled counterflow tapered-tube mercury system. As predicted, it was found that the mercury inlet static pressure initially dropped off rapidly with increasing condensing length but eventually leveled out.

Mercury Rankine Radiator–Condenser. Atomics International conducted a series of mercury-radiator development tests for a 3- to 5-kw(e) Rankine system with 19.8 lb/min flow. Quality of the 625°F mercury entering the prototype radiator was 97%. An exit temperature of 371°F was required with a flow-passage pressure drop of 2.5 psi against a 9-psi backpressure.[17]

The test radiator is an array of tapered Haynes 25 steel tubes with aluminum cooling fins. Versions with 24 and 36 tubes were tested (preheat, operate, drain, and shutdown). The condensing length of the array was ~120 in. Although the radiator temperature during operational tests was nearly constant at 625°F over the initial 100 in. of tube length, a very rapid drop to the rated exit temperature occurred in the last 10 to 20 in. of tubing. The configuration tested appeared to be successful, but experiments with other configurations were planned.

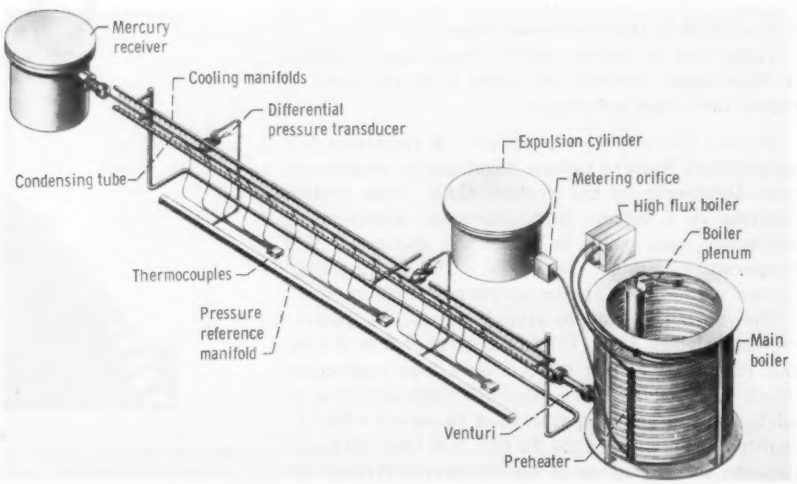

Fig. 20 Condensing mercury-vapor test rig.[16]

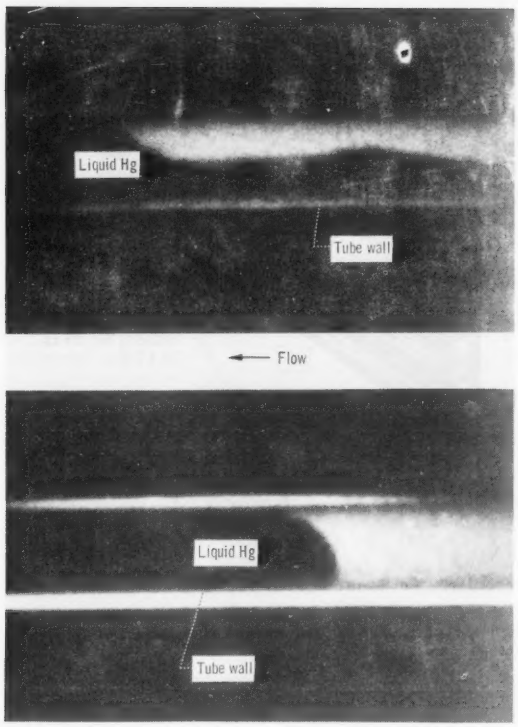

Fig. 21 Flow configurations at interface locations for wetting mercury condensation in copper tube (upper) and nonwetting condensation in stainless-steel tube.[16]

Two full-scale horizontal radiator–condensers simulating zero-gravity operation were tested. Over a range of conditions, no instabilities were noted. Satisfactory operation was also achieved against gravity by tilting the installation slightly.

Multitube Condenser for SNAP-8. Aerojet-General Nucleonics has tested a single-phase counterflow tube-in-shell NaK–mercury device containing 73 tapered 9% chromium–1% molybdenum steel tubes in a type 410 stainless-steel shell.[18] The 40-in.-long tubes are 0.25 in. in diameter at the inlet end and 0.20 in. at the exit. The total flow in the condenser is 11,500 lb/hr, and the variation in fluid quality is about linear with the tube length. The condenser pressure drop was successfully correlated with a modified Martinelli equation.

The only significant fabrication problem encountered in the assembly of the condenser was the welding of the 4° tapered tubes to the tube header support plate. A tapered-backbraze technique proved to be successful.

Tests showed that 420 kw(t) could be transferred, of which 15% was caused by subcooling of the condensate. Multitube-array performance differed little from results obtained earlier with a single-tube apparatus. This condenser appears to have satisfied all design requirements.

Direct-Condensing Potassium Radiators. A potassium, single-fluid, radiator–condenser for a space power system was tested at ORNL.[19] Each tube has copper radiator fins and is partially enclosed by a back reflector. A set of shutters attached to the reflector can be employed to open or completely enclose each condenser tube. These shutters, closed for launching, can be kept shut for low-power operation to control tube temperature and limit condensation. For operation at rated power, the shutters are opened and form part of the reflector.

Operational tests indicated satisfactory performance; no maldistribution or instability was observed. Data-gathering equipment included infrared films of the 800°F radiator surface.

Potassium-Condensing Tests. A 50-kw(t) condensing heat-transfer loop (Fig. 22) has been operated at the General Electric facility in Evendale, Ohio.[20] Single tubes $^3/_8$ and $^5/_8$ in. in inside diameter were flow tested with and without tapered-pin and helical inserts.

Potassium temperatures ranged from 1100 to 1400°F, and heat fluxes from 3×10^4 to 3×10^5 Btu/(hr)(sq ft) were obtained. Flow velocities of 100 to 1700 ft/sec were produced.

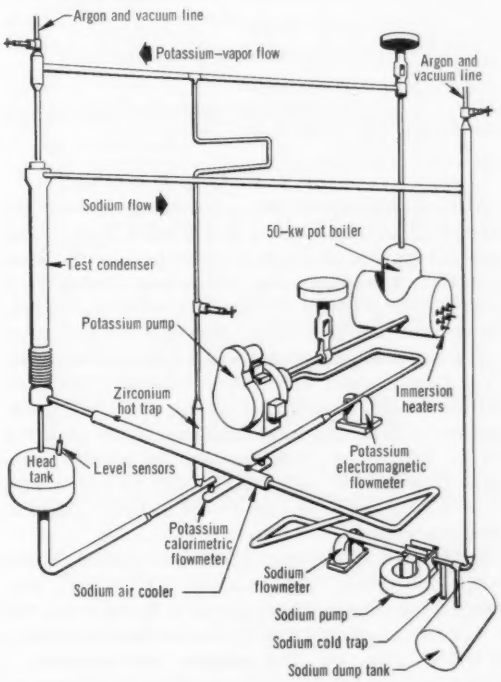

Fig. 22 Condensing potassium has been studied in this 50-kw(t) loop[20] *at heat fluxes up to 3×10^5 Btu/(hr)(sq ft).*

The Martinelli correlation successfully predicted pressure variations, and no evidence of flow instability was encountered. The data taken (Fig. 23 is typical) included the axial temperature distribution, heat-transfer coefficients vs. temperature, the variation of the Martinelli parameter with temperature, and the radial temperature variation in the condensing-tube walls.

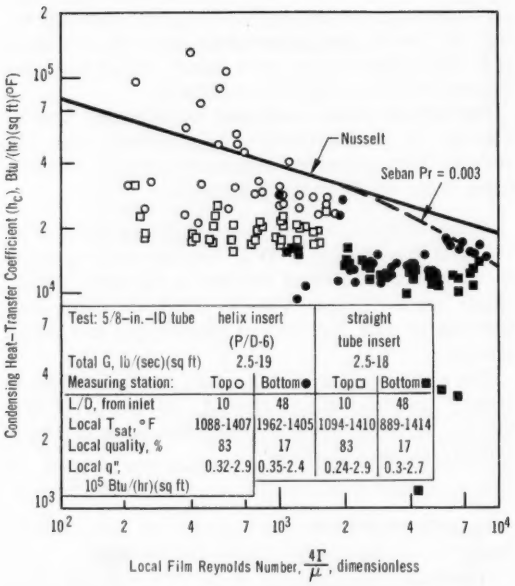
Condensing Heat-Transfer Coefficient (h_c), Btu/(hr)(sq ft)(°F)
Nusselt
Seban Pr = 0.003
Test: 5/8-in.-ID tube
helix insert (P/D-6)
straight tube insert
Total G, lb/(sec)(sq ft) 2.5-19 2.5-18
Measuring station: Top○ Bottom● Top□ Bottom■
L/D, from inlet 10 48 10 48
Local T_{sat}, °F 1088-1407 1962-1405 1094-1410 889-1414
Local quality, % 83 17 83 17
Local q", 10^5 Btu/(hr)(sq ft) 0.32-2.9 0.35-2.4 0.24-2.9 0.3-2.7
Local Film Reynolds Number, $\frac{4\Gamma}{\mu}$, dimensionless

Fig. 23 Potassium-condensing data obtained with the test loop shown in Fig. 22 (Ref. 20).

A three-loop potassium-condensing system was assembled at NASA Lewis Research Center.[21] This system consisted of a NaK primary loop, a two-phase potassium secondary loop, and a NaK cooling loop. Each NaK loop flowed 35,000 lb/hr, whereas the two-phase potassium loop design flow rate was 600 lb/hr.

The potassium condenser was a type 316 stainless-steel tube-in-shell assembly 16 ft long. The tubes had an outside diameter of 0.5 in. and a wall thickness of 0.03 in. The inside diameter of the shell was 2.0 in. Actual test conditions involved 1400°F potassium flow at 300 to 500 lb/hr with an inlet quality of 88%. Heat fluxes as high as 450,000 Btu/(hr)(sq ft) were observed.

A 14- by 3-ft radiator–condenser was also tested during this study. The radiator, ~ 10 ft long, consisted of an array of nine parallel, finned tubes with a wall thickness of 0.042 in. and an inside diameter of 0.5 in. (Fig. 24). The radiator was mounted in a cooled vacuum chamber to provide an environmental pressure of 10^{-3} mm Hg. Heat fluxes ranging from 23,000 to 49,000 Btu/(hr)(sq ft) were obtained.

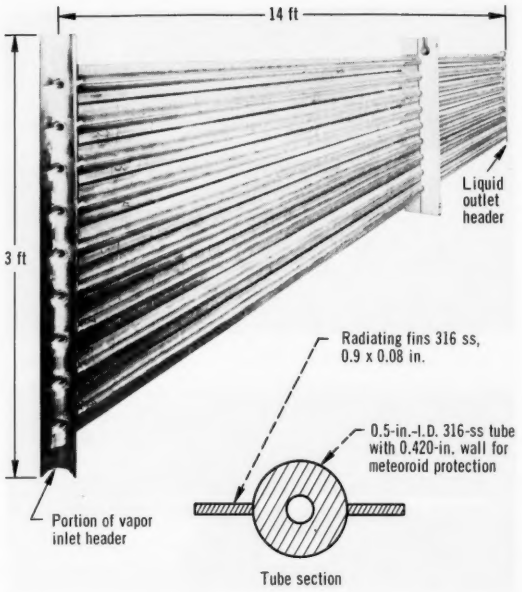
14 ft
3 ft
Liquid outlet header
Radiating fins 316 ss, 0.9 x 0.08 in.
0.5-in.-I.D. 316-ss tube with 0.420-in. wall for meteoroid protection
Portion of vapor inlet header
Tube section

Fig. 24 Potassium radiator–condenser with nine finned tubes.[21]

A typical condensing radiator wall-temperature profile was obtained in these tests over most of the length of the assembly; subcooling occurred near the radiator exit. With a vapor inlet temperature of 1426°F and inlet quality of 83%, a flow of 569 lb/hr was obtained. Pressure drop, temperature, and heat flux were measured. Satisfactory operation of the radiator–condenser was obtained over a range of pressures that included test conditions with a near-zero pressure drop.

Radiator Meteor Vulnerability. A program conducted by the NASA Lewis Research Center has attempted to provide some basic empirical data that would permit predicting how deeply a high-velocity particle would penetrate the wall of a radiator tube.[22]

Pyrex projectiles were fired into flat-plate targets of aluminum, type 316 stainless steel, niobium, nickel, and cobalt and into tubes of 2024T6 aluminum and type 316 stainless steel. Penetrations were correlated by an empirical relation. The flat-plate data were not, in most cases, very different from corresponding tube data. However, no general pattern of penetration was evident in tests that covered a range of penetrations from mild dimpling through severe spalling and perforation. These modes of damage are illustrated in Fig. 25.

In a series of impacts performed with lined tubes, spalling occurred with thick liners, but thin liners either dimpled or were penetrated. If mild dimpling could be tolerated, tube and liner weight could be reduced by about 45%.

A series of tests with beryllium armor over type 315 stainless-steel tubes revealed that damage could be expected consistently with unreinforced beryllium. A reinforcing scheme wherein kinked wire or steel screening was embedded in the beryllium considerably increased the efficacy of the armor. For a 500-day mission in which dimpled but not spalled radiator tubes would be tolerated, the minimum radiator specific weight [lb/kw(e)] would be obtained with lined beryllium tubes. In order of increasing weight, ATJ graphite, vanadium, and molybdenum follow beryllium.

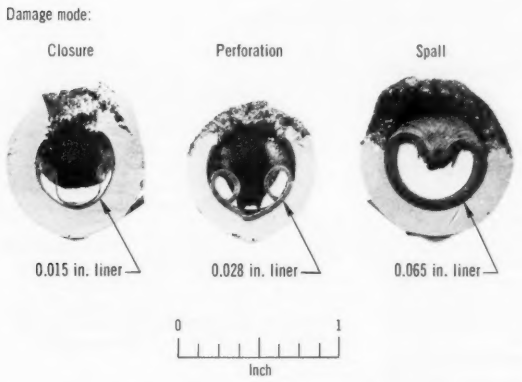

Fig. 25 Limiting damage modes in type 316 stainless-steel tubes armored with cast aluminum. Tubes were at room temperature and were impacted by $^3/_{32}$-in.-diameter pyrex projectiles at 25,000 ft/sec (Ref. 22).

Conclusions

Most of the current work in the field is directed toward building a backlog of component experience. Because of the complexity and cost of this kind of power system, development must proceed along a rather narrow front and in a somewhat piecemeal fashion. The total effort reported in this article was under the aegis of only four government and seven commercial organizations.

The prediction of heat-transfer coefficients in two-phase flow, wherein semiwetting conditions prevail, and the development of high-temperature turbines (1200 to 1800°F) and high-speed high-temperature bearings constitute the foremost technical problems. These represent a very straightforward projection of conventional rotating-machinery problems into a more severe and stringent environment. There is also the reliability problem—these Rankine systems must operate for relatively long periods without maintenance. At present an engineering approach to the solution of these problems is, for better or worse, being followed. Perhaps the seeming underemphasis on basic heat-transfer and dynamics research is only an apparent one, and fundamental design principles as well as practical techniques may emerge from current Rankine-cycle work.

References

All references are papers presented at the American Institute of Aeronautics and Astronautics Specialists Conference on Rankine Space Power Systems, in Cleveland, Ohio, October 26, 1965, USAEC Report CONF-651026, Vol. I.

1. R. Wallerstedt and D. Miller, Mercury Rankine Program Development Status and Multiple System Application.
2. E. S. Chalpin, J. R. Pope, and C. L. Foss, Development of the SNAP 8 Pump for Mercury Service.
3. J. A. Boppart, K. O. Parker, and P. J. Berenson, Multiple-Tube Potassium Boiler Development.
4. J. Malohn, Organic Working Fluid Cycle: Development Status.
5. R. C. Biering and Otto Decker, MRPC (SNAP 2) Turboalternator.
6. J. H. Dannan and L. E. Chadbourne, Potassium Turbine-Generator Development.
7. E. S. Chalpin, C. P. Colker, and C. L. Foss, Design and Development of Pumps for High Temperature NaK Service.
8. M. A. Perlow, H. H. Hanlin, and J. M. Hochman, Development of the MRP Thermoelectric NaK Pump.
9. L. V. Wilson, H. C. Young, and A. M. Smith, Experience with Turbine Driven Potassium Boiler Feed Pumps at ORNL.
10. A. H. Kreeger, A. J. Sellers, and J. N. Hodgson, Design and Development of the Mercury Boiler for the SNAP 8 System.
11. R. S. Carey and B. Farwell, Effects of Oil Contamination on Heat Transfer Performance.
12. J. R. Peterson, High Performance Once-Through Boiling of Potassium.
13. J. P. Lewis, Experimental Investigation of Forced Flow Boiling of Sodium.
14. M. G. Cherry and G. Oiye, Design and Development of a Turbine Alternator Assembly for the SNAP 8 System.
15. R. J. Rossback et al., Performance Test of Two-Stage 200-Hp Turbine in Wet Potassium Vapor.
16. D. Namkoong and J. Albers, An Experimental Study of the Condensing Characteristics of Mercury Vapor Flowing in Single Tubes.
17. D. H. Heiskala et al., Mercury Rankine Radiator Condenser Development Experience.
18. A. J. Kreeger and J. N. Hodgson, Design and Development of the SNAP 8 Multi-Tube Condenser.
19. A. P. Fraas, Design and Development Tests of Direct-Condensing Potassium Radiators.
20. S. C. Sawochka, Thermal and Fluid Dynamic Performance of Potassium During Condensing Inside a Tube.
21. Q. A. Gutierrez et al., Potassium Condensing Tests of Horizontal Multi-Tube Convective and Radiative Condensers Operating at Vapor Temperatures of 1250°F to 1500°F.
22. N. Clough and J. H. Diederich, Results of Hypervelocity Impacts into Space Radiator Materials.

Index

Power Reactor Technology

Volume 9

Note: The page range for each of the four issues of Vol. 9 is as follows:

No. 1, pages 1 to 63
No. 2, pages 65 to 100
No. 3, pages 101 to 152
No. 4, pages 153 to 213

A

Accidents
  loss-of-coolant, studies in fast breeder reactors by zone-loading experiments, 164-65
Aeroball system
  neutron-flux distribution measurement by, 28
Aluminum (SAP)
  use as fuel cladding in organic-cooled reactors, 138-39
Argon isotopes (^{40}Ar)
  use in neutron-flux distribution measurements, 28-29

B

Beacons
  lighting on offshore platforms, SNAP-7F power source for, 3
Bearings (liquid-metal)
  film-thickness measurement techniques, 125-26
Boilers
  development for Rankine-cycle power systems, 132-34, 200-04

C

Cavitation
  damage studies of metals in liquid alkali metals, instrument for, 128
Cobalt isotopes (^{60}Co)
  use as heat source in turbine-Rankine-cycle engine, 12-13
Computer programs
  development for loss-of-coolant accident, 47
  development for shielding analysis, 19-23
Condensers
  development for Rankine-cycle power systems, 210-13
  meteor vulnerability, 212-13
Conferences and meetings
  high-temperature instrumentation in liquid-metal experiments, 123-35
  two-phase fluid flow, 35-44
Copper alloys
  Cu-Fe-Zr, use as fuel cladding in organic-cooled reactors, 139
Critical experiments
  zone-loading for fast breeder reactors, 162-68
Critical mass
  estimating in fast breeders by zone-loading experiments, 166

D

Deep-submergence vehicles
  list, 7
  NR-1, 14-15
  nuclear powered for fisheries research, 4-8
  nuclear propulsion systems, 13-15
  SWR, 14
Density probes
  design of nuclear for measuring deep-sea sediments, 4
Divers
  scuba-suit heating by isotopic power, 6
Doppler effect
  measurement in zone-loaded fast breeder experiments, 164-65
Dowtherm A
  use as working fluid for turbine-Rankine-cycle engine, 13, 197-98
Drilling
  nuclear power sources for offshore, 2-3

E

Economics
  neutron-flux distribution measurements as aid in power increase, 25
  on-power refueling systems, 181
  organic coolants, 137-40
Engines (steam)
  radioisotope powered for oceanography applications, 12-13

F

Fishing industry
  nuclear power applications in, 4-8
Flowmeters
  for liquid-metal systems, 124-25
Fluid flow (two-phase)
  compressibility, effects on stability and burnout, 65-68
  inverse temperature profiles in boiling K, 129-30
  symposium on, review, 35-44
  volume-fraction measurements in liquid metals, 124-25
Foghorns
  on offshore platforms, SNAP-7A power source for, 3
Food
  harvesting from the ocean, nuclear power for, 4-8
Foils
  use in neutron-flux distribution measurements, 26, 86-94
France
  liquid-metal steam-generator program, 69-73

G

Gamma-adsorption analysis
  use in measuring volume fraction in two-phase flows, 124
Gases
  monitoring of inert in liquid metals, instrument for, 128
  use in neutron-flux distribution measurement, 28-29
Generators
  liquid-metal MHD, review, 188-92

H

Haynes 25 alloy
  performance as Hg boiler material, 134-35
HB-40
  properties as organic coolant, 137-40
Heat exchangers
  design for liquid metals, 177-79
Heat sources
  development of isotopic for oceanography applications, 9-10
Heat transfer
  coefficients for liquid metals, 174-79
  heat transfer in double-pipe liquid metal, method for determination of, 129
  inverse temperature profile in boiling two-phase flow of K, 129-30
Heaters
  for liquid-metal experiments, 123

I

Instruments
for high-temperature liquid-metal experiments, 123-35
Ion chambers
use in neutron-flux distribution measurement, 29-31
Iron alloys
Cu–Fe–Zr, use as fuel cladding in organic-cooled reactors, 139
Fe–Ni–Nb–Sb–Zr, use as fuel cladding in organic-cooled reactors, 139
Isotopic engines
development of steam piston, 13
development of turbine-Rankine-cycle system, 12-13
Isotopic thermal power systems
application in oceanography, 9-10
Isotopic thermoelectric systems
application in oceanography, 10-12

L

Liquid-metal steam generators
U. S. and French programs, 69-73

M

Magnetohydrodynamic power systems
review of technology, 187-92
Mercury
boiler development for Rankine-cycle power systems, 132-34, 200-02
condenser development for Rankine-cycle power systems, 210-11
pump development for Rankine-cycle power systems, 198
Metals (liquid)
cavitation damage studies, instrument for, 128
flowmeters, 124-25
heat-transfer coefficients, 174-79
heat transfer in double-pipe heat exchangers, method for determination of, 129
high-temperature instrumentation in experiments, 123-35
level measurement techniques, 126
monitoring for dissolved oxygen, instrument for, 128
monitoring for inert gases, instrument for, 128
pressure measurement, instrument for, 123-24
use in MHD power systems, 187-92
use in steam-generating systems, review of French program, 69-73
volume-fraction measurement in two-phase flow, 124-25
Minerals
exploration and production from the ocean floor, nuclear power for, 3-4
Mining
of minerals from the ocean floor, nuclear power for, 3-4

N

Neutron sources
design of high-flux research reactors for, 153-60
Neutron spectra
measurement in fast breeders by zone-loading experiments, 164
measurement in operating reactors, 25-33
measurement by two-detector cross-correlation, 142-43
measurement by pseudorandom binary inputs, 142-43
measurement of thermal and epithermal, 80-94
Nickel alloys
Fe–Ni–Nb–Sb–Zr, use as fuel cladding in organic-cooled reactors, 139
Niobium alloys
Fe–Ni–Nb–Sb–Zr, use as fuel cladding in organic-cooled reactors, 139
Nb–Zr, use as fuel cladding in organic-cooled reactors, 138-39
NR-1 deep-submergence vehicle
development, 7, 14
Nuclear ships
(see Ships (nuclear))

O

Oceanography
nuclear power applications, 1-17, 150-52
Ores
(see Minerals)
Organic materials
use as reactor coolants, 137-40
Organic Rankine-cycle power-system development, 197-98, 209-10
Oxygen
monitoring in liquid metals, instrument for, 126
Ozhennite
use as cladding in organic-cooled reactors, 139

P

Petroleum
offshore exploration and production, nuclear power for, 1-3
Potassium (liquid)
boiler development for Rankine-cycle power systems, 202-04
condenser development for Rankine-cycle power systems, 211-12
inverse temperature profiles in boiling two-phase flow of, 129-30
pump development for Rankine-cycle power systems, 199-200
Pressure
measurement in liquid-metal systems, devices for, 123-24
Pressure vessels
cladding failure in water reactors, 101-109
cladding with stainless steel, 102-104
Propulsion
nuclear power systems for deep-submergence vehicles, 6-9, 12-17, 150-52
Prospecting
for minerals on the ocean floor, nuclear power for, 4
Protein
harvesting from the ocean, nuclear power for, 4-5
Pumps
development for Rankine-cycle power systems, 198-200

R

Radiators
development for Rankine-cycle power systems, 210-13
meteor vulnerability, 212-13
Radioisotope Submersible Engine (RISE)
development, 12-13
Rankine-cycle power systems
component development, 194-213
use in RISE, 12-13
Reactor control systems
optimal theory, 169-71
Reactor coolants
dynamics in fast reactors, effects on safety, 46-49
loss in fast breeders, analysis by zone-loading experiments, 164-65
materials for organic, technology advances, 137-40
Reactor fuels
uniform burnup, neutron-flux distribution measurements as aid in, 25-26
Reactor safety
neutron-flux distribution measurements in, 26
Reactors
core design, use of neutron-spectra measurements in, 80-94
kinetics, measurement in fast breeders by zone-loading experiments, 165
kinetics, nonlinear analysis, 171-72
neutron-flux distribution measurement in operating, 25-33
neutron-noise analysis, 142-43
neutron-spectra measurement by differential techniques, 80-86
neutron-spectra measurement by integral techniques, 86-94
power rating increase, use of neutron-flux distribution measurement in, 25
on-power refueling systems, merits of, 180-86
role in magnetohydrodynamic power systems, 187-92
shielding analysis, advance methods in, 19-23
Reactors (Big Rock Point)
modifications, description and procedures, 76-78
operating experience, outages, 112, 120-21
neutron-flux distribution measurement system, 25
Reactors (cavity)
design concepts for high-flux research, 159
Reactors (Connecticut Yankee)
neutron-flux distribution measurement system, 25
Reactors (Dresden)
neutron-flux distribution measurement system, 25-26
operating experience, outages, 112, 119
Reactors (EBR-II)
neutron-flux distribution measurement systems, 26
Reactors (EBWR)
modifications, description and procedures, 78
neutron-flux distribution measurement system, 28
pressure-vessel cladding failure, 102-06
pressure-vessel cladding with stainless steel, 102
Reactors (Elk River)
pressure-vessel cladding failure, 107-09
Reactors (fast)
power excursions, effect of coolant dynamics on events, 46-49
Reactors (fast breeder)
zone-loaded critical experiments, 162-68

Reactors (gas-cooled)
applications for undersea power plants, 15
Reactors (HBWR)
neutron-flux distribution measurement system, 26
Reactors (Heavy Water Components Test) (HWCTR)
modifications, description and procedures, 78
Reactors (heavy-water moderated)
lattice calculations and measurements, 145-46
Reactors (high-flux research)
design concepts, 153-60
Reactors (Humboldt Bay)
neutron-flux distribution measurement system, 25
operating experience, outages, 112, 121-22
Reactors (Indian Point)
operating experience, outages, 119-120
Reactors (liquid-metal-cooled)
steam generators, U. S. and French programs, 69-73
Reactors (MH-1A)
development for floating power source, 15-16
Reactors (NPD)
on-power refueling system, 180-86
Reactors (NR-1)
design concept, 152
Reactors (NRU)
on-power refueling systems, 180
Reactors (Oak Ridge Graphite)
neutron-flux distribution measurement system, 26
Reactors (Plutonium Recycle Test)
neutron-flux distribution measurement system, 28
Reactors (San Onofre)
neutron-flux distribution measurement system, 25, 28
Reactors (Saxton)
neutron-flux distribution measurement system, 25
Reactors (SELNI)
neutron-flux distribution measurement system, 28
Reactors (Shippingport)
operating experience, outages, 112, 117-19
Reactors (SNAP-8A)
development for deep-submergence vehicle propulsion, 13-14
Reactors (SNAP-10A)
design, 2
power source for offshore oil and gas platforms, 3
use as undersea power units, 13-14 158-59
Reactors (Sodium Experiment) (SRE)
modifications, description and procedures, 74-76
Reactors (supercritical-water)
development for deep-submergence vehicle propulsion, 14-15
Reactors (thin shell)
design concepts for high-flux research, 159-60
Reactors (TURPS)
applications for surface and undersea power plants, 15, 17
Reactors (UHTREX)
design and projected operating characteristics, 51-62
Reactors (water-moderated)
lattice calculations and measurements, 146-49
Reactors (Yankee)
neutron-flux distribution measurement system, 25, 26-28
operating experience, outages, 112, 115-17
power-rating increase, 25
pressure-vessel cladding failure, 106-07
RISE
[see Radioisotope Submersible Engine (RISE)]

S

Safety
zone-loaded critical experiments, 166-68
Santowax OM
properties as organic coolant, 137-40
Shielding
analysis, advance methods in, 19-23
Ships (nuclear)
development for fishing industry, 4-5
Sodium
boiler development for Rankine-cycle power systems, 204
two-phase flow of boiling, properties of, 131-32
Sodium–potassium alloys (liquid)
pump development for Rankine-cycle power systems, 198-99
reaction with water, 72-73
Spheres
use in neutron-flux distribution measurements, 27-28
Stainless steel
crack analysis in pressure-vessel cladding, 101-109
Steam generators
liquid metal, U. S. and French programs, 69-73
Submarines
(see also Deep-submergence vehicles)
development for deep-sea research, 6-9
Systems for Nuclear Auxiliary Power (SNAP-2)
component development for Rankine-cycle power system, 194-96, 199, 205-6
Systems for Nuclear Auxiliary Power (SNAP-7A)
use in navigational buoy, 10
Systems for Nuclear Auxiliary Power (SNAP-7B)
use in lighthouses, 10-11
Systems for Nuclear Auxiliary Power (SNAP-7C)
use in Antarctic weather station, 11
Systems for Nuclear Auxiliary Power (SNAP-7D)
use in Gulf of Mexico weather station, 11
Systems for Nuclear Auxiliary Power (SNAP-7E)
use in sonobuoy near Bermuda, 11-12
Systems for Nuclear Auxiliary Power (SNAP-7F)
use for beacons and foghorns on offshore oil platforms, 3
Systems for Nuclear Auxiliary Power (SNAP-8)
component development for Rankine-cycle power systems, 132-33, 194, 196-99, 201-02, 206, 211
development for deep-submergence vehicle propulsion, 13-14
Systems for Nuclear Auxiliary Power (SNAP-10A)
design, 2
use for offshore platform power units, 3
use for undersea power units, 13-14
Systems for Nuclear Auxiliary Power (SNAP-15)
development for undersea power sources, 11-12
Systems for Nuclear Auxiliary Power (SNAP-21)
development for undersea power sources, 12
Systems for Nuclear Auxiliary Power (SNAP-50/SPUR)
component development for Rankine-cycle power system, 194, 197, 206-08
Symposia
(see Conferences and meetings)

T

Terphenyls
(see Santowax OM and HB-40)
Thermometers
use in neutron-flux distribution measurements, 31
Tin alloys
Fe–Ni–Nb–Sb–Zr, use as fuel cladding in organic-cooled reactors, 139
Turbines (potassium vapor)
pressure measurement, devices for, 123-24
Turbogenerators
development for Rankine-cycle power systems, 204-10

U

Uranium carbides
UC–D_2O, critical masses and neutron buckling in lattices of, 145
Uranium oxides
PuO_2–UO_2–H_2O, critical masses and neutron buckling in lattices of, 146-47
UO_2, testing of Zr–Nb alloy-clad, in organic-cooled reactors, 138
UO_2–H_2O, critical masses and neutron buckling in lattices of, 147

W

Welding
stainless-steel cladding to pressure vessels, 101-02
Wires
use in neutron-flux distribution measurements, 26

Z

Zircaloy-2
use as fuel cladding in organic-cooled reactors, 139
Zirconium alloys
Cu–Fe–Zr, use as fuel cladding in organic-cooled reactors, 139
Fe–Ni–Nb–Sb–Zr, use as fuel cladding in organic-cooled reactors, 139
Nb–Zr, use as fuel cladding in organic-cooled reactors, 138-39

U. S. GOVERNMENT PRINTING OFFICE: 1967—252338/2

LEGAL NOTICE

This journal was prepared under the sponsorship of the U. S. Atomic Energy Commission. Neither the United States, nor the Commission, nor any person acting on behalf of the Commission:

A. Makes any warranty or representation, expressed or implied, with respect to the accuracy, completeness, or usefulness of the information contained in this journal, or that the use of any information, apparatus, method, or process disclosed in this journal may not infringe privately owned rights; or

B. Assumes any liabilities with respect to the use of, or for damages resulting from the use of any information, apparatus, method, or process disclosed in this journal.

As used in the above, "person acting on behalf of the Commission" includes any employee or contractor of the Commission, or employee of such contractor, to the extent that such employee or contractor of the Commission, or employee of such contractor prepares, disseminates, or provides access to, any information pursuant to his employment or contract with the Commission, or his employment with such contractor.

NUCLEAR SCIENCE ABSTRACTS

The U. S. Atomic Energy Commission, Division of Technical Information, publishes *Nuclear Science Abstracts* (*NSA*), a semimonthly journal containing abstracts of the literature of nuclear science and engineering.

NSA covers (1) research reports of the U. S. Atomic Energy Commission and its contractors; (2) research reports of government agencies, universities, and industrial research organizations on a worldwide basis; and (3) translations, patents, books, and articles appearing in technical and scientific journals.

Complete indexes covering subject, author, source, and report number are included in each issue. These are cumulated quarterly, semiannually, and annually providing a detailed and convenient key to the literature.

Availability of *NSA*

SALE *NSA* is available on subscription from the Superintendent of Documents, U. S. Government Printing Office, Washington, D. C., 20402, at $30.00 per year for the semimonthly abstract issues and $22.00 per year for the four cumulated-index issues. Subscriptions are postpaid within the United States, Canada, Mexico, and all Central and South American countries, except Argentina, Brazil, Guyana, French Guiana, Surinam, and British Honduras. Subscribers in these Central and South American countries, and in all other countries throughout the world, should remit $37.00 per year for subscriptions to semimonthly abstract issues and $25.00 per year for the four cumulated-index issues.

EXCHANGE *NSA* is also available on an exchange basis to universities, research institutions, industrial firms, and publishers of scientific information. Inquiries should be directed to the Division of Technical Information Extension, U. S. Atomic Energy Commission, P. O. Box 62, Oak Ridge, Tennessee, 37830.

TECHNICAL PROGRESS REVIEWS may be purchased from Superintendent of Documents, U. S. Government Printing Office, Washington, D. C., 20402. *Nuclear Safety* at $3.00 per year for each subscription or $1.00 per issue; each of the other journals at $2.50 per year or $0.70 per issue. The use of the coupon below will facilitate the handling of your order.

POSTAGE AND REMITTANCE: Postpaid within the United States, Canada, Mexico, and all Central and South American countries except Argentina, Brazil, Guyana, French Guiana, Surinam, and British Honduras. For these Central and South American countries and all other countries, add $0.75 for each annual subscription or $0.20 for a single issue. Payment should be by check, money order, or document coupons, and MUST accompany order. Remittances from foreign countries should be made by international money order or draft on an American bank payable to the Superintendent of Documents or by UNESCO book coupons.

order form

SUPERINTENDENT OF DOCUMENTS
U. S. GOVERNMENT PRINTING OFFICE
WASHINGTON, D. C., 20402

Enclosed:
document coupons ☐ check ☐ money order ☐

Charge to Superintendent of Documents No._____

Please send a one-year subscription to

☐ ISOTOPES AND RADIATION TECHNOLOGY

☐ POWER REACTOR TECHNOLOGY

☐ REACTOR MATERIALS

(Each subscription $2.50 per year; $0.70 per issue.)

☐ NUCLEAR SAFETY

(Each subscription $3.00 per year; $1.00 per issue.)

SUPERINTENDENT OF DOCUMENTS
U. S. GOVERNMENT PRINTING OFFICE
WASHINGTON, D. C., 20402

(Print clearly)

_____
Name

_____
Street

_____
City, State, ZIP Code